Review

Sustainable Methods for Conversion of Lignocellulosic Biomass to Bioplastics: A Green Chemistry Approach

Mostafa M. Gaafar , Muhammad Hamza , Muhammad Husnain Manzoor , Islam Elsayed , El barbary Hassan *

Posted Date: 21 January 2026

doi: 10.20944/preprints202601.1587.v1

Keywords: biomass; pretreatment; 2,5-furandicarboxylic acid; lactic acid; bioplastics

Review

Sustainable Methods for Conversion of Lignocellulosic Biomass to Bioplastics: A Green Chemistry Approach

Mostafa M. Gaafar [1,2], Muhammad Hamza [1], Muhammad Husnain Manzoor [1], Islam Elsayed [1,2] and El barbary Hassan [1,*]

[1] Department of Sustainable Bioproducts, Mississippi State University, Mississippi State, MS 39762, USA

[2] Department of Chemistry, Faculty of Science, Damietta University, New Damietta, Egypt

* Correspondence: e.hassan@msstate.edu; Tel.: (16623258344)

Abstract

Plastic manufacturing depends heavily on petroleum-derived monomers like terephthalic acid, the main component of polyethylene terephthalate (PET). However, the depletion of fossil resources and increasing environmental concerns have heightened the need for sustainable alternatives. Lignocellulosic biomass has emerged as a promising resource due to its renewable, abundant, and eco-friendly nature. Understanding its chemical composition enables conversion of this biomass into platform chemicals, such as 2,5-furandicarboxylic acid (FDCA) and lactic acid, derived from cellulose and hemicellu-lose. These can be polymerized into bioplastics such as polyethylene furanoate (PEF) and polylactic acid (PLA), offering greener alternatives to fossil-based plastics. PEF features rigid furan rings that enhance thermal stability, mechanical strength, and barrier proper-ties, and reduce gas permeability compared to PET. PLA is a renewable, biodegradable plastic widely used in packaging and medical applications. This review covers the chem-ical makeup of lignocellulosic biomass cellulose, hemicellulose, and lignin, and various pretreatment strategies, chemical, physicochemical, and physical, to overcome biomass recalcitrance and improve conversion efficiency. It also highlights recent catalytic ad-vances in transforming lignocellulosic carbohydrates into bioplastic precursors such as FDCA and lactic acid. Lastly, the review discusses polymerization pathways for produc-ing PEF and PLA, emphasizing their role in reducing the environmental impact of poly-mer manufacturing and promoting green chemistry principles.

Keywords: biomass; pretreatment; 2,5-furandicarboxylic acid; lactic acid; bioplastics

1. Introduction

Plastics have revolutionized the modern world since the beginning of their large-scale production [1,2]. This remarkable material is used in thousands of applications due to its unique characteristics, i.e., light weight, flexibility, durability, and cost-effectiveness [3]. In 1833, the French chemist Henri Braconnot synthesized the first semi-synthetic plastic called xyloidine by treating plant-based materials, such as sawdust, starch, and cotton, with nitric acid. A few years later, Christian Friedrich Schönbein synthesized another cellulose derivative, *pyroxylin*, by treating cellulose (cotton) with a mixture of sulfuric and nitric acid, and it is commonly known as guncotton. The history of flexible plastics formally began in 1862, when Alexander Parkes introduced *Parkesine*, followed by the synthesis of *celluloid* by John Wesley Hyatt in 1870 [1]. In 1872, Baumann first developed polyvinyl chloride (PVC) by exposing tubes filled with vinyl chloride to sunlight [4]. Later, PVC showed some drawbacks, such as cracking and brittleness, when exposed to heat and light. In 1926, further research by Walter Semon led to plasticized PVC [5]. Growing research efforts and rising demand for plastic materials ultimately led to the production of the first fully synthetic plastic

 doi:10.20944/preprints202601.1587.v1

(Bakelite) by Leo Baekeland in 1907. Dr. Baekeland's invention marked the beginning of the "Age of Plastics," and he was the first to coin the term plastic [6].

In the following years, various forms of synthetic plastics, including high-density polyethylene, polyethylene terephthalate, acrylic, low-density polyethylene, polypropylene, and Styrofoam, were synthesized by different researchers, as shown in Figure 1. Plastic production expanded rapidly after World War II, fueled by industrial growth, and has now surpassed 400 million tons annually. Remarkably, half of all plastics ever produced have been manufactured in the past 15 years [7]. Global plastic production is projected to reach between 902 to 1124 million tons by 2050, two to three times higher than current levels [3,8,9]. The complete history timeline of plastic upgradation over the years is summarized in Figure 1.

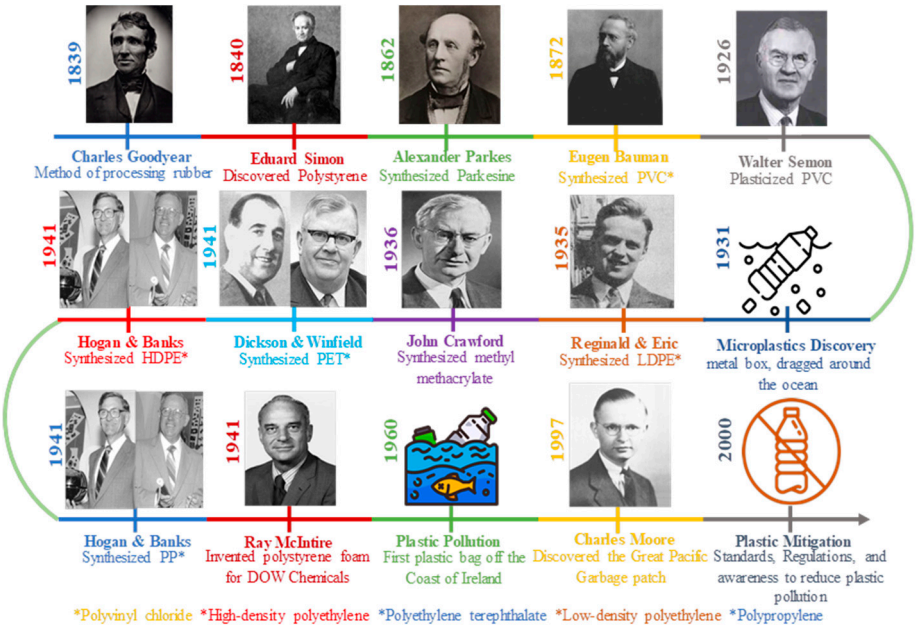

Figure 1. Timeline of plastic production and plastic pollution.

Conventional plastics are derived from petroleum-based products and are highly resistant to natural degradation. Due to their hydrocarbon nature, these materials retain their physicochemical properties even after remolding and thermal processing [10]. When subjected to incomplete degradation, plastics fragment into micro- and nanoscale particles that can easily infiltrate soil and aquatic environments [11]. Since the first documented scientific study on beach debris by Herms in 1907 [12]. Plastic waste has increasingly accumulated in marine and coastal regions worldwide [13]. The earliest recorded evidence of plastic pollution dates back to the Irish coast between 1960 and 1970 [14]. Since then, extensive research has been conducted to understand the fate, transport, and mitigation of plastics in both aquatic and terrestrial ecosystems. As shown in Figure 2, globally, about 34 million tons of plastic are produced each year, of which only about 7% is recycled [15], while the remaining 93% ends up in landfills or marine environments [16,17], leading to heavy economic loss of about 80 to 100 billion USD each year [18]. In the US, the government spends about 8.3 billion US dollars yearly to dispose of plastic waste in landfills [19]. Although plastics have wide usage, they pose a significant risk to human health and water ecosystems [20]. In addition, the production of plastics accounts for almost 13 percent of the world's carbon budget, and it also contributes significantly to fossil fuel use and the emission of greenhouse gases [21]. Together with the exhaustion of fossil resources, climate change, and health-related issues, these environmental and economic problems have triggered an international shift to more sustainable solutions [22]. This has led to the focus of research on renewable natural polymers, which are environmentally benign as feedstocks to produce bioplastics and other sustainable materials.

 doi:10.20944/preprints202601.1587.v1

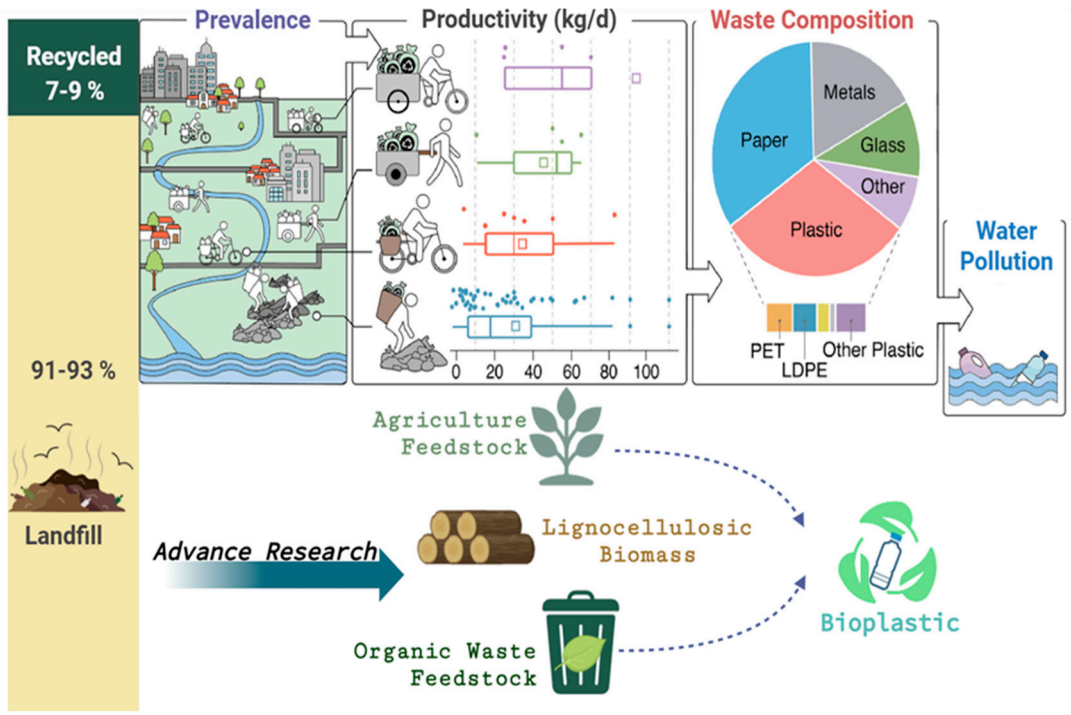

Figure 2. Plastic waste quantification and sources for bioplastics production. Figure were adapted with permission from the reference [23]. Copyright 2024, Elsevier.

Bioplastics are also a promising substitute to the petroleum-based plastics since they are made using natural materials that are sustainable, biodegradable, and have less greenhouse gas emissions throughout their life cycle [24]. In recent years, researchers have shifted their attention to the use of natural, sustainable feedstocks in the form of agricultural residues, lignocellulosic biomass, and organic wastes as raw materials to produce sustainable plastics [25]. The global research trend on sustainable bioplastics between 2000 and 2025 was extracted from the CAS SciFinder and Scopus databases, as shown in Figure 3. One can observe a sharp increase in publications after 2020, indicating growing scientific and industrial interest in environmentally friendly materials. The major area of research is on bioplastics, biodegradable materials, biomass refinery, packaging materials, and biodegradability, and to a large extent, it is the disciplines of environmental science, engineering, and materials science that have contributed to this. To align with the Sustainable Development Goals on responsible consumption and climate action, sustainable resources are being explored for the sustainable production of plastics to comply with environmental regulations.

Bioplastics are generally produced from biomass such as polysaccharides (cellulose, chitosan, alginate, and gelatin), proteins, and fats [26,27]. Lignocellulosic biomass, a renewable material, is abundantly available, with an estimated 130 billion tons of biomass produced each year globally, providing a low-cost and sustainable raw material [28]. However, fractionation of lignocellulosic biomass into cellulose and hemicellulose, which are tightly bound together by lignin, requires pretreatment, which often involves excessive use of harsh chemicals (organosolv, acid, alkaline, and supercritical CO_2) and harsh reaction conditions (high temperature and pressure) [29-31]. Abolore et al. and Sharma et al. critically reviewed green pretreatment methods that operate under mild reaction conditions, require minimal solvent use, and achieve high delignification efficiency [29,30]. Green solvents such as ionic liquids (ILs), deep eutectic solvents (DESs), and low-transition-temperature mixtures (LTTMs) are regarded as reliable alternatives to conventional solvents [31]. Their applications in cellulose modification, carbohydrate conversion, and lignin extraction have been comprehensively reviewed by Tang et al., Stalewal et al., Chen and Mu, and Ullah et al. [32-35]. Storz and Vorlop critically review the production of common bioplastics and discuss strengths, obstacles, and key trade-offs [36].

 doi:10.20944/preprints202601.1587.v1

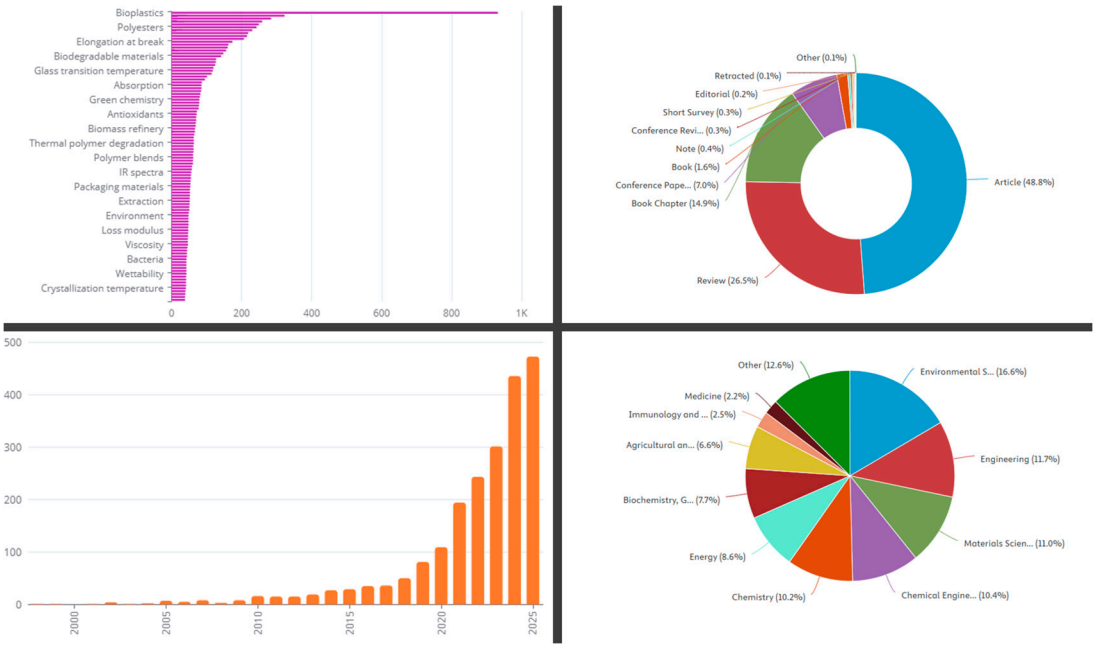

Figure 3. SciFinder (left) and Scopus (right) database summary of research trends for sustainable bioplastics.

2,5-furandicarboxylic acid (FDCA) is one of the substances produced from lignocellulosic biomass, which can be used as a monomer for polyester, polyurethane, and polyamide production [37-43]. Ethylene glycol can be copolymerized with FDCA to produce polyethylene furanoate (PEF), which is a promising bio-based alternative to polyethylene terephthalate (PET), a petroleum-derived polymer [43-46]. Two-step conversion is required for converting biomass-derived cellulose into FDCA, cellulose dehydration to 5-hydroxymethylfurfural (HMF), followed by oxidation to FDCA [43,47-49].

With the ongoing research efforts, bioplastics are replacing conventional plastics in developed countries. The most common types of bio-based biodegradable plastics, i.e., polylactic acid (PLA), polybutylene succinate (PBS), polyhydroxyalkanoates (PHA), polybutylene adipate terephthalate (PBAT), and thermoplastic starch (TPS) [50] accounted for approximately 40% of the global bioplastics market in 2020, and this share is projected to increase to about 70% by 2026. The total bioplastic production capacity is expected to reach 7.6 million tons by 2026. While the production of starch-based blends is projected to decline by 72.3%, the production of other biodegradable bioplastics such as PBAT, PBS, and PHA is expected to increase by 500%, 226.5%, and 166.7%, respectively, as shown in Figure 4 [26,51-53].

This review critically explains the sustainable conversion of lignocellulosic biomass components cellulose, hemicellulose, and lignin into bioplastics, along with the associated processing challenges. In the first section, different solvents used for the pretreatment of biomass are critically analyzed, followed by a detailed discussion on pretreatment strategies. In the subsequent section, conversion pathways from sugar monomers to bioplastics precursors are discussed. Furthermore, platforms for sustainable polymerization of bioplastics are discussed. At the end, we discussed sustainability considerations in terms of waste reduction, green solvents usage, and renewable resources, and creating eco-friendly production techniques by incorporating life cycle analysis.

 doi:10.20944/preprints202601.1587.v1

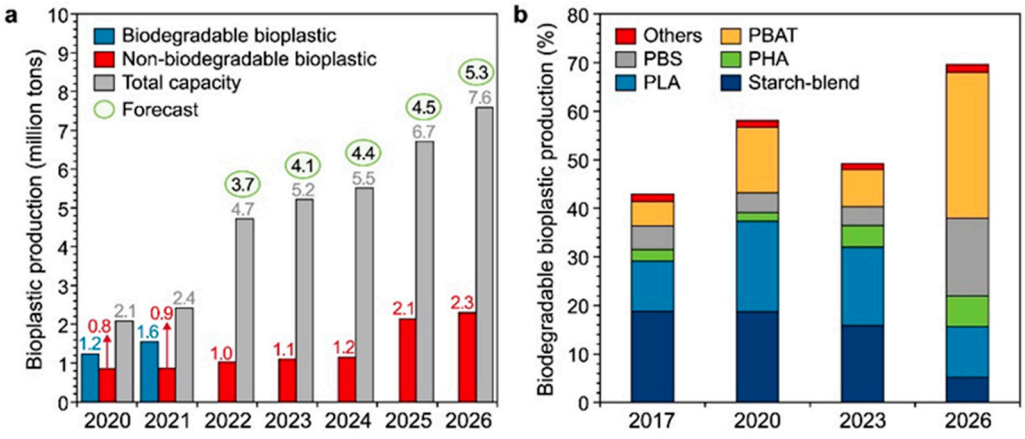

Figure 4. Forecast of global bioplastic production by 2026. Figure was adapted with permission from the reference [26]. Copyright 2023, Elsevier.

2. Lignocellulosic Biomass: Composition and Pretreatment Strategies

Lignocellulosic biomass (LCB) is the most abundant renewable resource on Earth, primarily composed of cellulose (50%), hemicellulose (25%), and lignin (15-35%), along with minor components such as pectin, resins, waxes, ash, and minerals [54]. These polymers form a complex 3D matrix where cellulose is embedded in a lignin-hemicellulose network. LCB varies by plant species, growth stage, and environment. Major sources include crop and forest residues, energy crops, waste, manure, pulp sludge, and forestry by-products [55]. Globally, LCB production is estimated at 10-50 billion tons annually, offering a sustainable, carbon-neutral alternative to fossil fuels for bioenergy and products [56].

Cellulose is the most abundant biopolymer on Earth, with an annual production of approximately 7.5×10^{10} tons [57]. It is a linear polysaccharide consisting of β-1,4-linked D-glucose units (Figure 5) with the general formula $(C_6H_{10}O_5)_n$ and a degree of polymerization ranging from 8000 to 10,000, depending on the biomass source [58]. In contrast, hemicellulose is an amorphous, branched heteropolymer composed of various sugar monomers, including pentoses (such as xylose and arabinose), hexoses (such as mannose, glucose, and galactose) and sugar acids. Its degree of polymerization is significantly lower than cellulose, typically ranging from 100 to 200, resulting in lower crystallinity and greater susceptibility to hydrolysis [59]. Lignin is the third major component, a complex, amorphous, and hydrophobic aromatic polymer that provides structural rigidity, impermeability, and resistance to microbial degradation [60]. It is synthesized through radical coupling of three primary monolignols: *p*-coumaryl, coniferyl, and sinapyl alcohol, which correspond to *p*-hydroxyphenyl (H), guaiacyl (G), and syringyl (S) units, respectively as shown in Figure 5.

LCB is a promising renewable feedstock for sustainable bioplastics due to its abundance, renewability, and non-food competition. Composed mainly of cellulose, hemicellulose, and lignin, it makes up 50-75% of plant dry mass and is versatile for producing bio-based monomers and polymers [61]. These polysaccharides can be converted into fermentable sugars and bioplastic precursors like lactic acid, succinic acid, HMF, and other chemicals used to synthesize PLA, PHAs, and PEF [62]. Valorizing lignocellulosic residues benefits the environment by reducing petrochemical plastics and waste. Demand for bio-based polymers is rising, with lignocellulosic-derived monomers expected to replace over 30% of fossil plastics in decades. Efficient fractionation and conversion technologies are needed to isolate key components: cellulose for glucose polymers, hemicellulose for pentose derivatives, and lignin for aromatic biopolymers. Thus, lignocellulosic biomass is vital for the circular bioeconomy, advancing renewable, low-carbon, biodegradable plastics [25].

 doi:10.20944/preprints202601.1587.v1

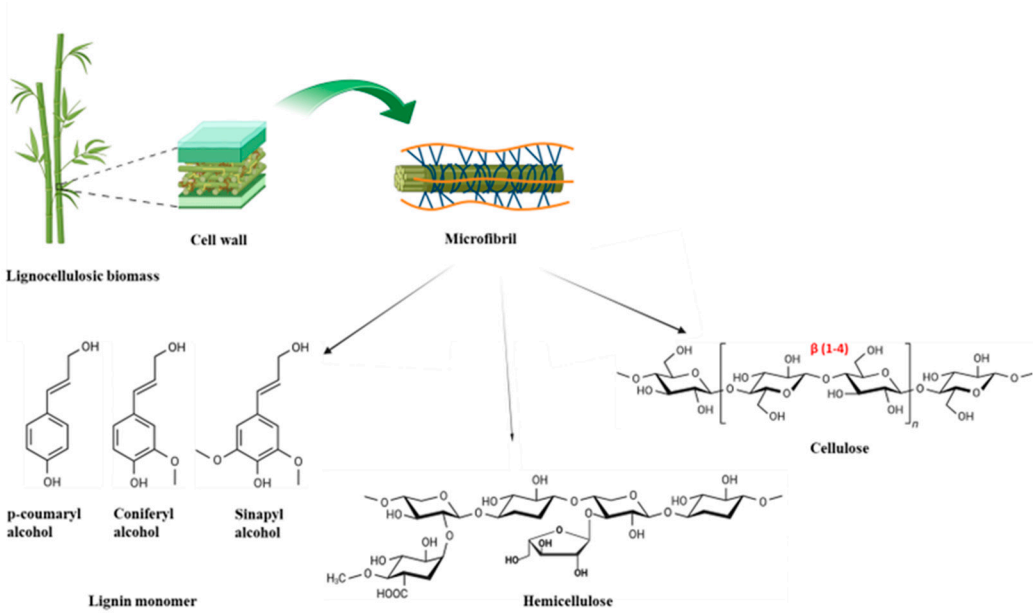

Figure 5. Structure of Cellulose, Hemicellulose and Lignin monomers in lignocellulosic biomass.

Lignocellulosic biomass pretreatment methods are classified into physical, chemical, physicochemical, and biological approaches, each targeting the disruption of cellulose-hemicellulose-lignin linkages to improve hydrolysis [63]. Physical methods like chipping, grinding, and milling reduce particle size, increase surface area, but are energy-intensive and often costly at scale [64]. Chemical methods use acids, alkalis, oxidizers, or solvents to solubilize hemicellulose and disrupt lignin, exposing cellulose; they are fast but can produce inhibitors and require costly recovery [65]. Physicochemical techniques such as steam explosion, liquid hot water, AFEX, and CO_2 explosion combine mechanical and chemical effects for delignification and hemicellulose solubilization, offering cost-effective, scalable solutions. Biological pretreatments employ fungi and bacteria to degrade lignin and hemicellulose under eco-friendly conditions with low energy, though they are slow. Each method has benefits and limitations depending on the biomass and desired product. Physical and chemical methods enable rapid biomass disruption, while biological and hybrid methods are greener, lower-energy alternatives. Optimizing pretreatment selection and operational conditions remains a critical step toward efficient biorefinery operations and sustainable bioplastic production from lignocellulosic feedstocks [66]. Table 1 summarizes the pros and cons of different pretreatment techniques for lignocellulosic biomass.

Table 1. Advantages and disadvantages of different pretreatment methods of lignocellulosic biomass.

Pretreatment Methods	Advantages	Disadvantages	Ref.
Acidic	Hydrolyzed hemicellulose sugars alter lignin structure	Corrosion of equipment, formation of degradation products, High cost, neutralization required	[67]
Alkaline	Cause cellulose swelling, disrupt lignin structure, increase surface area, remove lignin and hemicellulose	A long time and a high concentration of base are required for salt formation, which is not easily removed	[68]
Oxidative	Oxidize lignin, low inhibitors formation,	Soluble aromatic compounds formation due to the oxidation of lignin	[69]

 doi:10.20944/preprints202601.1587.v1

	decrease cellulose crystallinity		
Ozonolysis	Eco-friendly, no waste generation, mild operating conditions	Expensive, a large amount of ozone is required	[69]
Organosolv	Sulfur-free lignin yield, easily recovered by distillation	An extremely controlled environment is required. Solvent acts as an inhibitor	[70]
Ionic Liquid	High efficiency, disrupts cellulose structure, environmentally friendly	High cost, lignin condensation, recovery challenge	[71]
Steam Explosion	Low chemical usage, effectively hydrolyzed hemicellulose, and cost-effective	Inhibitor formation at high temperature, no lignin removal	[72]
Liquid Hot Water	Environment-friendly, high pentose recovery, minimal corrosion	Inhibitor formation at high temperature	[73]
AFEX	Increase accessible area, avoid inhibitor production	Not efficient with high lignin biomass, High cost of ammonia	[74]
Ultrasound	Disrupt lignin-cellulose-hemicellulose matrix, reduced reaction time, and no inhibitor production	High Energy consumption, scalability challenge	[75]
Mechanical	Decrease cellulose crystallinity	High power consumption, Difficult to scaling up.	[76]
Biological	Low energy required, degrade hemicellulose and lignin	Hydrolysis rate is slow	[67]

3. Green Catalytic Conversion Pathways for Bioplastic Precursors

Catalytic valorization of lignocellulosic biomass into bioplastic precursors is a key sustainable pathway. Renewable biomass intermediates are transformed into platform chemicals used as monomers for bioplastics like polylactic acid (PLA) and polyethylene furanoate (PEF). Lignocellulosic feedstocks, mainly cellulose, hemicellulose, and lignin are broken down into fermentable sugars such as glucose, xylose, and fructose. These carbohydrates are crucial for catalytic reactions that produce monomers with high selectivity, efficiency, and a lower ecological footprint.

3.1. Synthetic Pathway for FDCA Production

The goal of eco-friendly FDCA synthesis is to oxidize HMF under mild, sustainable conditions that reduce energy use, avoid harmful reagents, and generate less waste. HMF, a key platform chemical from lignocellulosic biomass, is usually made via acid dehydration of monosaccharides like fructose or directly from glucose [77,78]. Due to its multifunctional nature, HMF acts as a valuable precursor for producing high-value chemicals and polymer building blocks. Among these, FDCA stands out as one of the top twelve biomass-derived platform chemicals and is a key monomer used in making polyethylene furanoate (PEF) [79,80]. The catalytic oxidation of HMF to FDCA proceeds through successive transformations of its alcohol and aldehyde functionalities, with the dominant

 doi:10.20944/preprints202601.1587.v1

reaction pathway largely dictated by the catalyst composition and reaction environment. As illustrated in Figure 6, two principal and competing mechanisms are typically observed. In the first route, the aldehyde group is oxidized first to produce 5-hydroxymethyl-2-furancarboxylic acid (HMFCA). This intermediate undergoes further oxidation of the hydroxyl group to form FFCA. In the alternative route, the hydroxyl group, yielding 2,5-furandicarbaldehyde (DFF); subsequent oxidation of the aldehyde function forms 5-formyl-2-furancarboxylic acid (FFCA), which is then transformed into FDCA [81,82]. Overall, HMF can be oxidized to FDCA using metal-based catalytic systems via aerobic, electrochemical, or photocatalytic approaches.

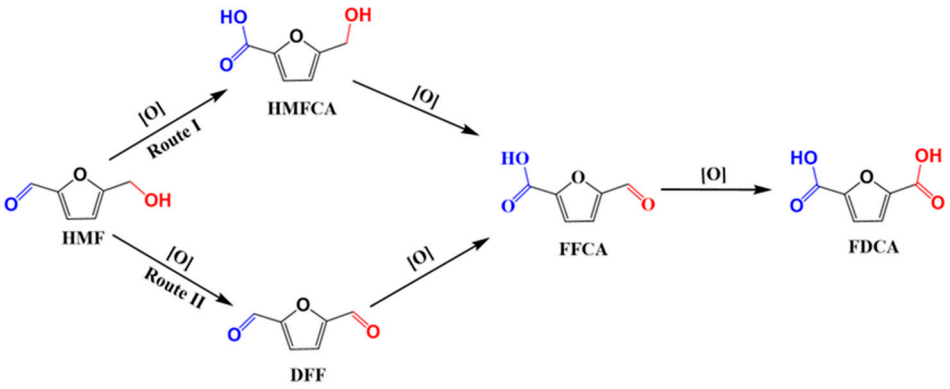

Figure 6. Schematic pathways for catalytic oxidation of HMF to FDCA.

3.1.1. Metal Catalyst for Oxidation of HMF to FDCA

The Mars-van Krevelen mechanism underscores the critical role of a catalyst's redox properties in governing HMF oxidation pathways [83]. Transition metals like Co, Mn, Cu,

Ni, and Fe are frequently utilized because of their accessible redox couples (Co^{3+}/Co^{2+}, $Mn^{4+}/Mn^{3+}/Mn^{2+}$, Cu^{1+}/Cu^{2+}, Ni^{4+}/Ni^{2+}, and Fe^{2+}/Fe^{3+}). Although noble metals, including Au, Pt, and Ru, exhibit high catalytic performance for FDCA synthesis, their high cost, environmental concerns, and challenging recovery procedures have shifted research interest toward more sustainable and economical non-noble metal catalysts, as summarized in Table 2 and Figure 7.

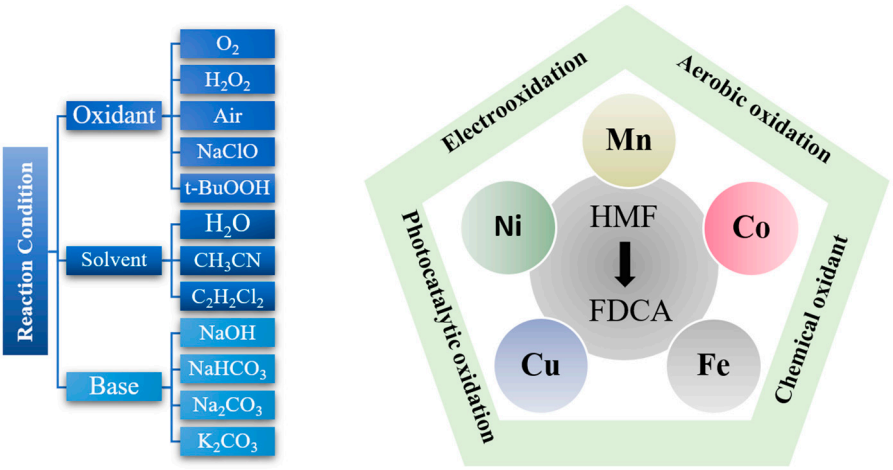

Figure 7. Reaction conditions using a single non-noble metal for the catalytic oxidation conversion of HMF to FDCA.

Numerous studies show that manganese-based catalysts exhibit excellent performance in HMF oxidation. The proposed aerobic metal-catalyzed oxidation mechanism of HMF to FDCA is illustrated in Figure 8. Beibei Liu et al. [84] described the preparation of MnO_2 nanorods via

 doi:10.20944/preprints202601.1587.v1

hydrothermal methods, which acted as efficient catalysts to the $NaHCO_3$-mediated oxidation of HMF, delivering 97.8% conversion to FDCA and maintaining performance at gram-scale reactions. Similarly, Hayashi et al. [85] conducted a comparative study of MnO_2 polymorphs and revealed that catalytic activity is strongly dependent on crystal structure. Among six examined phases (β-, α-, γ-, δ-, ε-, and λ-MnO_2), the β-phase, characterized by the lowest vacancy-formation energy, exhibited the highest activity at 100°C under an oxygen pressure of 10 bar for 24 hours, achieving a 91% FDCA yield when its surface area was enhanced. Bao et al. [86] developed porous two-dimensional Mn_2O_3 nanoflakes via high-temperature calcination of a Mn-based metal-organic framework (Mn-TPA). This catalyst enabled nearly quantitative conversion of HMF to FDCA over 24 h and retained catalytic stability over five successive cycles. However, despite their excellent FDCA yields, the relatively low productivity of manganese oxides remains a barrier to large-scale implementation. Consistent with these findings. Yao et al. [87] reported that β-MnO_2, owing to its minimal vacancy-formation energy and optimal FFCA adsorption characteristics, possesses the most reactive lattice oxygen, thereby promoting efficient FDCA formation.

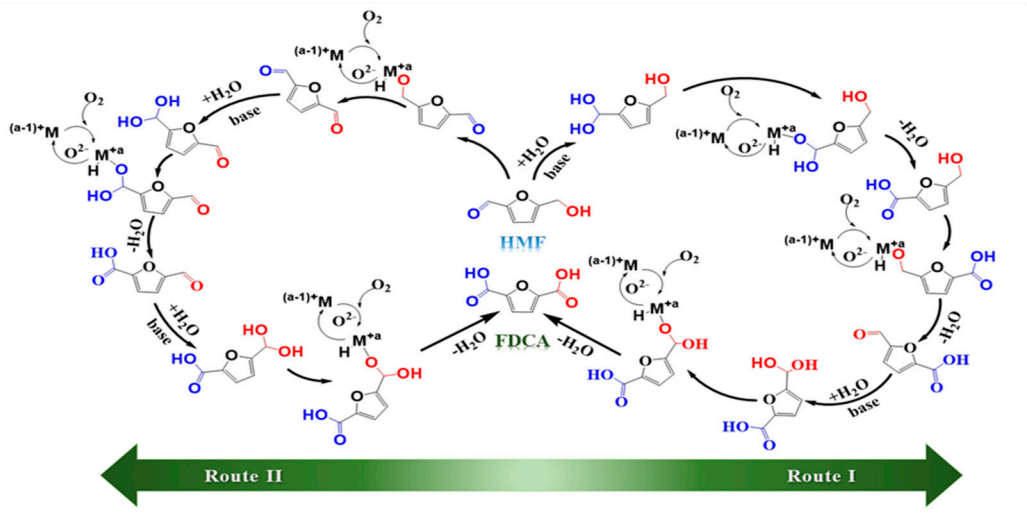

Figure 8. Mechanistic insights into the aerobic metal-catalyzed conversion of HMF to FDCA.

Liao et al. [88] introduced an environmentally benign and straightforward method to enhance the performance of MnO_2 catalysts by treating them with dilute nitric acid, producing the modified catalyst α-MnO_2-H^+. Their comparative evaluation showed that the acid treatment removed amorphous or poorly crystalline surface nanoparticles, increased the surface oxidation (OA) ratio, and markedly improved catalytic activity. Among the tested materials, α-MnO_2-H^+ delivered the highest efficiency, achieving 98.5% FDCA yield and over 99.9% HMF conversion under relatively moderate reaction conditions. The catalyst further demonstrated strong durability, retaining its activity across five consecutive reaction cycles.

Table 2. HMF oxidation over different metals.

Catalyst	Reaction Condition	Base	FDCA Yield %	HMF Con. %	Ref.
α-MnO_2-H^+	20 bar O_2, 120°C, 8 h	$NaHCO_3$	98.5 [d]	99.9	[88]
nanorods (MnO_2-R)	5 bar O_2, 110°C, 12 h	$NaHCO_3$	96.7 [d]	100	[84]
2 D Mn_2O_3 nanoflakes	14 bar O_2, 110°C, 24 h	$NaHCO_3$	99.5 [d]	100	[86]
La-MnO_2	5 bar O_2, 140°C, 4 h	NH_4OH	95.4 [d]	100	[89]
$Mn_6Ce_1O_x$	10 bar O_2, 120°C, 8 h	$KHCO_3$	97.2 [d]	99.4	[90]
Co@NC-a	2 bar O_2, 65°C, 16 h	Na_2CO_3	73.1 [f]	100	[91]
Co-NC	6 bar O_2, 130°C, 20 h	K_2CO_3	98 [a d]	99.9	[92]

 doi:10.20944/preprints202601.1587.v1

Co(II)–meso-tetra(4-pyridyl)-porphyrin	t-BuOOH, 100°C, 24 h	Free	60.3 [e]	95.6	[93]
Co@KIT-6	1 bar Air, 130°C, 20 h	Free	99 [d]	100	[94]
hexagon $MnCo_2O_4$	10 bar O_2, 130°C, 20 h	$KHCO_3$	70.9 [d]	99.5	[95]
CoMn-NC	t-BuOOH, 80°C, 12 h	Free MeCN [b]	95 [e]	99	[96]
Mn-Co	20 bar Air, 130°C, 8 h	$NaHCO_3$	98.7 [d]	100	[97]
Co-Mn-0.25	10 bar O_2, 120°C, 5 h	$NaHCO_3$	95 [d]	99	[98]
Co/Mn/Br	30 bar (molar CO_2/O_2 = 1), 100°C, 24 h	Free CH_3COOH [c]	90 [e]	99	[99]
$Li_2CoMn_3O_8$	55 bar O_2, 130°C, 8 h	Free CH_3COOH [c]	80 [d]	100	[100]
C-Fe_3O_4-Pd	30 mL/min O_2, 80°C, 4 h	K_2CO_3	91.8 [d]	98.2	[101]
Pt@$Fe_{1.7}Cr_{0.3}O_3$	1 bar O_2, 120°C, 12 h	Free	78.7 [d]	100	[102]
FeP-Co_0.2/NC	10 bar O_2, 150°C, 24 h	Na_2CO_3	91.6 [d]	100	[103]
Co_xFe_y@NC	5 bar O_2, 100°C, 7 h	$NaHCO_3$	91.1 [d]	100	[104]
MIL-100(Fe)	BuOOH, 100°C, 24 h	Free TEMPO [d]	74 [e]	100	[105]
$Fe_{0.6}Zr_{0.4}O_2$	20 bar O_2, 160°C, 24 h	Free [Bmim]Cl [b]	60.6 [d]	99.7	[106]
SBA-NH_2-VO^{2+}	O_2 rate of 20 mL/min, 110°C, 12 h	Free 4-chlorotoluene [b]	62.7 [d]	98.8	[107]
K-10 clay-Mo	O_2 rate of 20 mL/min, 110°C, 12 h	Free Toluene [b]	100 [d]	86.9	[108]
γ-Fe_2O_3@HAP-Mo	O_2 rate of 20 mL/min, 110°C, 12 h	Free Trifluorotoluene [b]	30.8 [d]	67.5	[109]
Mo_8O_{26}	H_2O_2, 100°C, 2 h	NaOH	100 [a d]	99.5	[110]
Ni foam modified (Ni_xB)	30 min	KOH	98.5 [f]	100	[111]
Ni_3S_2-MoS_2/NF	2 h	KOH	97 [f]	100	[112]
Au/TiO_2	VIS-LED, 40°C, 2h	NaOH	97 [g]	100	[113]
CoPz–g-C_3N_4	UV, RT. air flow at 20 mL, 14 h	pH = 9.18	96.1 [g]	99.6	[114]

[a] Selectivity, [b] Solvent, [c] Acid, [d] Aerobic, [e] chemical oxidant, [f] Electrooxidation, [g] Photocatalytic oxidation.

Mn-based bimetallic catalysts have demonstrated remarkable efficiency in HMF oxidation. For example, a MnOx-CeO_2 composite exhibited outstanding catalytic activity [115]. Compared with monometallic MnO_2, the synergistic interaction between Ce^{3+} and Mn^{4+} enhanced performance Mn^{4+} ions acted as the primary active sites, while lattice oxygen transfer from CeO_2 to MnOx promoted oxidation under mild conditions. Under optimized parameters, the MnOx-CeO_2 catalyst (Mn/Ce = 6) achieved a 91% FDCA yield and maintained stability over five successive reaction cycles without noticeable deactivation. Liu et al. [90] investigated the impact of various doping metals on the activation of lattice oxygen (OL) in Mn-based oxides, which demonstrates that Ce-doped MnOx (Mn_6Ce_1Ox) is highly effective for aerobic HMF oxidation to FDCA, achieving 97.2% yield and high formation rates under mild conditions with stable reusability. Ce doping creates asymmetric Mn-O-Ce sites, enhancing lattice oxygen mobility and the formation of oxygen vacancies, which act as active species in the Mars-van Krevelen mechanism. Other dopants (Zr, La, Sm) showed weaker or negative

 doi:10.20944/preprints202601.1587.v1

effects. A range of magnetic ferrite catalysts, including $CuFe_2O_4$, $CoFe_2O_4$, $MnFe_2O_4$, $MgFe_2O_4$, and Fe_3O_4, have also been investigated for HMF oxidation [116]. Among the evaluated ferrite catalysts, $MnFe_2O_4$ showed the highest catalytic efficiency, reaching an 85% yield of FDCA under a base-free environment when TBHP was employed as the oxidant. The enhanced performance was ascribed to the flexible redox behavior of Mn and the cooperative interaction between Mn species and the Fe_2O_4 framework. Additionally, the magnetic characteristics of $MnFe_2O_4$ enabled straightforward separation and allowed reuse for up to 4 reaction cycles without noticeable loss of catalytic performance. In a related investigation, Neatu et al. [117] developed a $Mn_{0.75}/Fe_{0.25}$ composite catalyst for the one-pot oxidation conversion of HMF to FDCA. During the initial reaction stage, only 9% FDCA was obtained, with FFCA (69%) forming as the predominant intermediate. Interestingly, in the absence of a catalyst, using eight equivalents of NaOH under 8 bar oxygen pressure, an 87% FFCA yield was achieved in just 30 minutes. Subsequent steps consisting of acidification, filtration, and catalytic oxidation of the isolated FFCA using $Mn_{0.75}Fe_{0.25}$ under optimized conditions consisting of 0.05 g catalyst, 2 mmol NaOH, 8 bar O_2, 90°C, and a reaction time of 24 h led to approximately 90% FDCA yield. In addition to manganese oxides, several other non-noble metal catalysts, including those based on cobalt, copper, iron, and molybdenum, are also extensively employed for the catalytic oxidation reaction of HMF. Gao et al. [91] prepared a Co-loaded activated carbon catalyst, Co@NC, which was subsequently graphitized, yielding an impressive 81.8% FDCA yield via electrooxidation. To identify the active sites, they performed acid etching to remove surface Co, revealing Co species originally bonded to the carbon matrix. The resulting catalyst, designated NC-900-a, showed a significant reduction in Co content from 28.2% to 0.71%, as confirmed by ICP analysis. Using the etched catalyst led to a 16% drop in FDCA yield after 12 hours compared to the unetched sample. Interestingly, when the reaction conditions were modified using the same amount of etched catalyst with five times more HMF (50 mM), a lower O_2 pressure, and an extended a reaction duration of 16 hours, leading to the FDCA yield increased to 94%. Li et al. [92] developed a Co-N-C catalyst by heating a Co-based ZIF. The process created well-dispersed cobalt sites strongly bonded with nitrogen. The catalyst shows a high conversion of HMF, 98% yield of FDCA within 3 h. under mild alkaline conditions and keeps its performance steady through repeated use. Co(II) complexes also showed activity; Gao et al. [93] evaluated the catalytic performance of Co(II)-meso-tetra(4-pyridyl)-porphyrin (M-resin-Co-Py for converting HMF to FDCA with tert-butyl hydroperoxide (t-BuOOH) as the oxidant, the catalyst yielded a 96% HMF conversion and a 90% yield of FDCA. Li. et al. [94] embedded ultrafine Co_3O_4 nanoparticles inside mesoporous KIT-6 (Co@KIT-6), reaching 99% FDCA yield within 2 h using air as oxidant and water and solvent. The nanoconfinement effect prevented Co_3O_4 aggregation and leaching, enabling stable activity over six cycles. Cobalt single-atom catalysts also performed well. Co-Mn heterogeneous catalysts have emerged as highly effective systems for HMF oxidation. Zhang et al. [95] examined a hollow-centered $MnCo_3O_4$ catalyst at the nanoscale, synthesized via a thermal method, which achieved full conversion of HMF and a 71% FDCA yield under mild oxygen as oxidant. The improved catalytic efficiency was attributed to increased oxygen mobility, as evidenced by the lowest reduction temperatures observed in H_2-TPR analysis. In a related investigation, Zhang et al. [96] developed a bimetallic CoMn-NC catalyst to oxidize HMF into FDCA. Under optimized conditions, the catalyst reached an outstanding FDCA yield of over 95%, highlighting its high catalytic performance. The porous hierarchical structure of CoMn-NC, along with the stable coordination of Co/Mn to N–C, effectively reduces metal leaching and maintains nanoparticle dispersion during extended cycles. The catalyst's structural stability was further demonstrated by maintaining FDCA selectivity above 90% across five successive cycles, indicating its potential for industrial applications. Li et al. [129] investigated a Mn-doped Co-based bimetallic catalyst with abundant oxygen vacancies ($MnCO_3$-$MnxCo_{3-x}O_4$-Ov) for converting HMF to FDCA via aerobic oxidation. The oxygen-vacancy-rich variant ($MnCO_3$-$MnxCo_{3-x}O_4$-Ov-1.0) showed outstanding activity, yielding a peak of 98.7% of FDCA. Mechanistic analysis suggested that increased oxygen vacancies enhance HMF adsorption and activate O_2, thereby promoting efficient oxidation. Additionally, Rao et al. [98]. Prepared Co-Mn mixed oxides with various Co/Mn

 doi:10.20944/preprints202601.1587.v1

proportions using a solid-state grinding approach. Among the samples, Co-Mn 0.25 achieved 99% conversion of HMF and FDCA yield of 95%. Compared with traditional liquid-state co-precipitation, this greener, more straightforward method yielded approximately 40% higher FDCA, attributed to its higher BET surface area, enhanced mobility of lattice oxygen, and multiple Mn oxidation states. The catalyst also showed excellent stability, maintaining performance over five cycles with minimal Co or Mn leaching, as verified by ICP analysis.

Zuo et al. [99] conducted a semi-continuous investigation on the oxidation of HMF, comparing its performance with the established *p*-xylene oxidation process Figure 9. Under the same conditions (160°C, 60 bar, Co/Mn/Br catalytic system), the oxidation of HMF yielded around 65% FDCA, significantly lower than the 95% yield of TPA obtained from *p*-xylene. This difference was due to the increased reactivity of the furan core and its -CH_2OH and -CHO functionalities compared to the more stable methyl substituents on benzene. By fine-tuning the reaction parameters to minimize secondary reaction such as the esterification of HMF to AcHMF and excessive oxidation to CO_x, the yield of FDCA was increased to ~90% at 180°C and 30 bars (CO_2/O_2 = 1) with 7 vol% added water. Future studies will focus on determining intrinsic kinetic parameters under these optimized conditions to facilitate process development and industrial scaling.

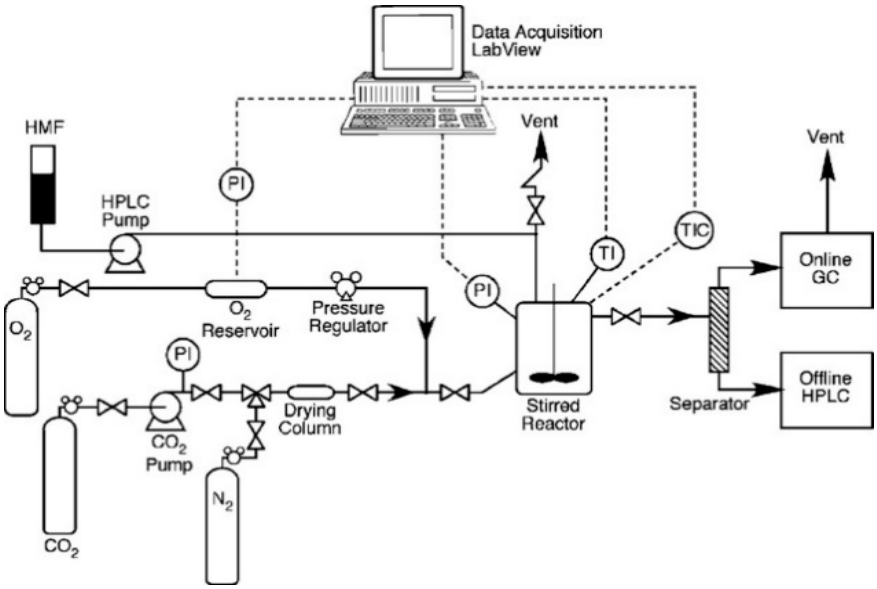

Figure 9. Schematic representation of the semicontiguous oxidation reaction of HMF to FDCA conducted in a Parr reactor setup. Figure was reproduced with permission from the reference [99]. Copyright 2016, American Chemical Society.

Jain et al. [100] reported that synergistic interactions between Co and Mn in the Co/Mn/Br system promote rapid generation of bromo radicals through a three-step redox cycle, enabling efficient completion of the catalytic oxidation pathway. Additional examples include $Li_2CoMn_3O_8$, prepared via pyrolysis with citric acid and urea, which produced an 80% isolated yield of FDCA was obtained in acetic acid with NaBr as a co-catalyst. As an inexpensive and earth-abundant metal, iron (Fe) has been widely employed either as a support or as an alloying component with noble metals in catalytic HMF oxidation. Representative systems include Fe-Pd alloys. Mei et al. [101] investigated a magnetically recoverable palladium supported on graphene oxide catalyst (C-Fe_3O_4-Pd), synthesized through a one-step solvothermal method procedure, for aerobic HMF oxidation. Under optimized conditions (80°C, 4 h, K_2CO_3/HMF = 0.5), this catalyst achieved 98.2% conversion of HMF and 91.8% yield of FDCA. Its magnetic separability enabled easy recovery and reuse without a substantial decrease in activity.

Perumal et al. [102] demonstrated Pt@$Fe_{2-x}Cr_xO_3$ acting as efficient catalyst applicable under base-free aerobic oxidation of HMF under mild conditions. Incorporating chromium into Fe_2O_3

 doi:10.20944/preprints202601.1587.v1

significantly enhanced catalytic activity by tuning surface acidity. The optimized Pt@$Fe_{1.7}Cr_{0.3}O_3$ catalyst delivered almost complete conversion of HMF and 78.7% FDCA yield, surpassing many noble-metal and transition-metal oxide catalysts. It also exhibited excellent durability, retaining over 90% activity after five cycles. Mechanistic studies indicated that improved Pt-support interactions and Cr-induced oxygen vacancies facilitated faster redox cycling and reduced overoxidation, enhancing activity and selectivity. Kalimuthu et al. [103] developed recyclable metal/metal phosphide catalysts supported by nitrogen-doped carbon (NC) via an eco-friendly synthesis approach. Among these, the FeP-$Co_{0.2}$/NC catalyst showed exceptional performance, achieving complete conversion of HMF and 91.6% FDCA yield under optimized conditions. The synergistic contributions of pyridinic nitrogen, Co-Fe alloy phases, and FeP species collectively enhanced catalytic activity and selectivity. Although the system required elevated temperatures and longer reaction times, the study emphasizes the strong potential of non-precious metal catalysts as efficient and sustainable candidates for industrial oxidation of HMF to FDCA. Liu et al. [104] prepared Co_2Fe_1@NC alloy catalysts via a simple solid-state approach and tuning the Co/Fe composition ratio resulted in outstanding HMF oxidation performance. The catalyst achieved 96.1% FDCA yield at 100°C and an oxygen pressure of 0.5 MPa, outperforming monometallic Fe and Co catalysts. It also maintained stability over five recycling cycles. The enhanced activity is attributed to strong Co-Fe interactions, which accelerated HMF oxidation, altered the rate-limiting step, and lowered activation energy barriers. This straightforward, cost-effective synthesis offers a promising strategy for scalable HMF to FDCA conversion. Fe-Co, nano Fe_3O_4-CoO_x, catalyst using base-free achieved a 68% FDCA yield using TBHP as the oxidant. Notably, when nano Fe_3O_4-SiO_2 was functionalized with -SO_3H groups for the two-stage catalytic conversion of fructose to FDCA, a 60% FDCA yield was obtained without any detectable Fe or Co leaching. The cost-effective synthesis, environmental compatibility, and strong catalytic performance make this system a promising candidate for large-scale applications reported by Wang et al. [118].

Under another base-free conditions, Sha et al. [119] achieved a 79% FDCA yield using Fe^{3+}-POP-1 as a catalyst under mild conditions without any base (100°C, 10 h, 10 bar O_2). The large surface area along with abundant Fe active centers of Fe^{3+}-POP-1 were key factors in promoting HMF oxidation. Furthermore, analysis of the recovered catalyst confirmed that the Fe^{3+} oxidation state remained stable after the reaction.

Chamberlain et al. [105] reports the use of MIL-100(Fe), utilized as a reusable catalyst for the oxidative transformation of HMF to FDCA under environmentally friendly conditions. In the presence of TEMPO as a co-catalyst, MIL-100(Fe) achieved complete HMF conversion in 24 h, with a maximum 57% yield of FDCA and 17% FFCA, giving a total selectivity of 74%. mutually enhancing interaction between TEMPO and MIL-100(Fe) was proposed to drive both alcohol and aldehyde oxidations. Unlike many other systems, this reaction uses water as a solvent and mild conditions rather than pure oxygen at high pressures. MIL-100(Fe) offers advantages over enzymes and electrocatalysts due to its ease of preparation, non-toxicity, and robust performance, marking a step toward scalable, green production of FDCA. The cost-effective and environmentally friendly synthesis of this catalyst, combined with its excellent performance, makes it a strong candidate for large-scale applications. Yan et al. [106] significantly advanced the utilization of biomass-derived materials in ionic liquids (ILs). They synthesized a series of Fe-based catalysts (Fe$xZr_{0.41-x}O_2$) for HMF oxidation, identifying $Fe_{0.6}Zr_{0.4}O_2$ as the most effective in [Bmim]Cl. Its small particle size, high surface area, and oxygen vacancies enhanced redox properties, boosting catalytic activity, while the catalyst demonstrated excellent reusability over five cycles.

Cu-based homogeneous catalysts have shown activity to produce DFF [120,121]. In recent studies, Ren et al. [121] employed DFT calculations to investigate adsorption of HMF on CuO (111) and Co_3O_4 (110) surfaces, identifying both as promising catalysts. In the adsorption process, Cu or Co ions interact with the oxygen atoms of HMF in an end-on manner, with the molecule adopting a bridging orientation. The adsorption energy is influenced by the coordination of surface oxygen to hydrogen and possible hydrogen bonding involving HMF's hydroxy and formyl groups.

 doi:10.20944/preprints202601.1587.v1

Experimental validation aligned with the DFT results, as CuO achieved a 99% FDCA yield and Co_3O_4 gave 96% under mild conditions, demonstrating their effectiveness for the oxidation HMF to FDCA.

Mannam et al. [122] described a CuO-based catalytic system for HMF oxidation, using CuCl as the catalyst and tert-butyl hydroperoxide (t-BuOOH) as the oxidant to transform primary alcohols into carboxylic acids in acetonitrile (MeCN) at ambient temperature. In a related study, Hansen et al. [123] employed CuCl with TBHP under mild, base-free conditions, obtaining a 50% FDCA yield in MeCN. The limited conversion was associated with the creation of an FDCA–Cu complex within the system, which impeded further oxidation.

Ventura et al. [124] showed that using O_2 as the oxidant without any added base led to conversion of only 33% of HMF, producing 9% FDCA and 14% FFCA, illustrating the difficulties of base-free oxidation even at elevated temperatures (100°C) or extended reaction times (15 h). In contrast, CuO-CeO_2 produced via high-energy milling (HEM) achieved complete HMF conversion with a 90% FFCA yield under the same conditions. A simple 1:1 physical mixture of CuO and CeO_2, however, gave low conversion 5% of HMF and FFCA yield of 3%, indicating that the superior activity of CuO-CeO_2 results from synergistic interactions rather than simple mixing. Characterization revealed that this improvement arises from an optimal distribution of the acid and base sites present on the surface of CuO-CeO_2.

Liu et al. [107] investigated SBA-NH_2-supported VO^{2+} (vanadyl) and Cu^{2+} (cupric) ions used for the oxidation of HMF, achieving a 29% yield of FDCA. The inclusion of Cu^{2+} facilitated the formation of active V^{5+} species, as Cu^{+} is easily reoxidized to Cu^{2+} by oxygen, maintaining the catalytic cycle. Recycling tests indicated minimal leaching of vanadium or copper, confirming the stable immobilization of VO^{2+} and Cu^{2+} on the SBA-NH_2 support.

Molybdenum-based catalysts are commonly used for HMF oxidation. For example, a Mo(VI) complex supported on montmorillonite K-10 (K-clay-Mo) was optimized regarding the supply of oxygen, solvent, base and temperature, achieving complete conversion of HMF and a 87% yield of HMFCA under optimal conditions (toluene as solvent, oxygen purging, 110°C, 3 h) [108].

The magnetic γ-Fe_2O_3@HAP-Mo catalyst was fine-tuned for recyclability by adjusting the temperature and solvent, resulting in 96% conversion of HMF with product distribution of 20% FDCA, 68% DFF, and 9% HMFCA in 4-chlorotoluene under an oxygen atmosphere [109]. The utilization of aromatic solvents, however, reduced selectivity toward intermediate products, restricting wider application. In a comparative study, ammonium octamolybdate and ammonium decatungstate were tested for HMF oxidation in aqueous H_2O_2. Both catalysts feature single and double epoxy groups, with the two epoxy groups acting as the primary active sites for FDCA production. The tungsten-based catalyst experienced reduced activity due to steric hindrance from the quaternary ammonium, while the molybdenum-based system showed no such limitation, allowing $[EMIM]_4Mo_8O_{26}$ to achieve a 99% FDCA yield [110].

Electrochemical oxidation has recently gained attention as an environmentally friendly method for HMF converting to FDCA, providing significant benefits compared to traditional thermal catalytic approaches [125]. In these systems, electrodes serve as catalysts. Various materials have been investigated for the development of electrocatalysts that facilitate the oxidation of biomass-derived compounds [126].

Zhu et al. [127] synthesized an Au/ZnO photocatalyst via a straightforward deposition-precipitation method for the visible-light-induced conversion of HMF to FDCA. The optimized 2.5% Au/ZnO-DP-H catalyst demonstrated exceptional performance, achieving 96.9% FDCA selectivity (Figure 10 (a)). The improved catalytic performance was ascribed to several factors: The localized surface plasmon resonance (LSPR) of Au improved absorption of visible light and generated hot electron generation; hydrogenation treatment lowered the size of Au particles particle size, strengthened metal support interactions, and introduced oxygen vacancies that promoted efficient charge separation; and the Schottky barrier at the Au-ZnO interface suppressed electron hole recombination. Despite the photocatalyst's renewable and environmentally friendly nature, its instability and high cost limit its industrial application for HMF oxidation to FDCA [128]. In parallel,

 doi:10.20944/preprints202601.1587.v1

Avantium has developed a pilot-scale process for FDCA and plans to scale up to commercial production [126]. A critical challenge for large-scale implementation is the synthesis of HMF, the unstable intermediate required for FDCA production. HMF is typically obtained via acid-catalyzed dehydration of the C6 sugars such as sucrose, fructose, and glucose. Because glucose exhibits lower yield and selectivity compared to fructose, it is commonly isomerized to fructose before dehydration to enhance HMF production efficiency [129].

Among the non-noble metal Nickel-based materials attracted attention has been attracted in recent studies as they are highly effective for HMF oxidation because of their strong activity toward aldehyde and hydroxyl groups. Barwe et al. [111] developed an efficient and cost-effective electrocatalyst for HMF oxidation by modifying high surface area nickel boride (Ni_xB) deposited on Ni foam. Electrolysis conducted under constant potential coupled with HPLC analysis indicated nearly 100% faradaic efficiency and a 98.5% FDCA yield. The oxidation of HMF mainly proceeded through the intermediate 5-hydroxymethyl-2-furancarboxylic acid rather than 2,5-diformylfuran, consistent with product analysis. Additionally, vertically aligned NiSe@NiOx core-shell nanowires grown electrochemically on nickel foam acted as an effective non-precious metal electrocatalyst for HMF electrooxidation to FDCA (Figure 10b). The NiSe@NiOx core-shell architecture provided abundant exposed active sites and improved electron transfer, achieving outstanding performance with 100% FDCA yield and 99% faradaic efficiency.

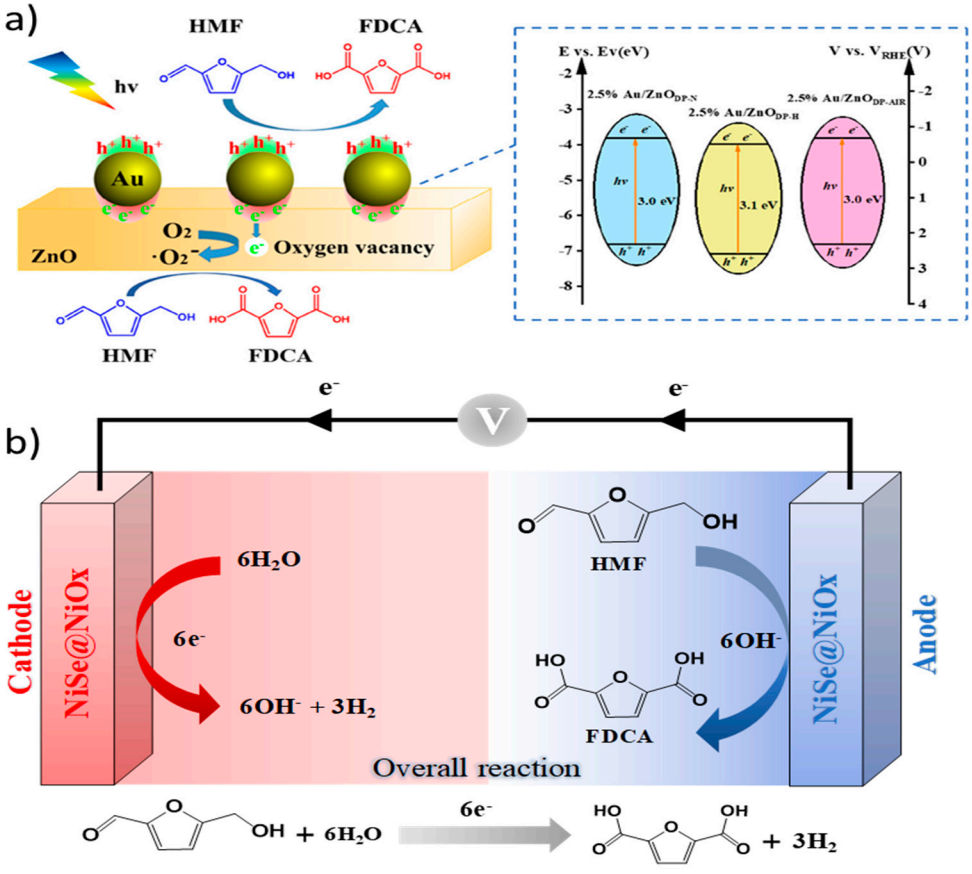

Figure 10. Depiction of *a)* the Visible-light-driven photocatalytic conversion of HMF to FDCA using Au/ZnO". The figure was reproduced with permission from the reference [127]. Copyright 2022, American Chemical Society, *b)* an electrochemical setup enabling concurrent oxidation of HMF and hydrogen evolution, employing a bifunctional NiSe@NiOx core-shell catalyst.

A flower-like Ni_3S_2-MoS_2 nano-heterojunction catalyst was designed via interface engineering. The Ni_3S_2-MoS_2/NF catalyst exhibited excellent electrocatalytic performance toward the hydrogen evolution reaction (HER) and HMF oxidation to produce FDCA, reaching complete conversion of

 doi:10.20944/preprints202601.1587.v1

HMF and a 97% FDCA yield. This remarkable performance is attributed to the high density of exposed active sites, strong interfacial electronic interactions, and the synergistic effect between Ni_3S_2 and MoS_2 [112]. Despite the promise of electrochemical HMF oxidation as a sustainable route for producing value-added chemicals from biomass, substantial carbon loss often occurs because the spontaneous degradation of HMF in basic electrolytes, particularly at higher concentrations, which presents a significant challenge for achieving high efficiency [130].

Photocatalytic methods have attracted attention because of their environmentally friendly nature, mild operating conditions, and ability to harness renewable light energy. When Upon light irradiation, electrons are excited from the valence band to the conduction band, where the valence band drives oxidation reactions and the conduction band enables reductions. Despite this potential, only a few studies have successfully achieved HMF oxidation to FDCA through photocatalysis. Recent findings suggest this singlet oxygen species ($^1O_2$) can catalyze the selective oxidation of HMF to FDCA. While noble metal-based catalysts like Ru and Au has the ability to efficiently produce $^1O_2$ when exposed to visible light, their high cost restricts broader application [131]. Non-noble metal photocatalysts, such as decatungstate (DT), ZnO/polypyrrole (ZnO/PPy), and cobalt thioporphyrazine supported on graphitic carbon nitride (CoPz/g-C_3N_4), have attracted growing research interest, Yang et al. [132] demonstrated that DT under visible light in CH_3CN at room temperature oxidized HMF, yielding 67.1% DFF and 5.8% FDCA in the presence of HBr. DT was found to interact with HBr and HMF, enhancing visible-light absorption and inhibiting HMF polymerization, though FDCA selectivity remained limited. Gonzalez-Casamachin et al. [133] employed ZnO/PPy composites under visible-light irradiation, achieving 30% HMF conversion and 30% FDCA yield, with HMFCA as the primary intermediate and FFCA formation identified as the rate-limiting step. Wang et al. [134] prepared α-Fe_2O_3/$Zn_{0.5}Cd_{0.5}S$ via hydrothermal methods, obtaining excellent activity for converting HMF selectively to DFF or FDCA in aqueous solution. The optimized 15% Fe_2O_3/$Zn_{0.5}Cd_{0.5}S$ catalyst reached 85% FDCA selectivity at 99% HMF conversion. Enhanced activity was attributed to efficient charge separation and reactive oxygen species (ROS) generation via a Z-scheme mechanism, with superoxide radicals ($\bullet O_2^-$) identified as key oxidizing species, demonstrating strong potential for solar-driven selective HMF oxidation.

Xu et al. [114] reported that deposition of CoPz on g-C_3N_4 markedly improved photocatalytic performance. Under alkaline conditions (pH 9.18), the system produced 96% FDCA yield, whereas under mildly acidic conditions, DFF was the predominant product. The study revealed that g-C_3N_4 generates hydroxyl radicals, which lead to CO_2 and H_2 formation, while $^1O_2$ from CoPz selectively oxidizes HMF to FDCA. Strong CoPz-g-C_3N_4 interactions enhanced active site availability, promoted $^1O_2$ generation, and minimized CoPz aggregation, providing an effective non-noble metal photocatalytic approach for transforming biomass-derived compounds into value-added chemicals. Additionally, a noble metal-based Au/TiO_2 catalyst with adjusted calcination allowed the preparation of materials with tunable oxygen vacancy (O_v) concentrations, atmosphere (H_2 or air), to investigate the effect of defects in photocatalytic selective oxidation of HMF. Hydrogen reduction generated abundant O_v sites by removing lattice oxygen, significantly enhancing photocatalytic activity. The O_v-rich Au/TiO_2-H_2 catalyst achieved a remarkable 97% FDCA yield from a concentrated 500 mM HMF solution following 20 hours of visible-light exposure. Mechanistic studies revealed that singlet oxygen ($^1O_2$) is the key oxidizing species for hydroxyl group oxidation, with O_v sites serving dual functions enhancing charge separation as electron traps and promoting O_2 activation to generate reactive intermediates. This work not only clarifies the defect-mediated photocatalytic mechanism but also offers a practical strategy for designing high-performance catalysts for selective photochemical oxidations [113].

3.2. Synthetic Pathway for Lactic Acid Production

Lactic acid (LA) is a widely used and chemically versatile compound, finding applications in industries such as food, cosmetics, pharmaceuticals, chemicals, and packaging [135]. The global need for lactic acid (LA) is expected to reach 130,000–150,000 tons per year. LA is present in two optical

 doi:10.20944/preprints202601.1587.v1

forms: D-(-)-lactic acid (D-LA) and L-(+)-lactic acid (L-LA), as illustrated in Figure 11. Chemical synthesis typically produces a racemic mixture containing both isomers, but the pure forms are more valuable due to their enhanced properties. For example, Lactic acid (LA) represents a vital building block for polylactic acid (PLA); nevertheless, employing a racemic mixture of L- and D-forms produces polymers that are largely amorphous and exhibit reduced stability. Conversely, microbial fermentation techniques can yield highly enantiomerically pure LA, as the biosynthetic enzymes display pronounced stereospecificity [136].

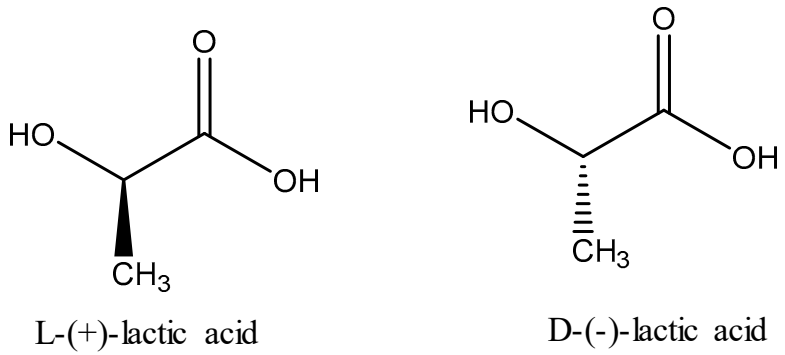

Figure 11. Chemical structures of the two optical isomers of lactic acid.

Crop residues are among the most significant renewable resources, accounting for about 3.5 billion tons each year. Feedstock selection for lactic acid production depends mainly on cost, supply, and carbohydrate quality [137]. Lignocellulosic biomass found in materials like agricultural residues such as distillers' grains, straw, and garden waste are rich sources of hemicellulose and cellulose. Its structure consists of cellulose molecules organized into microfibrils interconnected through hemicellulose and lignin, forming a dense, compact matrix [138]. Pretreatment is an essential stage in transforming lignocellulose into monosaccharides, as it removes lignin, increases the material's porosity, and exposes cellulose and hemicellulose to enzymatic action, thereby boosting hydrolysis efficiency [139]. Significant research has been devoted to pretreating cellulose-rich biomass wastes prior to lactic acid (LA) fermentation. For example, novel pretreatment strategies combining microwave-alkali and steam-alkali methods have been employed to enhance LA production from vinasse [140]. These pretreatments significantly improved LA production.

Various microorganisms have been employed for lactic acid (LA) fermentation, among them, Bacillus coagulans consistently ranks among the top species used, reflecting its widespread application across different studies and time periods. As fermentation technologies have advanced, genetically engineered microbial strains have also gained significant attention for enhancing LA yield, productivity, and stereochemical purity. The specific traits and advantages of these microorganisms used in LA fermentation are summarized in Figure 12.

Lactic acid (LA) bacteria refer to a broad group of microbes able to produce substantial quantities of lactic acid produced from fermentable sugars. These bacteria utilize various carbohydrates, including monosaccharides such as glucose, galactose and fructose, as well as disaccharides (e.g., sucrose, maltose, and lactose) utilized as carbon sources. In homolactic fermentation, more than 80% of the products consist of lactic acid, and common species that perform this process include *Lactococcus lactis*, *Lactobacillus delbrueckii*, *L. casei*, and *L. helveticus*. In contrast, heterolactic fermentation performed by species including *Leuconostoc*, *Lactobacillus*, and *Bifidobacterium*, produces not only lactic acid but also by-products formed, e.g., acetic acid, carbon dioxide, and ethanol [141]. Generally, lactic acid bacteria are anaerobic or microaerophilic in nature. Because of their fast growth rate, efficient reproduction, achieving significant lactic acid yields, and excellent productivity, these bacteria have attracted significant attention for their use in industrial lactic acid production [142].

 doi:10.20944/preprints202601.1587.v1

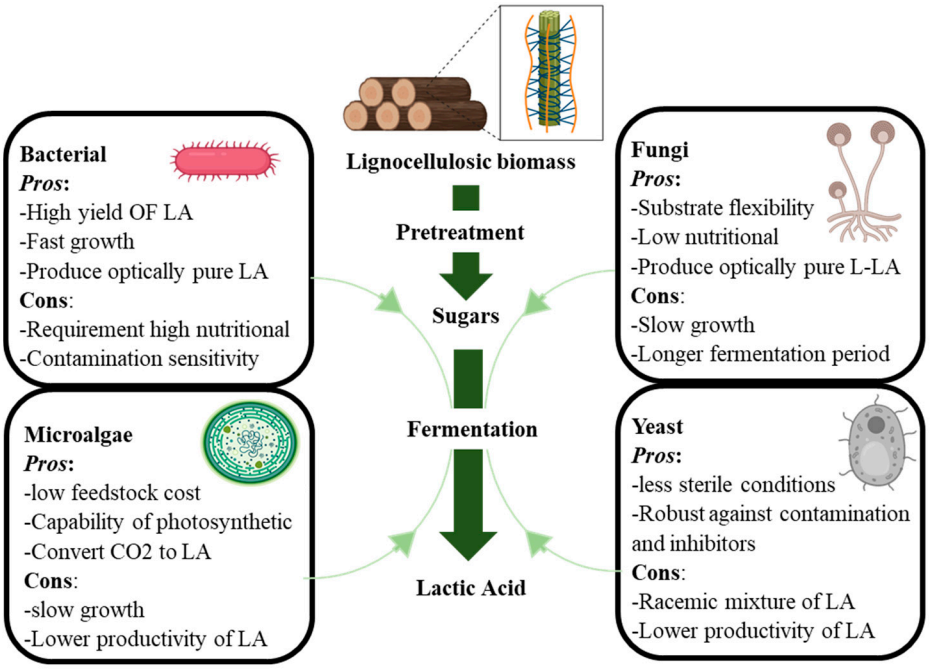

Figure 12. Features of microorganisms commonly utilized in LA production via fermentation.

Oonkhanod et al. [143] pretreated Sugarcane using bagasse in a two-step acid ethanolysis and alkaline peroxide process as depicted in Figure 13, achieving an 87.1% glucose yield. Fermentation with *Lactobacillus casei* produced 21.3 g/L lactic acid after 120 hours (0.63 g/L·h). Lactic acid was efficiently separated using a reduced flux nanofiltration membrane, showing 93.28% glucose exclusion and 82.48 selectivity at 6 bars.

He et al [144]. use an ethanol/H2O–oxalic acid system to demonstrate the separation of corn stover into the three primary components, cellulose, lignin, and hemicellulose (Figure 13). MgO was subsequently used to effectively convert the hemicellulose-derived fraction into lactic acid, resulting in a high yield (79.6 weight percent) and selectivity (90%). With a reusable catalyst and useful solid cellulose and lignin byproducts, the technique enables efficient biomass utilization.

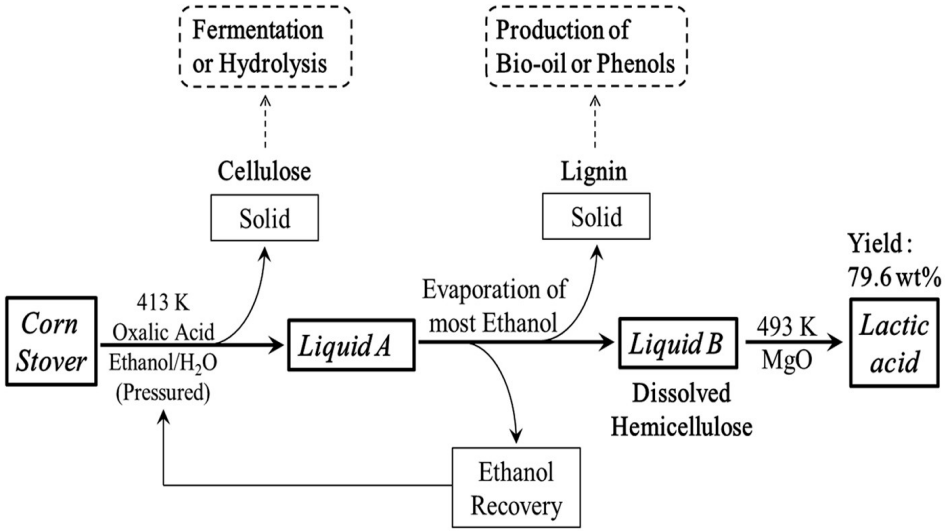

Figure 13. The schematic illustration of the process shows the fractionation of corn stover and its subsequent conversion into lactic acid. The figure was reproduced with permission from reference [144]. Copyright 2016, Springer Nature.

 doi:10.20944/preprints202601.1587.v1

Bacillus coagulans strain 36 is capable of utilizing C5 sugars through the pentose phosphate (PP) pathway, achieving yields of lactic acid as high as to 1.0 $g \cdot g^{-1}$ [145]. To take advantage of its thermophilic nature, open fermentation under non-sterile conditions has been developed as a simple and energy-efficient method for lactic acid production [146,147]. In addition, *Bacillus coagulans* can efficiently convert pentose sugars derived from cellulose hydrolysates into optically pure L-lactic acid. Lactic acid bacteria are also able to metabolize disaccharides such as maltose, sucrose, and lactose as carbon sources. Interestingly, *Lacticaseibacillus rhamnosus* has been reported to directly ferment cellobiose into lactic acid [148], indicating that lignocellulosic hydrolysates rich in cellobiose represent a promising and cost-effective substrate for lactic acid fermentation.

Lactic acid can also be produced by filamentous fungi like Rhizopus oryzae and Rhizopus arrhizus, however their main fermentation product is mostly L-lactic acid. These organisms share similar metabolic pathways. Studies on glucose metabolism in *R. oryzae* have revealed the presence of two independently regulated pyruvate pools: a cytosolic pool, which contributes to the synthesis of ethanol, lactate, oxaloacetate, malate, and fumarate, and a mitochondrial pool, which channels pyruvate into the tricarboxylic acid (TCA) cycle [149]. *Rhizopus* strains have been widely investigated for their ability to produce lactic acid (LA) from diverse renewable feedstocks. Miura et al. [150] utilized Rhizopus sp. MK-96-1196, an L-lactic acid producer, and Acremonium thermophilus ATCC 24622, a cellulase-producing microbe, which were used in a mixed-culture system aimed at boosting L-lactic acid synthesis using untreated raw corncob, Bai et al. [151] achieved about 77.2 $g \cdot L^{-1}$ of L-lactic acid from xylose in corncob employing Rhizopus oryzae strain HZS6. Additionally, R. oryzae has been used to produce lactic acid from a variety of renewable resources, such as waste office paper, wheat straw, xylose, chicken feather protein hydrolysate, sugar beets, and molasses. Huang et al. [152] mentioned 0.85–0.92 $g \cdot g^{-1}$ yields of lactic acid from the wastewater of potato starch using *R. oryzae* and *Rhizopus arrhizus*. Similarly, Zhang et al. [153] achieved lactic acid yield of 88 $g \cdot L^{-1}$ from the starch of potato waste using Acid-resistant precultures of *R. arrhizus* in a reactor with a bubble column. However, some *R. oryzae* strains also produce minor amounts of ethanol and fumaric acid as by-products during fermentation.

Yeasts can grow in highly acidic environments, tolerating as low as 1.5 pH levels, which removes the need for alkali-based pH neutralization during fermentation. Yet, native yeast strains typically produce only limited amounts of lactic acid. To address this, genetic engineering has been applied to enhance lactic acid preparation in yeasts [154,155]. For example, Osawa et al. [156] engineered *Candida boidinii* by disrupting its ethanol fermentation pathway and introducing a bovine LDH gene expressed under control of the PDC1 promoter. Under optimized conditions, a 48-hour batch fermentation produced 85.90 $g \cdot L^{-1}$ of lactic acid, resulting in a productivity of 1.79 $g \cdot L^{-1} \cdot h^{-1}$. Similarly, Wakai et al. [157] modified *Aspergillus oryzae* to produce lactic acid from starch-based substrates. Since *A. oryzae* naturally secretes amylases, the engineered strain LDHΔ871 efficiently converted starch, dextrin, or maltose (each at 100 $g \cdot L^{-1}$) into approximately 30 $g \cdot L^{-1}$ of lactic acid, simplifying the process compared to conventional mixed-culture or enzyme-assisted methods. Zhao et al. engineered an E. coli strain, *E. coli* JH12, by introducing the L-lactate dehydrogenase (LDH) gene derived from *Pediococcus acidilactici*. When fermenting 6% xylose as the sole carbon source, this strain generated 34.73 $g \cdot L^{-1}$ of lactic acid with 98% purity [158]. Although genetically modified *E. coli* strains offer shorter fermentation cycles than traditional lactic acid bacteria, conventional strains generally outperform them with respect to yield, productivity, and tolerance to lactic acid.

3.3. Production of Polyethylene Furanoate (PEF)

Polyethylene furanoate (PEF) is formed by copolymerizing 2,5-furandicarboxylic acid (FDCA) or its derivative dimethyl furan dicarboxylate with diol, typically monoethylene glycol (MEG). Its production can cut the use of fossil-based energy by about 40-50% and result in a 45–55% reduction in greenhouse gas emissions compared with polyethylene terephthalate (PET). Figure 14 shows the production of PEF and PET. PEF also shows better performance, with an increased glass transition temperature and a reduced melting point, and stronger resistance to oxygen, carbon dioxide, and

 doi:10.20944/preprints202601.1587.v1

water permeation than PET [159,160]. Research on FDCA-based polyesters has grown rapidly as advances in FDCA production have strengthened the push for renewable alternatives to petroleum-derived plastics. These biobased polymers are typically produced via direct esterification or transesterification, with FDCA or its derivatives react with diols for example ethylene glycol, 1,4-butanediol, 1,3-propanediol or with other monomers like 1,4-cyclohexanedicarboxylate, 2,2,4,4-tetramethyl-1,3-cyclobutanediol, or isosorbide. The resulting polymers PEF, PPF, PTF, PBF, PCHDMF, and PEIF shown in Figure 15, offer thermal stability, mechanical strength, and gas permeability performance that match or even exceed those of traditional terephthalate-based plastics [161]. Their processability and durability make them suitable for applications in packaging engineering and plastics.

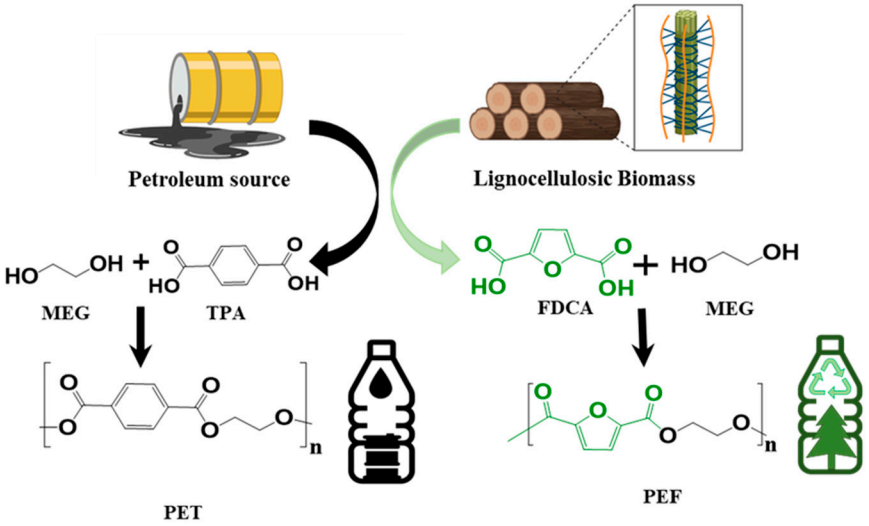

Figure 14. Illustration of the preparation of PEF and PET.

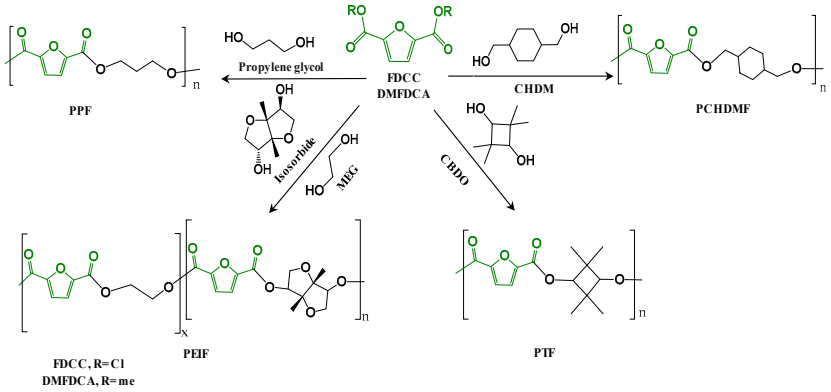

Figure 15. Reaction pathways for the synthesis of PPF, PEIF, PTF, and PCHDMF.

Among them, PEF stands positioned as a sustainable substitute for PET for food and beverage packaging because its strong gas-barrier effectiveness. At the same time, PPF and PBF offer enhanced toughness for industrial applications [162,163] as described in Table 3.

Table 3. Summary of the properties and usage of different FDCA-based polymers.

Polymer	Diol	Properties	Usage	Ref
PEF	Ethylene glycol	- Superior gas (O_2, CO_2, H_2O) barrier properties vs. PET,	Food and beverage packaging (soft drinks, water bottles, beer, juices), films for	[164]

 doi:10.20944/preprints202601.1587.v1

		- Higher glass transition temperature (Tg), good mechanical strength, fully recyclable, 100% bio-based when using bio-MEG.	fiber-based textiles, and flexible packaging.	
PPF	Propylene glycol (1,3-propanediol)	Higher polarity and lower Tg than PEF, good gas barrier properties, can be amorphous, can be blended or cross-linked to form degradable networks.	This material shows strong potential for use in bio-based packaging. When cross-linked with suitable agents, it can also be adapted for biological applications, including as tissue-engineering scaffolds and drug-delivery devices.	[165]
PTF	2,2,4,4-tetramethyl-1,3-cyclobutanediol (CBDO)	Amorphous, high transparency, high Tg (up to ~120°C in some blends), good heat resistance, and high impact resistance.	High-performance engineering plastics, potentially as a BPA-free alternative to polycarbonate in durable household items and baby bottles.	[166]
PBF	1,4-butanediol (BDO)	It exhibits good crystallization behavior, a relatively high melting temperature, excellent gas barrier performance, and can be readily electrospun into fibrous mats.	Packaging materials, as a blend component to improve foam morphology in bead foams, and in biomedical applications like drug delivery mats, due to biocompatibility.	[167]
PCHDMF	1,4-cyclohexanedimethanol (CHDM)	Higher Tg and enhanced barrier properties when used as a comonomer in FDCA-based polyesters (e.g., in PBCF-68, which has a Tg of 69°C), improved stiffness	Potential for use in high-performance, bio-based engineering plastics and improved packaging materials	[168]
PEIF	Ethylene glycol and Isosorbide	Inclusion of rigid diols like isosorbide leads to increased stiffness, higher Tg, and better barrier properties compared to linear diols, while maintaining bio-based content	Enhanced performance of bio-based packaging materials requiring higher thermal resistance and stiffness.	[169]

Current studies focus on refining polymerization strategies of PEF to optimize the quality and scalability of FDCA-based polyesters. Traditional synthesis routes, such as direct esterification [170], transesterification [171], and solution polymerization [172], remain the foundation for PEF production. However, recent advancements have introduced ring-opening polymerization (ROP) [173] as a promising alternative. This method enables rapid polymerization, better molecular weight control, and fewer side reactions, producing high-purity polymers suitable for large-scale manufacturing. The adoption of ROP is expected to streamline industrial processing, reduce energy requirements, and accelerate the transition toward fully biobased polyester materials [174].

3.3.1. Direct Esterification

Researchers are improving the synthesis of polyethylene furanoate (PEF) to enable industrial-scale production and expand its use in packaging and fibers. The direct esterification method is the

 doi:10.20944/preprints202601.1587.v1

most efficient and environmentally friendly route for PEF preparation, but it still faces challenges, such as oxidative degradation of the feedstock that can cause color changes and lower polymer quality [162,175] as shown in Figure 16 (a).

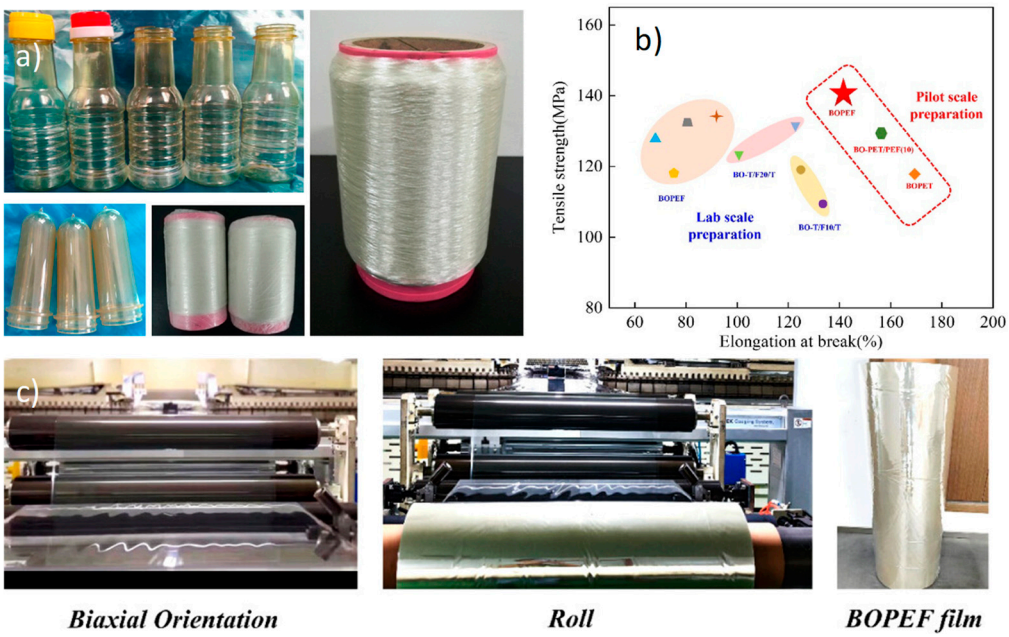

Figure 16. *a)* Photograph of the PET application. The figure was reproduced with permission from reference [175]. Copyright 2020, American Chemical Society, *b)* Tensile strength and elongation at break comparison of the designated polyesters, and *c)* preparation of BOPEF on a large scale. The figures was reproduced with permission from the reference [176]. Copyright 2024, American Chemical Society.

To overcome these issues, studies have focused on optimizing temperature, pressure, and catalyst systems to reduce side reactions. The process involves two stages: Esterification of ethylene glycol (EG) with 2,5-furandicarboxylic acid (FDCA), followed by polycondensation to extend polymer chains. Catalysts, including zinc acetate, manganese acetate, and tetrabutyl titanate, are commonly employed as shown in Table 4.

The esterification step proceeds at 165-200°C under nitrogen until water formation ceases, after which polycondensation occurs at 230-240°C under vacuum [177] as shown in Figure 17. The addition of catalysts such as antimony trioxide accelerates polymerization, and increased viscosity indicates polymer growth and chain elongation [178]. High reaction temperatures are required to achieve the thermal stability of FDCA, but this often results in dark-colored PEF, which affects optical and mechanical performance. Despite this drawback, direct esterification ensures high productivity and broad adaptability with different diols [164]. Stabilizers and anaerobic conditions are necessary to prevent degradation and maintain polymer integrity. Several furan-based polyesters, including PEF, polybutylene furanoate (PBF), and polytrimethylene furanoate (PTF), have been produced through this approach. The process can proceed without excess solvents or intermediates, using tetrabutyl titanate as the catalyst in a single-step, efficient, and low-energy reaction [179].

Table 4. Summary of the methods used for synthesis of PEF.

Aspect	1- Direct Esterification (DE) [164,170]	2- Transesterification (TE) [171,180]	3-Solution Polymerization (SP) [172]	4-Ring Opening Polymerization (ROP) [173]
Monomers	2,5-Furandicarboxylic acid (FDCA) + Mono ethylene glycol (MEG)	Dimethyl 2,5-furandicarboxylate (DMFD) +Mono	FDCC + MEG (in solvent medium)	Cyclic oligomers of PEF (e.g., cyclic ester or cyclic oligomer of FDCA & MEG)

 doi:10.20944/preprints202601.1587.v1

		ethylene glycol (MEG)		
Reaction Type	Direct condensation between carboxylic acid and alcohol	Ester exchange (methanol replaced by ethylene glycol)	Polycondensation is carried out in a solvent	Polymerization of cyclic monomers via ring opening
Catalysts	Metal oxides (e.g., Sb_2O_3, $Ti(OBu)_4$, GeO_2, $Zn(OAc)_2$)	Metal acetates (Mn, Co, Zn) + $Ti(OBu)_4$	Similar to DE/TE catalysts, may use organic catalysts	Tin octoate ($Sn(Oct)_2$), organometallic catalysts, or enzymes
Reaction Conditions	165-240°C, under vacuum or inert gas	180-220°C, stepwise removal of methanol	100-200°C depending on solvent; moderate pressure	150-200°C; often in bulk or solvent-free
By-products	Water (H_2O)	Methanol (CH_3OH)	Water or methanol (depends on monomer)	None (ideal step-growth ROP)
Advantages	- Direct use of bio-based FDCA - Environmentally friendly (no methanol) - High purity product possible	- Easier control of reaction - High reactivity of DMFD - Lower risk of side reactions	- Good molecular weight control - Easy to incorporate additives - Moderate temperature	- Solvent-free and energy efficient - High molecular weight polymer - Narrow molecular weight distribution
Drawbacks	- Poor solubility of FDCA in MEG - High reaction temperature required - Difficult water removal	- DMFD preparation adds cost - Methanol by product handling - Possible color formation (discoloration)	- Solvent recovery needed - Lower productivity - Possible chain degradation in solvent	- Requires cyclic monomer synthesis step - Expensive catalyst - Limited scalability
Molecular Weight	Moderate to high	Moderate to high	Moderate	High
Polymer Quality	High clarity, good color if well-controlled	Often slight yellowing, good mechanical properties	Good control, but may contain solvent residues	Excellent control, high molecular weight, narrow distribution

Studies such as those by Thiyagarajan et al. [181] demonstrate that polyesters derived from 2,4-FDCA and 3,4-FDCA exhibit thermal stability similar to or exceeding that of traditional 2,5-FDCA-based polymers, with similar glass transition temperatures. Structural analysis revealed that 2,4-PEF is amorphous while 2,5-PEF and 3,4-PEF are semicrystalline, indicating that FDCA isomer type significantly influences morphology and crystallinity.

Wang et al [182]. demonstrate poly(ethylene furanoate) (PEF) as a highly promising bio-based polyester for advanced barrier packaging applications. BOPEF achieved a beneficial combination of high mechanical strength, good ductility, and exceptional resistance to oxygen, carbon dioxide, and water vapor permeability through optimal biaxial orientation, as shown in Figure 16 b. By including 20% PEF in the PET/PEF/PET multilayer, greater performance improvements were achieved. structures, which performed better than traditional BOPET films. Pilot-scale experiments demonstrated the industrial feasibility of PEF-based films by confirming the scalability and reproducibility of these improved qualities as seen in figure 16 c. When taken as a whole, the results present PEF as a high-performance, sustainable substitute for conventional petrochemical polymers, highlighting the crucial part process optimization plays in facilitating widespread use.

Papageorgiou et al. [183] examined the effect of molecular weight on melting and crystallization kinetics. Higher-molecular-weight PEFs crystallized more slowly, while lower-molecular-weight

 doi:10.20944/preprints202601.1587.v1

polymers recrystallized faster during cooling. The activation energy for melting and cold crystallization shifted with temperature, showing complex thermal behavior characteristic of semicrystalline polymers. Microscopic analysis indicated denser nucleation at lower crystallization temperatures. These findings help refine polymerization parameters, improve processing stability, and enhance the mechanical and thermal performance of biobased PEF, supporting its transition toward commercial application. Further research by Codou et al. [184] confirmed similar crystallinity and unit cell structures between glassy and melt-crystallized samples. Thermal analysis revealed consistent early crystallization dynamics and distinct

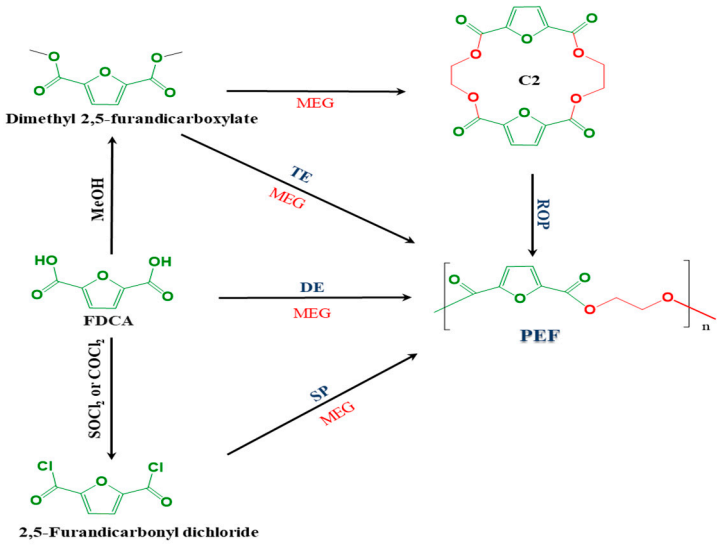

Figure 17. Polymerization routes for PEF, Direct esterification (SE), Solution polymerization (SP), Transesterification (TE), and ring-opening polymerization (ROP).

Transitions in crystal growth below 171°C. A study by Banella et al. [185] explored more practical and cost-effective method involving direct esterification of 2,5-furandicarboxylic acid. Two environmentally friendly and food-safe catalysts, zinc acetate and aluminum acetylacetonate, were evaluated under controlled conditions using minimal diol excess and short reaction times as illustrated in Figure 17.

As illustrated in Figure 18, ^{1}H NMR spectrum of the polymer synthesized using the $Al(acac)_3$ catalyst, the resulting PEF exhibited favorable properties, including desirable viscosity, color, and low diethylene glycol content, which are crucial for its thermal and barrier performance. The non-crystalline polymers developed are excellent for creating packaging materials such as oriented sheets and bottles. Industrial-scale synthesis of PEF by Wang et al. [186] reported that when PEF and PTF were synthesized in a 150 L stainless-steel reactor, their tensile strengths increased by 33.3% and 39.2%, respectively, compared with the same polymers produced in a small 100 mL flask. This enhancement was largely due to the improved control of temperature, vacuum, and mixing that is possible in larger reactors. FDCA-based polyesters with higher intrinsic viscosities ([η] > 0.9 dL/g) showed particularly strong mechanical performance, reaching tensile strengths of 93.2 MPa for PEF and 80.2 MPa for PTF, along with elastic moduli of 2.1 GPa and 1.8 GPa. In addition to their mechanical strength, both polymers demonstrated excellent barrier properties against oxygen, CO_2, and water vapor. The study also highlighted successful ton-scale production of PEF resin using a 3000 L pilot reactor, confirming that industrial-scale manufacturing of FDCA-based polyesters is not only feasible but already well within reach.

 doi:10.20944/preprints202601.1587.v1

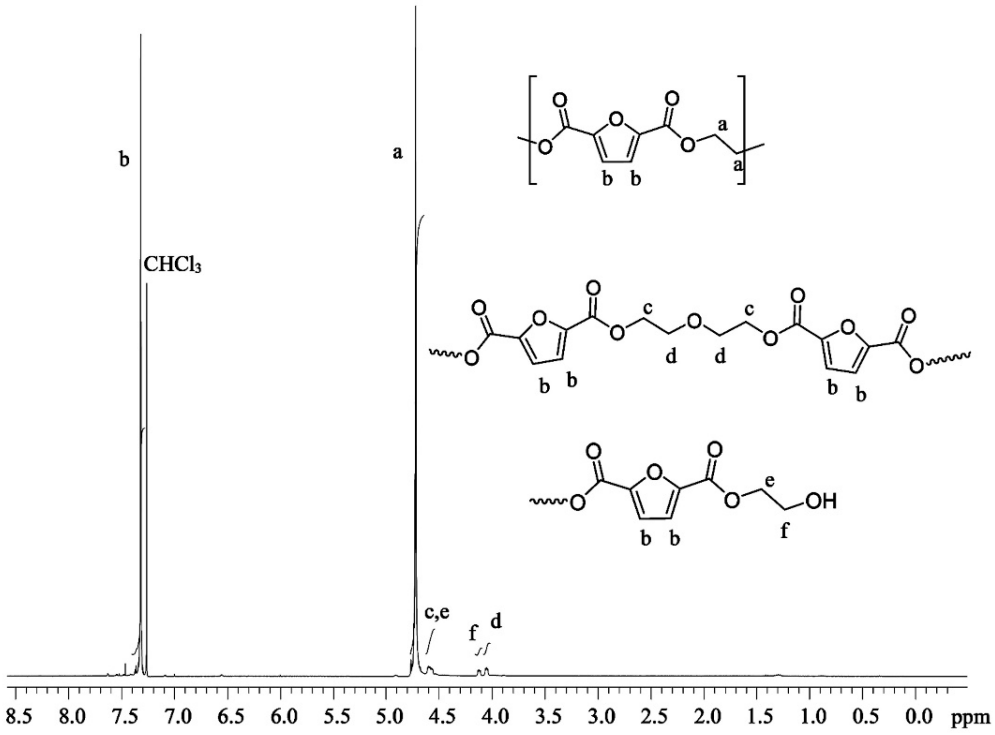

Figure 18. ^{1}H NMR spectrum of the sample synthesized using the Al(acac)$_3$ catalyst, showing the signal assignments corresponding to diethylene glycol (DEG) and the polymer's terminal groups. The figure was reproduced with permission from the reference [185]. Copyright 2019, American Chemical Society .

3.3.2. Polycondensation Through Solution Polymerization

Melt polymerization can produce high-molecular-weight polymers quickly, but it demands high temperatures and strong vacuum conditions. These requirements become harder to manage as the diol chain length increases. Longer-chain diols slow down the polycondensation reaction, reduce efficiency, and increase the likelihood of thermal degradation and discoloration. In contrast, solution polymerization can be performed under gentler conditions, with better temperature control and less oxidative damage, making it easier to tune the final polymer's average molecular weight and its distribution profile [172]. In this method, 2,5-FDCA is converted to the reactive (FDCC) 2,5-dicarbonylfuran chloride by reaction with $SOCl_2$ or $COCl_2$ (Figure 17), which combines with diols to yield lighter-colored polyesters as mentioned in Table 4. Gomes et al. [187] applied solution polymerization to take advantage of the monomers' reactivity and volatility. Instead of using standard aliphatic diols, they employed bis(hydroxyalkyl)-2,5-furan dicarboxylates, which enabled the formation of high-molecular-weight, semicrystalline PEF with excellent thermal stability. The polymerization was carried out at 240-250°C under vacuum in the presence of an Sb_2O_3 catalyst. The resulting semicrystalline polymers were both infusible and insoluble, behaving similarly to fully aromatic polyesters. In contrast, when nonvolatile diols such as isosorbide or isostearyl alcohol were used, the resulting polyesters were completely amorphous. Overall, these findings demonstrate that by tailoring the monomer structure, reaction conditions, and catalyst choice, it is possible to precisely tune polymer molecular weight, crystallinity, and thermal properties. Gandini et al. [188] prepared low-molecular-weight PEF oligomers by reacting FDCA dichloride with MEG in tetrachloroethane at room temperature in the presence of pyridine. Subsequent addition of 1% Sb_2O_3 followed by high-vacuum treatment at 220°C yielded solid PEF with well-controlled molecular weight. When higher-boiling diols such as isosorbide were used, their corresponding dichlorides were formed, leading to polymers with distinctly different thermal behaviors, including glass transition temperatures spanning from 90 to 180°C.

 doi:10.20944/preprints202601.1587.v1

3.3.3. polymerization Through Ring-Opening

Most PEF described in the literature is made using condensation polymerization, the standard approach for polyesters. However, this approach has significant drawbacks: as polymer chains lengthen, the melt becomes more viscous, which makes mixing challenging and slows the elimination of byproducts like water or alcohol. Lower response efficiency, longer manufacturing times, and higher energy consumption are the results of these diffusion-related problems. Ring-opening polymerization (ROP), on the other hand, has become a viable method for creating high-molecular-weight furan-based polyesters such as PEF and PBF. In ROP, cyclic oligomers are opened by an initiator and then join to create polymers. In contrast to polycondensation, ROP is entropy-driven, low-viscosity, and creates no byproducts, allowing for quicker reactions and more consistent polymer development. The molecular weight can be precisely tuned by adjusting the initiator-to-monomer ratio, and the polydispersity can be controlled through optimized reaction parameters [189-191]. A critical factor for successful ROP is the high purity of the cyclic oligomers, since any residual end groups can trigger premature chain initiation, thereby lowering molecular weight. Preparing such oligomers remains a major challenge. Rosenboom et al. [185] demonstrated that cyclic depolymerization of FDCA and EG can yield cyclic PEF oligomers, but the resulting size distribution was nonuniform due to solidification and diffusion limits during the reaction. To overcome this, selective precipitation and cyclic dimer purification methods have been developed to create oligomers with excellent purity suitable for scalable ROP. Ultimately, PEF synthesized by optimized ROP has achieved molecular weights up to 50,000 g/mol and thermal properties comparable to those of melt-polymerized PEF, confirming ROP as an efficient and industrially viable alternative for producing bottle-grade PEF. ROP has been successfully applied to produce high molecular weight PEF with properties comparable to melt-polymerized material. Liu et al. [191] demonstrated a green, economically competitive ROP process using FDCA and EG, forming cyclic oligomers from prepolymerized linear PEF under dilution and depolymerization, (SEC) profile indicates that neat ROP of 99% pure cyclic oligomeric ethylene furanoate (cyOEF) at 280°C, without any additional catalyst, rapidly converts trimers (C3) and larger rings into PEF. However, the dimer (C2) reacts much more slowly and remains only partially polymerized (black arrow). As the reaction continues, the mixture gradually becomes heterogeneous, accompanied by noticeable discoloration and a drop in molecular weight. This is reflected in Figure 19(a), where the PEF peak shifts toward higher elution volumes. To accelerate polymerization at 280°C, several ROP conditions were evaluated, as shown in Figure 19(b): a neat reaction (black squares); dry grinding of cyOEF with 0.1 mol% cyclic stannoxane initiator for mechanical mixing (blue diamonds); feeding fresh cyOEF into a reactive PEF melt already converted by more than 90% and containing the same initiator level (purple triangles); and adding 33 wt% tetraglyme as an inert liquid plasticizer together with 0.1 mol% initiator (red circles). Notably, tetraglyme alone without any initiator (grey circles) provided a moderate increase in polymerization rate, as illustrated in Figures 19(c, d). When ROP was performed at 260°C using 0.1%, 0.2%, or 0.3% cyclic stannoxane in the presence of 33 wt% tetraglyme, the reaction reached nearly complete conversion (>96%) within 20 minutes, producing high-molecular-weight PEF (>30 kg mol^{-1}) suitable for bottle-grade applications. As shown in Figure 19(e), the optimized ROP condition (0.1% cyclic stannoxane + 33% tetraglyme at 260°C for 25 min) generated a colorless, high-molecular-weight PEF (right). compared to a non-optimized ROP utilizing 97% pure cyOEF at 280°C with the same initiator for 60 min resulted in a noticeably discolored product (middle). For reference, industrial PEF produced by polycondensation (Mn ≈ 15 kg mol^{-1}) displayed similar discoloration (left).

 doi:10.20944/preprints202601.1587.v1

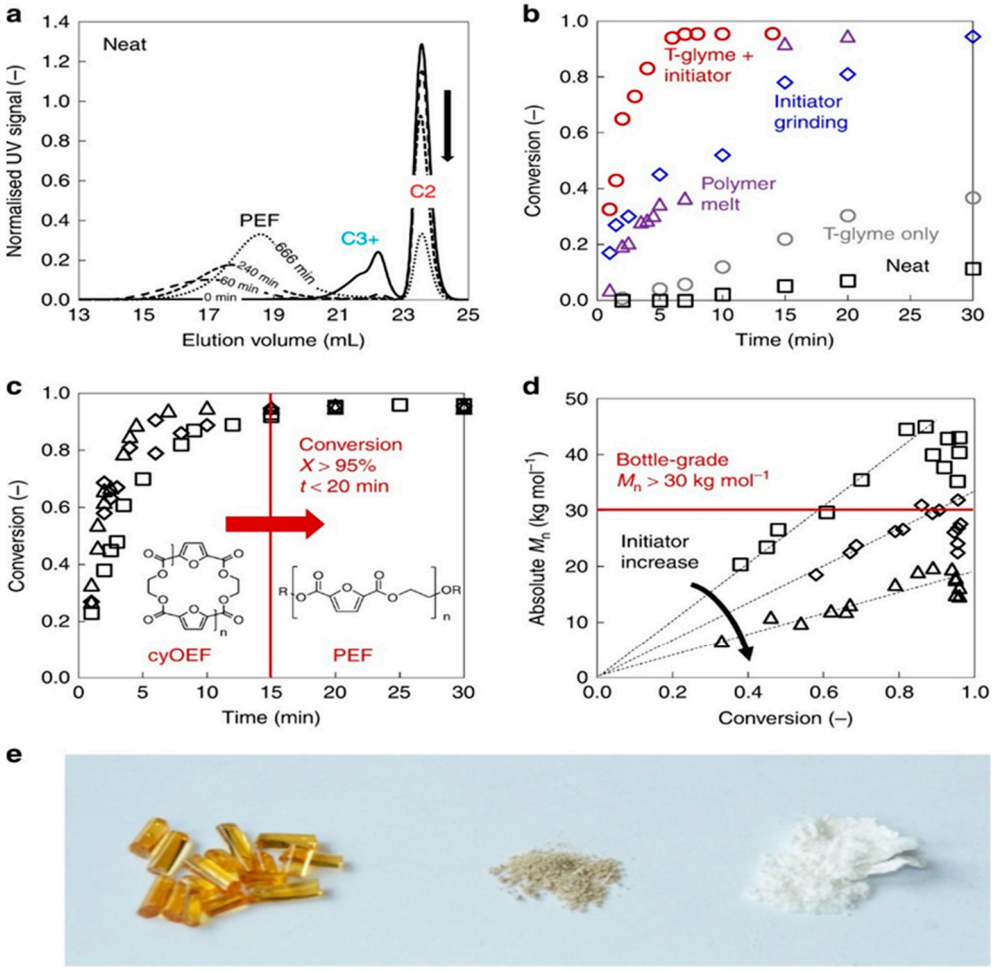

Figure 19. *(a)* The size exclusion chromatography (SEC) profile, *(b)* Different ROP conditions, *(c, d)* The influence of various stannoxane ratios with respect to the conversion to PEF, *(e)* The resulting PEFs show clear visual and structural differences The figures was reproduced with permission from the reference [174]. Copyright 2019, Springer Nature. .

Li et al. prepared multiblock copolymers of poly(ethylene2,5-furandicarboxylate)-block poly (tetramethylene oxide) using cascade condensation coupling ROP (PROP). Reaction of cyclic oligo(ethylene 2,5-furandicarboxylate) with PTMO diols under vacuum, producing bicrystalline structures with controlled molecular weight, block length, and phase distribution. Increasing the PEF content elevated the melting temperature and crystallinity of the PEF segments, while PTMO properties remained stable. These amphiphilic, biodegradable thermoplastic elastomers exhibit tailored mechanical properties, demonstrating the effectiveness of ROP-based strategies for producing sustainable, high-performance PEF-based polymers and providing a foundation for further polymer design and applications [192].

Huerta et al. [193] have effectively created cyclic low-molecular-weight polyesters using thermal ring depolymerization and high-dilution polycondensation techniques, producing mixtures of tiny cyclic oligomers. Using $Sn(Oct)_2$ as a catalyst, these cyclic oligomers, principally dimers, trimers, and tetramers, were subsequently polymerized by ring-opening polymerization (ROP) to create PEF and PBF. The oligomers, purified using semipreparative chromatography, were crystalline solids with melting temperatures between 140-200°C. In both mixed and pure oligomer systems, polymerization tests showed that smaller ring diameters resulted in faster reaction rates. The ROP technique yielded high-molecular-weight polymers (50,000-60,000 g/mol), equivalent to or exceeding those made with conventional polycondensation. Additionally, PBF polymerized more quickly than PEF, and as ring size decreased, polymerization rates marginally rose. The thermal characteristics of PEF and PBF

 doi:10.20944/preprints202601.1587.v1

formed from ROP were similar to those of polymers produced by melt polycondensation, demonstrating that ROP is an extremely effective and commercially viable method of producing furan-based polyesters.

3.3.4. Polycondensation Through Transesterification

Discoloration and sluggish crystallization are two ongoing issues in the manufacturing of polyethylene furanoate (PEF). Impurities in FDCA, decarboxylation during polymerization, and the use of metal catalysts like titanium or manganese can all cause discoloration. Researchers investigated ring-opening polymerization and chloride-solution techniques utilizing manganese catalysts to reduce these effects. [164]. Still, these approaches involve complex steps and solvent-intensive processes, unsuitable for large-scale production. An alternative route involves converting FDCA into dimethyl 2,5-furandicarboxylate (DMFD), followed by transesterification with ethylene glycol (EG) as shown in Figure 20, to form PEF [194,195]. This approach yields lighter-colored PEF with better quality, but careful control of reaction time and temperature is essential since high thermal exposure (230-250°C) increases costs and intensifies discoloration. Developing stable, colorless catalysts for DMFD and EG transesterification, as mentioned in Table 4, can enable industrial-scale synthesis of high-quality, colorless PEF with strong market potential.

Transesterification remains a preferred route for biobased PEF synthesis because it offers lower activation energy, greater product purity, and improved reactant stability compared to direct esterification. In this process, DMFD reacts with EG, exchanging ester and hydroxyl groups to form polymer chains. The ideal esterification temperature is 180-190°C, with polycondensation occurring around 235-245°C. Catalysts such as tetrabutyl titanate, manganese acetate, zinc acetate, and stannous oxalate boost polymerization efficiency and product quality. Studies showed that PEF synthesized via transesterification exhibits a glass transition temperature (Tg) of 80°C, higher than that of PET (75°C), and a melting temperature (Tm) of 215°C, lower than PET's 260°C. These results confirm that PEF offers suitable mechanical and thermal properties for replacing PET in packaging and industrial applications [196,197].

Knoop et al. [199] effectively synthesized high-molecular-weight, semi-aromatic FDCA-based polyesters using high-purity DMFDCA through a two-step commercial melt polymerization technique. They produced polyesters with low coloring, narrow molecular weight distribution (PDI < 2), and moderate molecular weights by reacting DMFDCA with a number of linear aliphatic diols. Poly(ethylene furanoate) (PEF), poly(propylene furanoate) (PPF), and poly(butylene furanoate) (PBF) displayed comparable molecular weights and color to their terephthalate counterparts, The molecular weight of PEF was further increased by almost an order of magnitude through subsequent solid-state polymerization (SSP), demonstrating that PEF may be made in industrial settings similar to PET. After annealing, the high-molecular-weight PEF showed enhanced mechanical strength above its glass transition temperature and a young's modulus of about 2450 MPa on par with PET, demonstrating its great promise for advanced material applications. PEF was prepared by Papageorgiou et al. [200] via a two-step melt polycondensation method employing dimethyl 2,5-furandicarboxylate (DMFDCA) and ethylene glycol (EG), and its thermal characteristics were compared with those of PET and PEN. The results showed that PEF had an equilibrium melting point of 265°C and a heat of fusion of approximately 137 J g^{-1}. Crystallization kinetics were examined using several models, and the impact of synthesis parameters such as monomer ratio, catalyst type, and reaction temperature on the structure and characteristics of furanoate polyesters were carefully explored. It was revealed that the molecular chain configuration substantially impacts the final polymer quality. Wang et al. [198] Dimethyl 2,5-furandicarboxylate (DMFD) was transesterified with various diols to create PEF, PTF, and PBF, with intrinsic viscosities of 0.92, 0.88, and 0.96 dL g^{-1}, respectively. As shown in Figure 20 (a & b), copolymers containing 2,2,4,4-tetramethyl-1,3-cyclobutanediol (CBDO) showed exceptional mechanical strength, barrier performance, and glass transition temperatures. These characteristics imply that these furan-based copolyesters could be attractive biobased, high-performance substitutes for traditional PET, PPT, and PBT, particularly in

 doi:10.20944/preprints202601.1587.v1

packaging applications. Bimestre et al. [201] successfully created PEF using a transesterification melt polycondensation method, demonstrating a direct connection between the monomer structure and the polymerization process. The glass transition temperature (Tg) of the generated PEF was 80°C higher than that of PET (75°C), and its melting temperature (Tm) was 215°C lower than that of PET (260°C). These thermal properties demonstrate PEF's great potential as a PET substitute in a variety of applications.

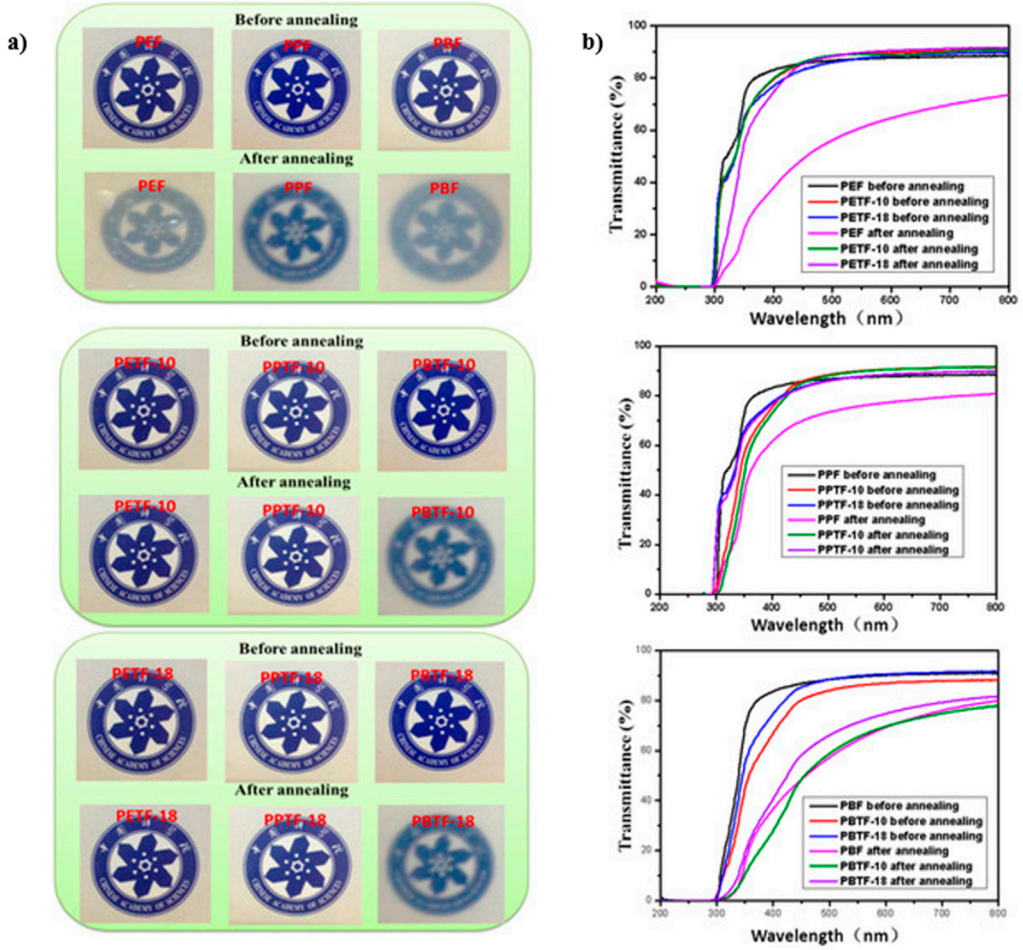

Figure 20. *a)* Optical images and *b)* UV-visible spectra of PBF, PEF, PPF, and their CBDO-modified copolyester films were captured before and after annealing at 150°C for 30 minutes [198].

3.4. Production of Polylactic Acid (PLA)

Made from renewable resources, polylactic acid (PLA) is a completely biodegradable polymer. It can be generated from lactic acid using chemical or enzymatic processes. PLA is classified into three main types based on the optical isomer of lactic acid employed: Different physical and chemical properties are displayed by poly(D-lactic acid) (PDLA), poly(L-lactic acid) (PLLA), and poly(DL-lactic acid) (PDLLA). PDLA is mostly amorphous, while PLLA is semi-crystalline. PLLA stands out in particular for having a glass transition temperature of 67°C, a melting temperature of about 180°C, and a crystallinity of about 37% [202-204].

Both PLLA and PDLA are highly thermally stable polymers, making them suitable for a range of applications. PDLA, which is amorphous and optically inactive, is one of the two enantiomers derived from L(+)- and D(-)-lactic acid. When combined with PLLA through co-precipitation, it forms a stereo-complex polylactide (sc-PLA) that exhibits improved physicochemical characteristics, including a higher melting point of approximately 230°C [205]. Polysaccharides (such as cellulose

 doi:10.20944/preprints202601.1587.v1

and starch), lipids (such as vegetable oils and fats), and proteins (such as gelatin) are examples of sustainable biomass sources from which PLA can be made. The first step in its manufacture is the microbial fermentation of carbohydrates into lactic acid, which is subsequently polymerized into PLA. This polymerization can proceed via three main methods (Figure 21): (i) direct polycondensation, yielding low-molecular-weight PLA that requires subsequent chain extension Table (5 entry 1); (ii) azeotropic dehydration, which similarly produces short-chain PLA Table (5 entry 2); and (iii) ring-opening polymerization (ROP) of lactide, a three-step process involving polycondensation, depolymerization, and final polymerization to produce high-molecular-weight PLA. Catalysts for ROP include metal complexes of aluminum, zinc, magnesium, calcium, iron, tin, yttrium, samarium, lutetium, titanium, and zirconium, with stannous octoate ($Sn(Oct)_2$) being the most commonly used for generating high-molecular-weight products [206]. Although condensation polymerization is cost-effective, it does not yield high-molecular-weight PLA directly. Additional expenses arise from the use of coupling agents and esterification accelerators. The process typically involves two stages: first, dehydration condensation between hydroxyl and carboxyl groups forms low-molecular-weight PLA; second, chain-extending additives are applied to lengthen polymer chains and modify structural properties. Byproducts and residual additives generated during this process are non-biodegradable, which can be problematic for biomedical applications. Triphosgene is sometimes employed to remove impurities and residual catalysts, but its use raises production costs and safety concerns due to flammable solvents. While new chain extenders have been developed to replace conventional agents, issues related to toxicity and non-biodegradability remain unresolved. Although condensation polymerization is cost-effective, it does not yield high-molecular-weight PLA directly. Additional expenses arise from the use of coupling agents and esterification accelerators. The process typically involves two stages: first, dehydration condensation between hydroxyl and carboxyl groups forms low-molecular-weight PLA; second, chain-extending additives are applied to lengthen polymer chains and modify structural properties. Byproducts and residual additives generated during this process are non-biodegradable, which can be problematic for biomedical applications. Triphosgene is sometimes employed to remove impurities and residual catalysts, but its use raises production costs and safety concerns due to flammable solvents. While new chain extenders have been developed to replace conventional agents, issues related to toxicity and non-biodegradability remain unresolved [207-209].

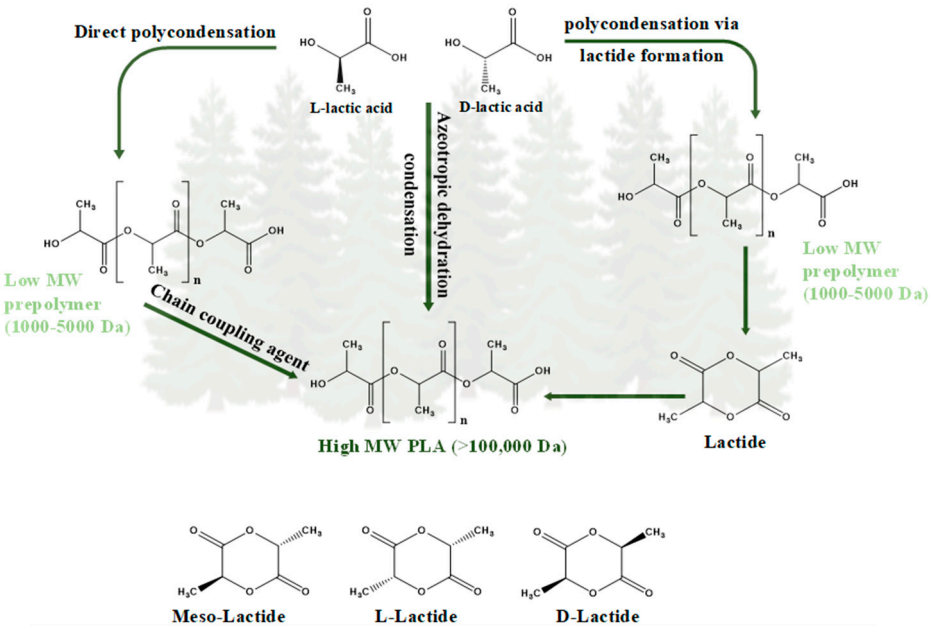

Figure 21. Polymerization routes for PLA preparation and Lactide stereochemistry.

 doi:10.20944/preprints202601.1587.v1

Senila et al. [210] developed a two-step polymerization strategy to synthesize PLA from lignocellulosic residues. In the first phase, lactic acid was produced from sugars liberated via pressurized hot water pretreatment and subsequent fermentation utilizing Lacticaseibacillus rhamnosus. The purified lactic acid then underwent two polymerization stages: initially, azeotropic dehydration at 140°C for 24 hours in xylene with tin(II) chloride ($SnCl_2$) to generate lactide, followed by microwave-assisted polymerization at 140°C for 30 minutes using 0.4% $SnCl_2$. This methodology offers an efficient route to convert lignocellulosic biomass into PLA. Although the azeotropic dehydration-condensation approach avoids extensive additives, solvents such as dibasic acids and glycols are still used, and catalysts remain present in the final polymer.

In practice, lactic acid is initially distilled under reduced pressure at 130°C for 2-3 hours to eliminate most water. The mixture is then refluxed over a molecular sieve for 30 to 40 hours at 130°C after the catalyst and diphenyl ether are added. Efficient water removal increases the solvent's boiling point, accelerating polymerization. Among the catalysts tested, tin-based compounds demonstrated the highest efficiency, though residual impurities can partially inhibit the reaction. Industrial studies later confirmed that most catalyst residues can be removed without degrading PLA [211]. To create high-molecular-weight PLA, ring-opening polymerization (ROP) of lactide is frequently utilized in industry (Table 5, entry 3). Lactide, a cyclic dimer of lactic acid, exists as L-lactide, D-lactide, and meso-lactide, and can be produced under mild, solvent-free dehydration conditions. High-purity L- or D-lactide appropriate for ROP is produced commercially by condensing lactic acid at 115-179°C, eliminating water, and recrystallizing to separate meso-lactide and low-molecular-weight polymers [212,213]. For instance, reduced-pressure reflux was employed by Cargill Inc.[214] to eliminate partial lactide, oligomers, lactic acid, and leftover water. While prior techniques used inert-gas or gas-phase recrystallization to increase yield, Nemphos added multistage melt recrystallization to remove unreacted monomers and low-molecular-weight species. For extraction, weakly alkaline aqueous solvent systems have also been studied.

Table 5. Comparison of different PLA production methods.

Method	Process Description	Catalyst(s)	Molecular Weight	Advantages	Disadvantages	Ref
Direct Polycondensation	Lactic acid monomers are condensed directly, releasing water as a byproduct.	SnO, ZnO, $Ti(OBu)_4$	Low	Simple and low-cost process	Reaction equilibrium limits MW: water removal is difficult	[215]
Azeotropic Dehydration Polycondensation	Lactic acid polymerized under azeotropic conditions with continuous removal of water using solvents.	$SnCl_2$, $Zn(Ac)_2$, Ti-based catalysts	Low to Medium	Efficient water removal; improved polymer quality over direct condensation	Solvent use increases cost and purification steps	[216]
Ring-Opening Polymerization (ROP)	High-MW PLA is produced by first converting lactic acid to lactide (cyclic dimer), which then goes through ring-opening polymerization.	$Sn(Oct)_2$, $Al(O\text{-}iPr)_3$, Zinc lactate	High	Produces high-MW, high-purity PLA; most common industrial method	Requires multi-step process and catalyst removal	[217]
Enzymatic Polymerization	Enzymes catalyze the polymerization of lactic acid or	Lipases (e.g., *Candida antarctica*	Medium	Green process; no toxic catalysts	Slow reaction rate; limited scalability	[218]

 doi:10.20944/preprints202601.1587.v1

	lactide under mild, eco-friendly conditions.	lipase B), Proteinase K	

Following purification, high purity lactide undergoes ROP through cationic, anionic, or coordination/insertion mechanisms depending on the catalyst. Cationic initiators, such as triflic acid or methyl triflate, efficiently promote polymerization, whereas anionic initiators can cause racemization and uneven molecular weight distributions [219]. To reduce toxicity, industrial processes prefer less active metal catalysts such as tin(II) or zinc compounds. Tin(II) 2-ethylhexanoate ($Sn(Oct)_2$) is the most widely used FDA-approved catalyst due to its high efficiency and low toxicity, though aluminum alkoxides and rare-earth compounds are also employed, the latter offering faster polymerization rates. Enzymatic polymerization (Table 5, entry 4) provides a sustainable alternative for PLA synthesis, operating under mild conditions with high specificity. Zahra et al. [220] reported that ultrasound-assisted dehydration during ROP effectively reduced water content and enhanced polymer properties. Using ultrasonic treatment at 109.6 W for 98.85 minutes, they achieved a moisture content of 1.9%, yielding PLA with 60.01% crystallinity, a melting temperature of 165°C, and a molecular weight of 40,567 g/mol. These findings suggest that ultrasonic-assisted dehydration is a promising strategy for improving PLA synthesis via ROP. Enzymatic approaches are increasingly explored as environmentally friendly alternatives [221]. Unlike chemical methods, which require highly pure monomers, anhydrous conditions, and elevated temperatures to prevent side reactions, enzymatic polymerization enables the production of well-defined polymers from inexpensive raw materials. A fully biosynthetic route for PLA could offer significant advantages if remaining technical challenges are addressed [222], although reports on enzymatic PLA synthesis remain limited. Using lactic acid-polymerizing enzymes (LPEs) as alternatives to chemical catalysts represents a promising strategy. Discovering natural PLA-producing microorganisms would be ideal, but this remains an ongoing challenge requiring further research. Using lipase B from Candida antarctica (Novozyme 435), Chanfreau et al. [223] demonstrated the enzymatic synthesis of poly-L-lactide (PLLA) in the ionic liquid 1-hexyl-3-ethylimidazolium hexafluorophosphate ([HMIM][PF_4]). At 90°C, the maximum PLLA yield was 63%, with a molecular weight of 37.8×10^3 g/mol.

4. Sustainability Considerations

Single-use plastics are not sustainable and produce a higher level of carbon emissions. Bioplastics are a viable substitute because they are mechanically stronger and more elastic. Yet, the biggest problem facing bioplastics adoption is ambiguity in production cost, end-of-life handling, and a lack of adequate biodegradability [224]. To promote sustainable bioplastic production and consumption, several key factors should be considered, as shown in Figure 22. These include the use of renewable and sustainable raw materials, along with the use of green solvents, as addressed in previous sections. Additionally, an integrated life cycle assessment (LCA) is necessary to evaluate the energy balance and the environmental fate of bioplastics, specifically their biodegradation behavior after disposal. In addition, waste minimization during production can be achieved through closed-loop recycling systems, thereby maintaining resource efficiency and reducing the overall carbon footprint.

 doi:10.20944/preprints202601.1587.v1

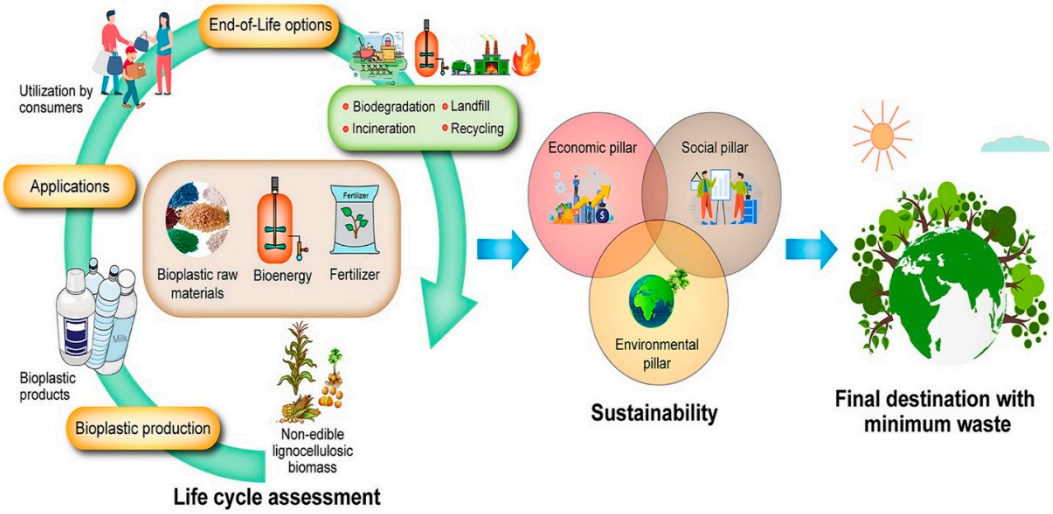

Figure 22. Sustainability considerations for bioplastics production, use, and disposal. The figure was reproduced with permission from the reference [26]. Copyright 2023, Elsevier.

4.1. Life Cycle Assessment (LCA)

The life cycle assessment (LCA) tool is typically used to compare the environmental and economic footprints of bioplastics. Bioplastics' sustainability is dependent upon several interconnected stages, including raw material procurement to their end-of-life management [26]. During the raw material procurement stage, the key issues are land use change [225,226], non-renewable energy consumption, and greater eutrophication potential due to agricultural inputs such as fertilizers for starch-based feedstocks. To resolve these issues, process optimization and the use of renewable energy sources are required to reduce the total environmental impact. In the course of manufacturing or production, bioplastics such as polyhydroxyalkanoates (PHA) face issues of high production costs, slow microbial growth, low raw material conversion efficiency, and high energy requirements [26,227]. Process optimization and waste minimization in this stage can lead to a huge reduction in environmental impacts [228]. In addition, the use of renewable energy sources may help reduce greenhouse gases and carbon footprints overall [229]. Although the use phase has little environmental impact compared to production, the material's performance and durability influence overall sustainability. In the end-of-life (EOL) phase, sound management of waste through recycling, composting, and biodegradation is important to limit waste generation and environmental impacts. Therefore, the application of circular approaches, such as waste recycling and decision-making based on environmental analysis, can also enhance sustainability. Overall, both environmental and economic aspects must be considered in the life cycle for responsible bioplastic production and disposal. In several research articles, LCA is used to compare the environmental footprints of different polymers. Senila et al. conducted an LCA of two bioplastics, PLA and PHB. They reported that in PLA production, biomass processing, pretreatment, and bioprocessing significantly impact the environment. But in PHB production, the initial biomass processing and pretreatment are energy-intensive processes and emit a high carbon footprint [50]. Yadav and Nikalje did a detailed LCA comparison of energy reduction strategies during the synthesis of bioplastics by use of eco-friendly chemical solvents [230]. Benavides and Mehrjerdi performed a comprehensive life cycle assessment (LCA) of biodegradable polylactic acid (PLA) and bio-based polyethylene (bio-PE) across their entire life cycle, from raw material extraction to end-of-life (EOL), to evaluate the environmental impacts. Compared to conventional fossil-based plastics such as HDPE and LDPE, bio-PE and PLA both exhibited lower greenhouse gas emissions and fossil energy consumption, with bio-PE and PLA emitting 1.0 and 1.7 kg CO_2 eq/kg and consuming 29 and 46 MJ/kg, respectively. Research found that the environmental profile of PLA worsens when biodegradation occurs in landfills or composting environments, resulting in a 16-163% increase in life-cycle GHG emissions. These findings emphasize the critical role of end-of-life management in determining biodegradable plastics' true sustainability

 doi:10.20944/preprints202601.1587.v1

[231]. Roijen and Miller provided an EOL analysis of three bioplastics (PLA, PHA, and thermoplastic starch) by composting, landfill, and anaerobic digestion (AD). They asserted that the literature on LCA studies of biodegradation is insufficiently aligned with projected uses of bioplastics. Landfilling as an EOL option was used by 60% of the studies, while 12% used biodegradation. Assigning utilitarian outputs on anaerobic digestion significantly improved the environmental output of the bioplastics, reducing their carbon emission by nearly half, some 55 per cent. Concerning composting, 38 per cent of the studies were carried out on a full-time, continuous basis- requirements that are deemed to be important regarding complete material composting [232].

4.2. Environmental and Socio-Economic Impacts

Sustained economic growth over the last few years has raised grave concerns about its environmental impacts, especially in rapidly growing economies. To address these issues, Moshood et al. [233] carried out research on sustainable bioplastics, exploring their economic nature, environmental impact, and social qualities; among these, the environment has been declared the most critical factor. Bioplastics can minimize the carbon emissions by 241-316 million metric tons per year [234]. On the economic front, bioplastics still have an uphill climb against biofuels in terms of biomass resources. Furthermore, there are substantial financial obstacles related to biomass utilization, as research and development in the field require significant investment. Investors and governments, however, tend to be more hesitant to fund such initiatives compared to the well-established infrastructure supporting fossil-based plastic production [235]. Bio-based plastics have potential in all three pillars of sustainability (environment, economy, and social) [234].

4.3. Waste Minimization

Biorefineries consist of multiple interconnected processes that work together to convert feedstocks into a variety of valuable products. Over the past few decades, numerous studies have focused on individual bioprocesses for producing either biofuels such as bioethanol, biomethane, biohydrogen, and biodiesel or bioproducts, including pharmaceuticals, enzymes, and bioplastic monomers, from organic materials. By examining the process flow diagrams of these bioprocesses, different standalone processes can be strategically integrated to design a conceptual bioplastic biorefinery. Moreover, understanding the feedstock characteristics and the fate of by-products at each stage is essential to achieving complete valorization [236]. Figure 23 shows that designing products for reuse and recycling helps keep them in use longer, with less material and energy use. When products can no longer be repaired, processes like mechanical recycling and depolymerization can recover their material value. Even if some bio-based plastics end up in the environment, they can still support a circular economy. This is because they can break down into CO_2 and water, allowing the carbon to return to nature and be used again in making new materials, which helps move toward a zero-waste and sustainable production cycle [237].

 doi:10.20944/preprints202601.1587.v1

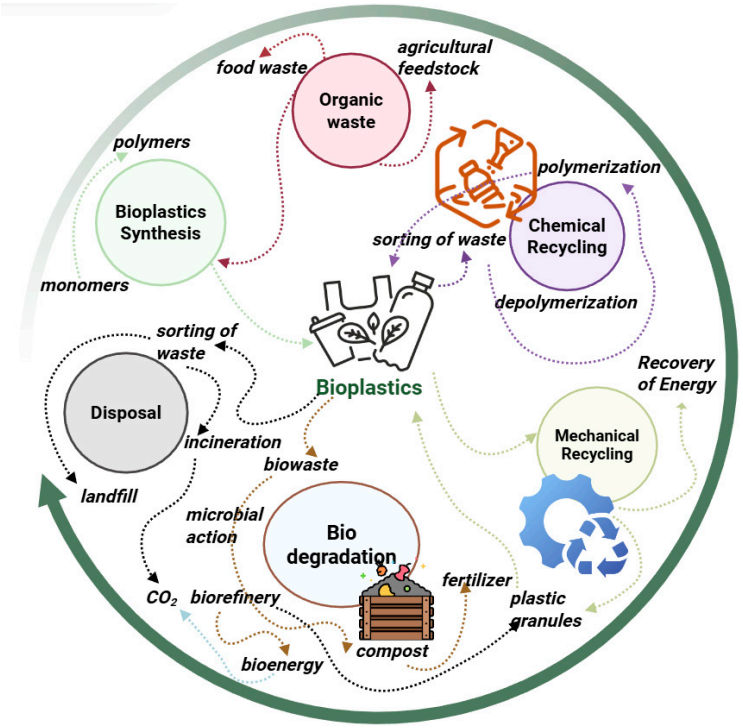

Figure 23. Circular economy for bioplastics.

5. Conclusion & Outlook

Lignocellulosic biomass is a sustainable source for the production of bioplastics. It not only reduces dependence on petroleum-based polymers but also mitigates plastic pollution at the source. This review comprehensively discusses green chemistry approaches for biomass pretreatment and the synthesis of precursors for the efficient utilization of biomass-derived carbohydrates and aromatics as renewable feedstocks for high-performance bioplastics. Moreover, chemical, physical, physicochemical, and biological pretreatment methods are critically compared based on reaction rates, working conditions, monomeric sugar yields, and their advantages and drawbacks. New green solvents, such as ILs, DESs, and LHWs, achieve higher delignification rates under milder conditions, in a more environmentally friendly setting, and produce sugar monomers that can be further processed for bioplastic production. In the same vein, the catalytic valorization of sugars into major platform chemicals, 5-hydroxymethylfurfural (HMF) and its oxidation product, 2,5-furandicarboxylic acid (FDCA), has been significantly advanced by the development of non-noble-metal catalysts that are highly yielding, selective, and reusable. Despite significant research, several key factors negatively affect the synthetic process, including biomass heterogeneity, enzyme inhibition, and difficulty in solvent recovery. The overall process requires significant energy inputs, which ultimately increase the cost of production. Therefore, to achieve cost competitiveness with traditional petroleum-based plastics, catalyst performance must be upgraded, solvent recycling enhanced, and reaction rates increased. However, the shift toward circular bioeconomy, combined with increased environmental awareness and supportive policy instruments, is accelerating the exploration and industrial interest in bio-based polymers, including PLA, PHA, PBS, and PEF. The following recommendations and key points need further exploration:

i. No single pretreatment is completely eco-friendly; more research is necessary to develop greener protocols that maintain yields.
ii. The lack of standardized analytical methods leads to yield variations caused by biomass differences, which must be addressed to ensure process consistency.
iii. Few studies have examined scaling laboratory processes to pilot or commercial levels, highlighting the need for further research.

 doi:10.20944/preprints202601.1587.v1

iv. Genetically engineered plants could improve yields by tackling biomass heterogeneity and recalcitrance.
v. Bioplastics require comprehensive cost assessments and end-of-life analyses to confirm their economic and environmental viability.

Generally, the lignocellulosic biomass is a strong, renewable, and untapped source of next-generation bioplastics. New environmentally friendly pretreatment technologies, catalytic mechanisms, and green polymerization processes will remain important in the full exploitation of its potential. Further innovations will be based on interdisciplinary cooperation, process optimization informed by life-cycle assessment, and the development of scalable, cost-effective biorefinery models. With sustained research and technological refinement, biomass-derived bioplastics can play a pivotal role in shaping a low-carbon, circular, and environmentally responsible materials future.

Author Contributions: Conceptualization, M. M. G., M. H., and M. H. M.; methodology, M. M. G.; writing-original draft preparation, M. M. G., M. H., and M. H. M.; writing-review and editing, E. H. and I. E; visualization, M. M. G., M. H., and M. H. M.; supervision, E. H. All authors have read and agreed to the published version of the manuscript.

Funding: This publication is based upon work supported by the McIntire-Stennis project under accession number 70011735.

Institutional Review Board Statement: Not applicable.

Informed Consent Statement: "Not applicable.

Data Availability Statement: Data are contained within the article.

Acknowledgments: This manuscript is publication #SB1179 of the Sustainable Bioproducts, Mississippi State University. This publication is a contribution of the Forest and Wildlife Research Center, Mississippi State University.

Conflicts of Interest: The authors declare no conflicts of interest.

References

1. Rasmussen, S.C. From parkesine to celluloid: the birth of organic plastics. *Angewandte Chemie* **2021**, *133*, 8090-8094, doi:https://doi.org/10.1002/anie.202015095.
2. Pilapitiya, P.N.T.; Ratnayake, A.S. The world of plastic waste: A review. *Cleaner Materials* **2024**, *11*, 100220, doi:https://doi.org/10.1016/j.clema.2024.100220.
3. Dokl, M.; Copot, A.; Krajnc, D.; Van Fan, Y.; Vujanović, A.; Aviso, K.B.; Tan, R.R.; Kravanja, Z.; Čuček, L. Global projections of plastic use, end-of-life fate and potential changes in consumption, reduction, recycling and replacement with bioplastics to 2050. *Sustainable Production and Consumption* **2024**, *51*, 498-518, doi:https://doi.org/10.1016/j.spc.2024.09.025.
4. Mulder, K.; Knot, M. PVC plastic: a history of systems development and entrenchment. *Technology in Society* **2001**, *23*, 265-286, doi:https://doi.org/10.1016/S0160-791X(01)00013-6.
5. Lambert, S. Environmental risk of polymer and their degradation products. University of York, 2013.
6. Martín, A.J.; Mondelli, C.; Jaydev, S.D.; Pérez-Ramírez, J. Catalytic processing of plastic waste on the rise. *Chem* **2021**, *7*, 1487-1533, doi:https://doi.org/10.1016/j.chempr.2020.12.006.
7. Agenda, I. The new plastics economy rethinking the future of plastics. In Proceedings of the World economic forum, 2016.
8. Allen, S.; Allen, D.; Moss, K.; Le Roux, G.; Phoenix, V.R.; Sonke, J.E. Examination of the ocean as a source for atmospheric microplastics. *PloS one* **2020**, *15*, e0232746, doi:https://doi.org/10.1371/journal.pone.0232746.
9. Geyer, R.; Jambeck, J.R.; Law, K.L. Production, use, and fate of all plastics ever made. *Science advances* **2017**, *3*, e1700782, doi:https://doi.org/10.1126/sciadv.1700782.

10. Mülhaupt, R. Green polymer chemistry and bio-based plastics: dreams and reality. *Macromolecular Chemistry and Physics* **2013**, *214*, 159-174, doi:https://doi.org/10.1002/macp.201200439.
11. Iroegbu, A.O.C.; Ray, S.S.; Mbarane, V.; Bordado, J.C.; Sardinha, J.P. Plastic pollution: a perspective on matters arising: challenges and opportunities. *ACS omega* **2021**, *6*, 19343-19355, doi:https://doi.org/10.1021/acsomega.1c02760.
12. Herms, W.B. *An ecological and experimental study of Sarcophagidae with relation to lake beach debris*; 1907.
13. Williams, A.T.; Rangel-Buitrago, N. The past, present, and future of plastic pollution. *Marine Pollution Bulletin* **2022**, *176*, 113429, doi:https://doi.org/10.1016/j.marpolbul.2022.113429.
14. Ostle, C.; Thompson, R.C.; Broughton, D.; Gregory, L.; Wootton, M.; Johns, D.G. The rise in ocean plastics evidenced from a 60-year time series. *Nature communications* **2019**, *10*, 1622, doi:https://doi.org/10.1038/s41467-019-09506-1.
15. Stubbins, A.; Law, K.L.; Muñoz, S.E.; Bianchi, T.S.; Zhu, L. Plastics in the Earth system. *Science* **2021**, *373*, 51-55, doi:https://doi.org/10.1126/science.abb0354.
16. Pathak, S.; Sneha, C.; Mathew, B.B. Bioplastics: its timeline based scenario & challenges. *J. Polym. Biopolym. Phys. Chem* **2014**, *2*, 84-90, doi:https://doi.org/10.12691/jpbpc-2-4-5.
17. Arif, A.; Azeem, F.; Rasul, I.; Siddique, M.H.; Zubair, M.; Muneer, F.; Zaheer, W.; Nadeem, H. Bioplastics from waste biomass of marine and poultry industries. *Journal of Biosciences* **2023**, *48*, doi:https://doi.org/10.1007/s12038-023-00332-8.
18. Nizamuddin, S.; Baloch, A.J.; Chen, C.; Arif, M.; Mubarak, N.M. Bio-based plastics, biodegradable plastics, and compostable plastics: biodegradation mechanism, biodegradability standards and environmental stratagem. *International Biodeterioration & Biodegradation* **2024**, *195*, 105887, doi:https://doi.org/10.1016/j.ibiod.2024.105887.
19. Garcia, J.M.; Robertson, M.L. The future of plastics recycling. *Science* **2017**, *358*, 870-872, doi:https://doi.org/10.1126/science.aaq0324.
20. Rashid, S.; Majeed, L.R.; Mehta, N.; Radu, T.; Martín-Fabiani, I.; Bhat, M.A. Microplastics in terrestrial ecosystems: sources, transport, fate, mitigation, and remediation strategies. *Euro-Mediterranean Journal for Environmental Integration* **2025**, 1-27, doi:https://doi.org/10.1007/s41207-025-00766-6.
21. Sharma, S.; Sharma, V.; Chatterjee, S. Contribution of plastic and microplastic to global climate change and their conjoining impacts on the environment-A review. *Science of the total environment* **2023**, *875*, 162627, doi:https://doi.org/10.1016/j.scitotenv.2023.162627.
22. Zhang, Y. Circular economy innovations: Balancing fossil fuel impact on green economic development. *Heliyon* **2024**, *10*, doi:https://doi.org/10.1016/j.heliyon.2024.e36708.
23. Cook, E.; Cano, N.S.d.S.L.; Velis, C.A. Informal recycling sector contribution to plastic pollution mitigation: A systematic scoping review and quantitative analysis of prevalence and productivity. *Resources, Conservation and Recycling* **2024**, *206*, 107588, doi:https://linkinghub.elsevier.com/retrieve/pii/S0921344924001824.
24. Asif, M.; Siddique, M.; Abbas, A.; Abubakar, A.M.; Pandit, G.K.; Selele, M.I. Production of sustainable bioplastic derived from renewable lignocellulosic agricultural biomass: a comprehensive review. *Frontiers in Water and Environment* **2024**, *4*, 1-14, doi:https://doi.org/10.37934/fwe.4.1.114.
25. Mujtaba, M.; Fraceto, L.F.; Fazeli, M.; Mukherjee, S.; Savassa, S.M.; de Medeiros, G.A.; Santo Pereira, A.d.E.; Mancini, S.D.; Lipponen, J.; Vilaplana, F. Lignocellulosic biomass from agricultural waste to the circular economy: a review with focus on biofuels, biocomposites and bioplastics. *Journal of cleaner production* **2023**, *402*, 136815, doi:https://doi.org/10.1016/j.jclepro.2023.136815.
26. Ali, S.S.; Abdelkarim, E.A.; Elsamahy, T.; Al-Tohamy, R.; Li, F.; Kornaros, M.; Zuorro, A.; Zhu, D.; Sun, J. Bioplastic production in terms of life cycle assessment: A state-of-the-art review. *Environmental Science and Ecotechnology* **2023**, *15*, 100254, doi:https://doi.org/10.1016/j.ese.2023.100254.
27. Kour, M.; Chaudhary, S.; Kumar, R. Cellulose based bioplastics: A sustainable approach toward environmental safety-A review. *Sustainable Materials and Technologies* **2025**, e01694, doi:https://doi.org/10.1016/j.susmat.2025.e01694.

28. Raj, T.; Chandrasekhar, K.; Kumar, A.N.; Kim, S.-H. Lignocellulosic biomass as renewable feedstock for biodegradable and recyclable plastics production: A sustainable approach. *Renewable and Sustainable Energy Reviews* **2022**, *158*, 112130, doi:https://doi.org/10.1016/j.rser.2022.112130.
29. Abolore, R.S.; Jaiswal, S.; Jaiswal, A.K. Green and sustainable pretreatment methods for cellulose extraction from lignocellulosic biomass and its applications: A review. *Carbohydrate Polymer Technologies and Applications* **2024**, *7*, 100396, doi:https://doi.org/10.1016/j.carpta.2023.100396.
30. Sharma, G.; Kumar, M.; Pandey, A.K.; Kumari, S.; Singh, A.; Ansari, N.A.; Gaur, N.A. Pretreatment technologies for valorisation of lignocellulosic biomass towards sustainable biorefineries: Comprehensive insights and advances. *Bioresource Technology Reports* **2025**, 102336, doi:https://doi.org/10.1016/j.biteb.2025.102336.
31. Wong, J.L.; Khadaroo, S.N.B.A.; Cheng, J.L.Y.; Chew, J.J.; Khaerudini, D.S.; Sunarso, J. Green solvent for lignocellulosic biomass pretreatment: An overview of the performance of low transition temperature mixtures for enhanced bio-conversion. *Next Materials* **2023**, *1*, 100012, doi:https://doi.org/10.1016/j.nxmate.2023.100012.
32. Tang, X.; Zuo, M.; Li, Z.; Liu, H.; Xiong, C.; Zeng, X.; Sun, Y.; Hu, L.; Liu, S.; Lei, T. Green processing of lignocellulosic biomass and its derivatives in deep eutectic solvents. *ChemSusChem* **2017**, *10*, 2696-2706, doi:https://doi.org/10.1002/cssc.201700457.
33. Satlewal, A.; Agrawal, R.; Bhagia, S.; Sangoro, J.; Ragauskas, A.J. Natural deep eutectic solvents for lignocellulosic biomass pretreatment: recent developments, challenges and novel opportunities. *Biotechnology advances* **2018**, *36*, 2032-2050, doi:https://doi.org/10.1016/j.biotechadv.2018.08.009
34. Chen, Y.; Mu, T. Application of deep eutectic solvents in biomass pretreatment and conversion. *Green Energy & Environment* **2019**, *4*, 95-115, doi:https://doi.org/10.1016/j.gee.2019.01.012.
35. Ullah, A.; Zhang, Y.; Liu, C.; Qiao, Q.; Shao, Q.; Shi, J. Process intensification strategies for green solvent mediated biomass pretreatment. *Bioresource Technology* **2023**, *369*, 128394, doi:https://doi.org/10.1016/j.biortech.2022.128394.
36. Storz, H. Bio-based plastics: status, challenges and trends. *Appl Agric Forestry Res* **2013**, *4*, 321-332, doi:https://doi.org/10.3220/LBF_2013_321-332.
37. Ling, M.H.Y.; Hooper, J.; Pushpamalar, J. Sustainable production of polyethylene glycol and furandicarboxylic acid copolymer (PEG-co-FDCA) from oil palm empty fruit bunch. *Industrial Crops and Products* **2025**, *227*, 120740, doi:https://doi.org/10.1016/j.indcrop.2025.120740.
38. Fei, X.; Wang, J.; Zhang, X.; Jia, Z.; Jiang, Y.; Liu, X. Recent progress on bio-based polyesters derived from 2, 5-furandicarbonxylic acid (FDCA). *Polymers* **2022**, *14*, 625, doi:https://doi.org/10.3390/polym14030625.
39. Annatelli, M.; Sánchez-Velandia, J.E.; Mazzi, G.; Pandeirada, S.V.; Giannakoudakis, D.; Rautiainen, S.; Esposito, A.; Thiyagarajan, S.; Richel, A.; Triantafyllidis, K.S. Beyond 2, 5-furandicarboxylic acid: status quo, environmental assessment, and blind spots of furanic monomers for bio-based polymers. *Green Chemistry* **2024**, *26*, 8894-8941, doi:https://doi.org/10.1039/d4gc00784k.
40. Bello, S.; Salim, I.; Méndez-Trelles, P.; Rodil, E.; Feijoo, G.; Moreira, M.T. Environmental sustainability assessment of HMF and FDCA production from lignocellulosic biomass through life cycle assessment (LCA). *Holzforschung* **2018**, *73*, 105-115, doi:https://doi.org/10.1515/hf-2018-0100.
41. Chen, G.; van Straalen, N.M.; Roelofs, D. The ecotoxicogenomic assessment of soil toxicity associated with the production chain of 2, 5-furandicarboxylic acid (FDCA), a candidate bio-based green chemical building block. *Green Chemistry* **2016**, *18*, 4420-4431, doi:https://doi.org/10.1039/C6GC00430J.
42. Yuan, H.; Li, J.; Shin, H.-d.; Du, G.; Chen, J.; Shi, Z.; Liu, L. Improved production of 2, 5-furandicarboxylic acid by overexpression of 5-hydroxymethylfurfural oxidase and 5-hydroxymethylfurfural/furfural oxidoreductase in Raoultella ornithinolytica BF60. *Bioresource technology* **2018**, *247*, 1184-1188, doi:https://doi.org/10.1016/j.biortech.2017.08.166.
43. Kim, H.; Lee, S.; Ahn, Y.; Lee, J.; Won, W. Sustainable production of bioplastics from lignocellulosic biomass: technoeconomic analysis and life-cycle assessment. *ACS Sustainable Chemistry & Engineering* **2020**, *8*, 12419-12429, doi:https://doi.org/10.1021/acssuschemeng.0c02872.

44. Luo, K.; Wang, Y.; Yu, J.; Zhu, J.; Hu, Z. Semi-bio-based aromatic polyamides from 2, 5-furandicarboxylic acid: toward high-performance polymers from renewable resources. *RSC Advances* **2016**, *6*, 87013-87020, doi:https://doi.org/10.1039/C6RA15797A.
45. Sajid, M.; Zhao, X.; Liu, D. Production of 2, 5-furandicarboxylic acid (FDCA) from 5-hydroxymethylfurfural (HMF): recent progress focusing on the chemical-catalytic routes. *Green chemistry* **2018**, *20*, 5427-5453, doi:https://doi.org/10.1039/C8GC02680G.
46. Wang, J.; Liu, X.; Jia, Z.; Sun, L.; Zhu, J. Highly crystalline polyesters synthesized from furandicarboxylic acid (FDCA): Potential bio-based engineering plastic. *European Polymer Journal* **2018**, *109*, 379-390, doi:https://doi.org/10.1016/j.eurpolymj.2018.10.014.
47. Tang, Z.; Su, J. Direct conversion of cellulose to 5-hydroxymethylfurfural (HMF) using an efficient and inexpensive boehmite catalyst. *Carbohydrate research* **2019**, *481*, 52-59, doi:https://doi.org/10.1016/j.carres.2019.06.010
48. Zhang, Y.; Jin, P.; Liu, M.; Pan, J.; Yan, Y.; Chen, Y.; Xiong, Q. A novel route for green conversion of cellulose to HMF by cascading enzymatic and chemical reactions. *AIChE Journal* **2017**, *63*, 4920-4932, doi:https://doi.org/10.1002/aic.15841.
49. Nakajima, H.; Dijkstra, P.; Loos, K. The recent developments in biobased polymers toward general and engineering applications: Polymers that are upgraded from biodegradable polymers, analogous to petroleum-derived polymers, and newly developed. *Polymers* **2017**, *9*, 523, doi:https://doi.org/10.3390/polym9100523.
50. Senila, L.; Kovacs, E.; Resz, M.-A.; Senila, M.; Becze, A.; Roman, C. Life Cycle Assessment (LCA) of Bioplastics Production from Lignocellulosic Waste (Study Case: PLA and PHB). *Polymers* **2024**, *16*, 3330, doi:https://doi.org/10.3390/polym16233330.
51. Bioplastics, E. Bioplastics market development update 2023. *European Bioplastics eV: Berlin, Germany* **2023**.
52. Bioplastics, E. Global Production Capacities of Bioplastics 2019–2024. *Europe Bioplastics: Berlin, Germany* **2019**.
53. Chinthapalli, R.; Skoczinski, P.; Carus, M.; Baltus, W.; De Guzman, D.; Käb, H.; Raschka, A.; Ravenstijn, J. Biobased building blocks and polymers—global capacities, production and trends, 2018–2023. *Industrial Biotechnology* **2019**, *15*, 237-241, doi:https://doi.org/10.1089/ind.2019.29179.rch.
54. Di Sabatino, R.; Kersten, S.R.; Lange, J.-P.; Ruiz, M.P. Lignocellulosic biomass to glycols: Simultaneous conversion of cellulose, hemicellulose and lignin using an organic solvent. *Biomass and Bioenergy* **2024**, *187*, 107307, doi:https://doi.org/10.1016/j.biombioe.2024.107307.
55. Sharma, H.K.; Xu, C.; Qin, W. Biological pretreatment of lignocellulosic biomass for biofuels and bioproducts: an overview. *Waste and Biomass Valorization* **2019**, *10*, 235-251, doi:https://doi.org/10.1007/s12649-017-0059-y.
56. Assad, H.; Lone, I.A.; Kumar, A.; Kumar, A. Leveraging lignocellulosic biomass for sustainable energy storage solutions. In *Materials for Boosting Energy Storage. Volume 2: Advances in Sustainable Energy Technologies*; ACS Publications: 2024; pp. 177-201.
57. Okolie, J.A.; Nanda, S.; Dalai, A.K.; Kozinski, J.A. Chemistry and specialty industrial applications of lignocellulosic biomass. *Waste and Biomass Valorization* **2021**, *12*, 2145-2169, doi:https://doi.org/10.1007/s12649-020-01123-0.
58. Rosson, L.; Tan, B.; Best, W.; Byrne, N. Applications of regenerated bacterial cellulose: a review. *Cellulose* **2024**, *31*, 10165-10190, doi:https://doi.org/10.1007/s10570-024-06220-0.
59. Chakraborty, P.; Kumar, R.; Chakrabortty, S.; Saha, S.; Chattaraj, S.; Roy, S.; Banerjee, A.; Tripathy, S.K.; Ghosh, A.K.; Jeon, B.-H. Technological advancements in the pretreatment of lignocellulosic biomass for effective valorization: A review of challenges and prospects. *Journal of Industrial and Engineering Chemistry* **2024**, *137*, 29-60, doi:https://doi.org/10.1016/j.jiec.2024.03.025.
60. Creteanu, A.; Lungu, C.N.; Lungu, M. Lignin: an adaptable biodegradable polymer used in different formulation processes. *Pharmaceuticals* **2024**, *17*, 1406, doi:https://doi.org/10.3390/ph17101406.
61. Haberzettl, J.; Hilgert, P.; von Cossel, M. A critical review on lignocellulosic biomass yield modeling and the bioenergy potential from marginal land. *Agronomy* **2021**, *11*, 2397, doi:https://doi.org/10.3390/agronomy11122397.

62. Megías-Sayago, C.; Navarro-Jaén, S.; Drault, F.; Ivanova, S. Recent advances in the Brønsted/lewis acid catalyzed conversion of glucose to HMF and lactic acid: pathways toward bio-based plastics. *Catalysts* **2021**, *11*, 1395, doi:https://doi.org/10.3390/catal11111395.
63. Rathour, R.K.; Behl, M.; Sakhuja, D.; Kumar, N.; Sharma, N.; Walia, A.; Bhatt, A.K.; Bhatia, R.K. Recent Updates in Biomass Pretreatment Techniques for a Sustainable Biofuel Industry: A Comprehensive Review. *Waste and Biomass Valorization* **2025**, 1-26, doi:https://doi.org/10.1007/s12649-025-03016-6.
64. Woźniak, A.; Kuligowski, K.; Świerczek, L.; Cenian, A. Review of lignocellulosic biomass pretreatment using physical, thermal and chemical methods for higher yields in bioethanol production. *Sustainability* **2025**, *17*, 287, doi:https://doi.org/10.3390/su17010287.
65. Ilangovan, A.; Balakrishnan, A.; Kanchinadham, S.B.K. Conversion of lignocellulosic waste biomass into valuable derivatives and their pretreatment potential: An overview. *Environmental Progress & Sustainable Energy* **2025**, *44*, e70021, doi:https://doi.org/10.1002/ep.70021.
66. Tessera, G.M.; Habtu, N.G.; Abera, M.K.; Misganaw, F.W. Advances in electromagnetic radiation-assisted pretreatment of lignocellulosic biomass as a green method: a review. *Biomass Conversion and Biorefinery* **2025**, *15*, 13165-13189, doi:https://doi.org/10.1007/s13399-024-06301-x.
67. Chen, J.; Ma, X.; Liang, M.; Guo, Z.; Cai, Y.; Zhu, C.; Wang, Z.; Wang, S.; Xu, J.; Ying, H. Physical–chemical–biological pretreatment for biomass degradation and industrial applications: A review. In Proceedings of the Waste, 2024; pp. 451-473.
68. Woiciechowski, A.L.; Neto, C.J.D.; de Souza Vandenberghe, L.P.; de Carvalho Neto, D.P.; Sydney, A.C.N.; Letti, L.A.J.; Karp, S.G.; Torres, L.A.Z.; Soccol, C.R. Lignocellulosic biomass: Acid and alkaline pretreatments and their effects on biomass recalcitrance–Conventional processing and recent advances. *Bioresource technology* **2020**, *304*, 122848, doi:https://doi.org/10.1016/j.biortech.2020.122848.
69. Di Fraia, A.; Di Fraia, S.; Massarotti, N. Role of advanced oxidation processes in lignocellulose pretreatment towards biorefinery applications: a review on emerging trends and economic considerations. *Green Chemistry* **2024**, doi:https://doi.org/10.1039/D3GC05108K.
70. Chowdari, R.K.; Ganji, P.; Likozar, B. Solvent-Free Catalytic Hydrotreatment of Lignin to Biobased Aromatics: Current Trends, Industrial Approach, and Future Perspectives. *Energy & Fuels* **2024**, *39*, 2943-2985, doi:https://doi.org/10.1021/acs.energyfuels.4c05174.
71. Ovejero-Pérez, A.; Nakasu, P.Y.; Hopson, C.; Costa, J.M.; Hallett, J.P. Challenges and opportunities on the utilisation of ionic liquid for biomass pretreatment and valorisation. *npj Materials Sustainability* **2024**, *2*, 7, doi:https://doi.org/10.1038/s44296-024-00015-x.
72. Gladysheva, E.K. Liquid Hot Water and Steam Explosion Pretreatment Methods for Cellulosic Raw Materials: A Review. *Polymers* **2025**, *17*, 1783, doi:https://doi.org/10.3390/polym17131783.
73. Manzoor, M.H.; Elsayed, I.; Hassan, E.B. Optimization of Hemicellulosic Carbohydrate Extraction from Corncobs via Hydrothermal Treatment: A Response Surface Methodology Approach. *Sustainable Chemistry* **2025**, *6*, 27, doi:https://doi.org/10.3390/suschem6030027.
74. Balan, V.; Mohammadi, M.; Dale, B.E. Advancements in ammonia-based pretreatment: key benefits and industry applications. *RSC Sustainability* **2025**, doi:https://doi.org/10.1039/D5SU00070J.
75. Kıdak, R. Enhancement of biogas production by means of ultrasonic pre-treatment: State of art and review. *Environmental Research and Technology* **2025**, *8*, 487-498, doi:https://doi.org/10.35208/ert.1521758.
76. Joshi, M.; Manjare, S. Chemical approaches for the biomass valorisation: a comprehensive review of pretreatment strategies. *Environmental Science and Pollution Research* **2024**, *31*, 48928-48954, doi:https://doi.org/10.1007/s11356-024-34473-6.
77. Steinbach, D.; Kruse, A.; Sauer, J. Pretreatment technologies of lignocellulosic biomass in water in view of furfural and 5-hydroxymethylfurfural production- A review. *Biomass Conversion and Biorefinery* **2017**, *7*, 247-274, doi:https://dx.doi.org/10.1007/s13399-017-0243-0.
78. Wu, Z.; Yu, Y.; Wu, H. Hydrothermal Reactions of Biomass-Derived Platform Molecules: Mechanistic Insights into 5-Hydroxymethylfurfural (5-HMF) Formation during Glucose and Fructose Decomposition. *Energy & Fuels* **2023**, *37*, 2115-2126, doi:https://dx.doi.org/10.1021/acs.energyfuels.2c03462.

79. Jiang, Z.; Zeng, Y.; Hu, D.; Guo, R.; Yan, K.; Luque, R. Chemical transformations of 5-hydroxymethylfurfural into highly added value products: present and future. *Green Chemistry* **2023**, *25*, 871-892, doi:https://doi.org/10.1039/d2gc03444a.
80. Maleki, F.; Bararzadeh Ledari, M.; Fani, M. Integrated analysis of a hydrogen-based port: Energy, exergy, environmental, and economic sustainability. *International Journal of Hydrogen Energy* **2025**, *100*, 1402-1420, doi:https://doi.org/10.1016/j.ijhydene.2024.12.332.
81. Oyegoke, T.; Dumeignil, F.; E.-Yakubu Jibril, B.; Michel, C.; Wojcieszak, R. Exploring catalytic oxidation pathways of furfural and 5-hydroxymethyl furfural into carboxylic acids using Au, Pt, and Pd catalysts: a comprehensive review. *Catalysis Science & Technology* **2024**, *14*, 6761-6774, doi:https://doi.org/10.1039/d4cy00821a.
82. Sayed, M.; Gaber, Y.; Junghus, F.; Martín, E.V.; Pyo, S.H.; Hatti-Kaul, R. Oxidation of 5-hydroxymethylfurfural with a novel aryl alcohol oxidase from Mycobacterium sp. MS1601. *Microbial Biotechnology* **2022**, *15*, 2176-2190, doi:https://dx.doi.org/10.1111/1751-7915.14052.
83. Arias, P.L.; Cecilia, J.A.; Gandarias, I.; Iglesias, J.; López Granados, M.; Mariscal, R.; Morales, G.; Moreno-Tost, R.; Maireles-Torres, P. Oxidation of lignocellulosic platform molecules to value-added chemicals using heterogeneous catalytic technologies. *Catalysis Science & Technology* **2020**, *10*, 2721-2757, doi:https://doi.org/10.1039/d0cy00240b.
84. Liu, B.; Liu, H.; Sun, S.; Ma, Z.; Zhang, Y.; Nie, R.; Fu, J. Hydrothermal Redox Driven Phase and Defect Engineering of MnO₂ for Enhanced HMF Oxidation at Ambient Oxygen Pressure. *Advanced Functional Materials* **2025**, doi:https://doi.org/10.1002/adfm.202504172.
85. Hayashi, E.; Yamaguchi, Y.; Kamata, K.; Tsunoda, N.; Kumagai, Y.; Oba, F.; Hara, M. Effect of MnO₂ Crystal Structure on Aerobic Oxidation of 5-Hydroxymethylfurfural to 2,5-Furandicarboxylic Acid. *Journal of the American Chemical Society* **2019**, *141*, 890-900, doi:https://doi.org/10.1021/jacs.8b09917.
86. Bao, L.; Sun, F.Z.; Zhang, G.Y.; Hu, T.L. Aerobic Oxidation of 5-Hydroxymethylfurfural to 2,5-Furandicarboxylic Acid over Holey 2 D Mn₂O₃ Nanoflakes from a Mn-based MOF. *ChemSusChem* **2020**, *13*, 548-555, doi:https://doi.org/10.1002/cssc.201903018.
87. Yao, Y.-F.; Wang, G.-C. Mechanism Insights into the Aerobic Oxidation of 5-Hydroxymethylfurfural to 2,5-Furandicarboxylic Acid over MnO₂ Catalysts. *The Journal of Physical Chemistry C* **2021**, *125*, 3818-3826, doi:https://doi.org/10.1021/acs.jpcc.0c09545.
88. Liao, W.; Yang, S.; Liu, Y.; Yin, Q.; Tang, X.; Lin, L.; Sun, Y. Aerobic oxidation of 5-hydroxymethylfurfural to 2,5-furandicarboxylic acid by modification of the crystalline structure of MnO2 for catalytic purposes. *Molecular Catalysis* **2025**, *578*, 114995, doi:https://doi.org/10.1016/j.mcat.2025.114995.
89. Yu, L.; Chen, H.; Wen, Z.; Jin, M.; Ma, X.; Li, Y.; Sang, Y.; Chen, M.; Li, Y. Efficient Aerobic Oxidation of 5-Hydroxymethylfurfural to 2, 5-Furandicarboxylic Acid over a Nanofiber Globule La-MnO₂ Catalyst. *Industrial & Engineering Chemistry Research* **2021**, *60*, 1624-1632, doi:https://doi.org/10.1021/acs.iecr.0c05561.
90. Liu, Q.; Gong, Y.; Zeng, J.; Zhao, Y.; Lv, J.; Jiang, Z.; Hu, C.; Zhou, Y. Strategic Metal Doping in MnO_x Catalysts Unlocks High-Yield 2,5-Furandicarboxylic Acid Production via Tailored Lattice Oxygen Activity and Oxygen Vacancies. *ACS Sustainable Chemistry & Engineering* **2025**, *13*, 2107-2119, doi:https://doi.org/10.1021/acssuschemeng.4c09055.
91. Gao, Y.; Fan, S.; Zhu, B.; El-Hout, S.I.; Lyu, J.; Zhang, J.; Chen, C. Cobalt and nitrogen co-modified graphitic carbon: A bifunctional catalyst for thermocatalytic and electrocatalytic oxidation of HMF to FDCA. *Catalysis Today* **2024**, *440*, 114847, doi:https://doi.org/10.1016/j.cattod.2024.114847.
92. Li, Y.; Wang, Y.; Gao, H.; Zhang, Z.; Chen, L.; Liao, X. Tunable products of 5-hydroxymethylfurfural oxidation by Zn/Co-ZIF derived catalysts. *Applied Catalysis A: General* **2024**, *678*, 119712, doi:https://doi.org/10.1016/j.apcata.2024.119712.
93. Gao, L.; Deng, K.; Zheng, J.; Liu, B.; Zhang, Z. Efficient oxidation of biomass derived 5-hydroxymethylfurfural into 2,5-furandicarboxylic acid catalyzed by Merrifield resin supported cobalt porphyrin. *Chemical Engineering Journal* **2015**, *270*, 444-449, doi:https://doi.org/10.1016/j.cej.2015.02.068.

94. Fang, R.; Tian, P.; Yang, X.; Luque, R.; Li, Y. Encapsulation of ultrafine metal-oxide nanoparticles within mesopores for biomass-derived catalytic applications. *Chemical Science* **2018**, *9*, 1854-1859, doi:https://doi.org/10.1039/c7sc04724j.
95. Zhang, S.; Sun, X.; Zheng, Z.; Zhang, L. Nanoscale center-hollowed hexagon MnCo2O4 spinel catalyzed aerobic oxidation of 5-hydroxymethylfurfural to 2,5-furandicarboxylic acid. *Catalysis Communications* **2018**, *113*, 19-22, doi:https://dx.doi.org/10.1016/j.catcom.2018.05.004.
96. Zhu, R.; Gao, F.; Li, X. Bimetallic Co-Mn catalyzed chemselective oxidation of 5-hydroxymethylfurfural to 2,5-furandicarboxylic acid. *Molecular Catalysis* **2025**, *580*, 115135, doi:https://dx.doi.org/10.1016/j.mcat.2025.115135.
97. Li, M.; Hu, S.; Zhang, Y.; Qin, J.; Min, D.; Chen, C.; Zhang, P.; Jiang, L.; Zhang, J. Regulation of oxygen vacancy in Mn-Co oxides to enhance selective oxidation of 5-hydroxymethylfurfural to 2,5-furandicarboxylic acid. *Applied Catalysis B: Environment and Energy* **2025**, *368*, 125130, doi:https://doi.org/10.1016/j.apcatb.2025.125130.
98. Rao, K.T.V.; Rogers, J.L.; Souzanchi, S.; Dessbesell, L.; Ray, M.B.; Xu, C. Inexpensive but Highly Efficient Co–Mn Mixed-Oxide Catalysts for Selective Oxidation of 5-Hydroxymethylfurfural to 2,5-Furandicarboxylic Acid. *ChemSusChem* **2018**, *11*, 3323-3334, doi:https://dx.doi.org/10.1002/cssc.201800989.
99. Zuo, X.; Venkitasubramanian, P.; Busch, D.H.; Subramaniam, B. Optimization of Co/Mn/Br-Catalyzed Oxidation of 5-Hydroxymethylfurfural to Enhance 2,5-Furandicarboxylic Acid Yield and Minimize Substrate Burning. *ACS Sustainable Chemistry & Engineering* **2016**, *4*, 3659-3668, doi:https://dx.doi.org/10.1021/acssuschemeng.6b00174.
100. Jain, A.; Jonnalagadda, S.C.; Ramanujachary, K.V.; Mugweru, A. Selective oxidation of 5-hydroxymethyl-2-furfural to furan-2,5-dicarboxylic acid over spinel mixed metal oxide catalyst. *Catalysis Communications* **2015**, *58*, 179-182, doi:https://doi.org/10.1016/j.catcom.2014.09.017.
101. Mei, N.; Liu, B.; Zheng, J.; Lv, K.; Tang, D.; Zhang, Z. A novel magnetic palladium catalyst for the mild aerobic oxidation of 5-hydroxymethylfurfural into 2,5-furandicarboxylic acid in water. *Catalysis Science & Technology* **2015**, *5*, 3194-3202, doi:https://dx.doi.org/10.1039/C4CY01407C.
102. Perumal, S.K.; Yu, H.; Je, H.; Lee, H.; Kim, Y.; Kim, H.S. Cr-Promoted Pt@Fe_{2–x}Cr_xO₃ Hematite-Type Catalysts for Efficient Base-Free HMF Oxidation under Mild Conditions. *ACS Sustainable Chemistry & Engineering* **2025**, *13*, 17470-17482, doi:https://dx.doi.org/10.1021/acssuschemeng.5c07366.
103. Kalimuthu, K.; Poonsawat, T.; Chumkaeo, P.; Somsook, E. Oxidation of 5-HMF Catalyzed by N-Doped Carbon-Supported Non-Noble Metal Catalysts. *ACS Omega* **2025**, *10*, 44415-44424, doi: https://doi.org/10.1021/acsomega.5c06288.
104. Liu, B.; Liu, H.; Wang, H.; Ma, Z.; Cheng, X.; Chang, C.; Nie, R. Solid-state synthesis of CN-encapsulated CoFe alloy catalysts for mild HMF oxidation to FDCA: insights into the kinetics and mechanism. *Dalton Transactions* **2025**, *54*, 1013-1020, doi:https://doi.org/10.1039/d4dt02890b.
105. Chamberlain, T.W.; Degirmenci, V.; Walton, R.I. Oxidation of 5-Hydroxymethyl Furfural to 2,5-Furan Dicarboxylic Acid Under Mild Aqueous Conditions Catalysed by MIL-100(Fe) Metal-Organic Framework. *ChemCatChem* **2022**, *14*, doi:https://doi.org/10.1002/cctc.202200135.
106. Yan, D.; Xin, J.; Zhao, Q.; Gao, K.; Lu, X.; Wang, G.; Zhang, S. Fe–Zr–O catalyzed base-free aerobic oxidation of 5-HMF to 2,5-FDCA as a bio-based polyester monomer. *Catalysis Science & Technology* **2018**, *8*, 164-175, doi:https://dx.doi.org/10.1039/C7CY01704A.
107. Liu, X.; Xiao, J.; Ding, H.; Zhong, W.; Xu, Q.; Su, S.; Yin, D. Catalytic aerobic oxidation of 5-hydroxymethylfurfural over VO2+ and Cu2+ immobilized on amino functionalized SBA-15. *Chemical Engineering Journal* **2016**, *283*, 1315-1321, doi:https://doi.org/10.1016/j.cej.2015.08.022.
108. Zhang, Z.; Liu, B.; Lv, K.; Sun, J.; Deng, K. Aerobic oxidation of biomass derived 5-hydroxymethylfurfural into 5-hydroxymethyl-2-furancarboxylic acid catalyzed by a montmorillonite K-10 clay immobilized molybdenum acetylacetonate complex. *Green Chemistry* **2014**, *16*, 2762, doi:https://dx.doi.org/10.1039/C4GC00062E.

109. Wang, S.; Liu, B.; Yuan, Z.; Zhang, Z. Aerobic oxidation of 5-hydroxymethylfurfural into furan compounds over Mo-hydroxyapatite-encapsulated magnetic γ-Fe 2 O 3. *Journal of the Taiwan Institute of Chemical Engineers* **2016**, *58*, 92-96, doi:https://dx.doi.org/10.1016/j.jtice.2015.06.002.
110. Li, S.; Su, K.; Li, Z.; Cheng, B. Selective oxidation of 5-hydroxymethylfurfural with H₂O₂ catalyzed by a molybdenum complex. *Green Chemistry* **2016**, *18*, 2122-2128, doi:https://doi.org/10.1039/c5gc01991e.
111. Barwe, S.; Weidner, J.; Cychy, S.; Morales, D.M.; Dieckhöfer, S.; Hiltrop, D.; Masa, J.; Muhler, M.; Schuhmann, W. Electrocatalytic Oxidation of 5-(Hydroxymethyl)furfural Using High-Surface-Area Nickel Boride. *Angewandte Chemie International Edition* **2018**, *57*, 11460-11464, doi:https://doi.org/10.1002/anie.201806298.
112. Yang, S.; Guo, Y.; Zhao, Y.; Zhang, L.; Shen, H.; Wang, J.; Li, J.; Wu, C.; Wang, W.; Cao, Y.; et al. Construction of Synergistic Ni₃S₂-MoS₂ Nanoheterojunctions on Ni Foam as Bifunctional Electrocatalyst for Hydrogen Evolution Integrated with Biomass Valorization. *Small* **2022**, *18*, 2201306, doi:https://doi.org/10.1002/smll.202201306.
113. Xiao, R.; Zhao, W.; Yang, Q.; He, A.; Tang, X.; Shen, C. Oxygen vacancies modulate reactive oxygen species for high-efficiency photocatalytic synthesis of 2,5-furandicarboxylic acid. *Journal of Catalysis* **2025**, 116472, doi:https://dx.doi.org/10.1016/j.jcat.2025.116472.
114. Xu, S.; Zhou, P.; Zhang, Z.; Yang, C.; Zhang, B.; Deng, K.; Bottle, S.; Zhu, H. Selective Oxidation of 5-Hydroxymethylfurfural to 2,5-Furandicarboxylic Acid Using O₂ and a Photocatalyst of Co-thioporphyrazine Bonded to g-C₃N₄. *Journal of the American Chemical Society* **2017**, *139*, 14775-14782, doi:https://dx.doi.org/10.1021/jacs.7b08861.
115. Han, X.; Li, C.; Liu, X.; Xia, Q.; Wang, Y. Selective oxidation of 5-hydroxymethylfurfural to 2,5-furandicarboxylic acid over MnO_x–CeO₂ composite catalysts. *Green Chemistry* **2017**, *19*, 996-1004, doi:https://doi.org/10.1039/c6gc03304k.
116. Zhao, D.; Su, T.; Wang, Y.; Varma, R.S.; Len, C. Recent advances in catalytic oxidation of 5-hydroxymethylfurfural. *Molecular Catalysis* **2020**, *495*, 111133, doi:https://dx.doi.org/10.1016/j.mcat.2020.111133.
117. Neațu, F.; Marin, R.S.; Florea, M.; Petrea, N.; Pavel, O.D.; Pârvulescu, V.I. Selective oxidation of 5-hydroxymethyl furfural over non-precious metal heterogeneous catalysts. *Applied Catalysis B: Environmental* **2016**, *180*, 751-757, doi:https://doi.org/10.1016/j.apcatb.2015.07.043.
118. Wang, S.; Zhang, Z.; Liu, B. Catalytic Conversion of Fructose and 5-Hydroxymethylfurfural into 2,5-Furandicarboxylic Acid over a Recyclable Fe₃O₄–CoO_x Magnetite Nanocatalyst. *ACS Sustainable Chemistry & Engineering* **2015**, *3*, 406-412, doi:https://dx.doi.org/10.1021/sc500702q.
119. Saha, B.; Gupta, D.; Abu-Omar, M.M.; Modak, A.; Bhaumik, A. Porphyrin-based porous organic polymer-supported iron(III) catalyst for efficient aerobic oxidation of 5-hydroxymethyl-furfural into 2,5-furandicarboxylic acid. *Journal of Catalysis* **2013**, *299*, 316-320, doi:https://dx.doi.org/10.1016/j.jcat.2012.12.024.
120. Tong, X.; Yu, L.; Chen, H.; Zhuang, X.; Liao, S.; Cui, H. Highly efficient and selective oxidation of 5-hydroxymethylfurfural by molecular oxygen in the presence of Cu-MnO2 catalyst. *Catalysis Communications* **2017**, *90*, 91-94, doi:https://dx.doi.org/10.1016/j.catcom.2016.11.024.
121. Lin, J.-Y.; Yuan, M.-H.; Lin, K.-Y.A.; Lin, C.-H. Selective aerobic oxidation of 5-hydroxymethylfurfural to 2,5-diformylfuran catalyzed by Cu-based metal organic frameworks with 2,2,6,6-tetramethylpiperidin-oxyl. *Journal of the Taiwan Institute of Chemical Engineers* **2019**, *102*, 242-249, doi:https://doi.org/10.1016/j.jtice.2019.06.008.
122. Mannam, S.; Sekar, G. CuCl catalyzed selective oxidation of primary alcohols to carboxylic acids with tert-butyl hydroperoxide at room temperature. *Tetrahedron Letters* **2008**, *49*, 2457-2460, doi:https://doi.org/10.1016/j.tetlet.2008.02.031.
123. Hansen, T.S.; Sádaba, I.; García-Suárez, E.J.; Riisager, A. Cu catalyzed oxidation of 5-hydroxymethylfurfural to 2,5-diformylfuran and 2,5-furandicarboxylic acid under benign reaction conditions. *Applied Catalysis A: General* **2013**, *456*, 44-50, doi:https://doi.org/10.1016/j.apcata.2013.01.042.

 doi:10.20944/preprints202601.1587.v1

124. Ventura, M.; Aresta, M.; Dibenedetto, A. Selective Aerobic Oxidation of 5-(Hydroxymethyl)furfural to 5-Formyl-2-furancarboxylic Acid in Water. *ChemSusChem* **2016**, *9*, 1096-1100, doi:https://dx.doi.org/10.1002/cssc.201600060.
125. Chen, B.; Hou, Q.; Smith, R.L.; Qi, X.; Guo, H. Electrocatalytic oxidation of biomass-derived furans to 2,5-furandicarboxylic acid – a review. *Green Chemistry* **2025**, *27*, 8414-8447, doi:https://doi.org/10.1039/d5gc01181g.
126. Li, X.-L.; Zhu, R.; Xu, H.-J. Recent Advances in Direct Synthesis of 2,5-Furandicarboxylic Acid from Carbohydrates. *ACS Sustainable Chemistry & Engineering* **2025**, *13*, 2223-2259, doi:https://doi.org/10.1021/acssuschemeng.4c09659.
127. Zhu, P.; Zhang, W.; Li, Q.; Xia, H. Visible-Light-Driven Photocatalytic Oxidation of 5-Hydroxymethylfurfural to 2,5-Furandicarboxylic Acid over Plasmonic Au/ZnO Catalyst. *ACS Sustainable Chemistry & Engineering* **2022**, *10*, 8778-8787, doi:https://dx.doi.org/10.1021/acssuschemeng.2c01143.
128. Zhang, X.; Liu, A.; Li, X.; Xu, W.; Duan, X.; Shi, J.; Li, X. Research progress of deep eutectic solvents in lignocellulosic biomass pretreatment. *Cellulose* **2025**, 1-14, doi:https://doi.org/10.1007/s10570-025-06553-4.
129. de Jong, E.; Dam, M.A.; Sipos, L.; Gruter, G.J.M. Furandicarboxylic Acid (FDCA), A Versatile Building Block for a Very Interesting Class of Polyesters. In *Biobased Monomers, Polymers, and Materials*; ACS Symposium Series; American Chemical Society: 2012; Volume 1105, pp. 1-13.
130. Qu, L.; Kong, F.; Chen, X.; Zhang, Y.; Lin, Z.; Ni, X.; Zhang, X.; Lu, Q.; Zhao, Y.; Zou, B. Progress in Research on the Preparation of 2, 5-Furandicarboxylic Acid by Hydroxymethylfurfural Oxidation. *Catalysts* **2025**, *15*, 373, doi:https://dx.doi.org/10.3390/catal15040373.
131. Zhang, Y.; Jia, G.; Wang, W.; Jiang, L.; Guo, Z. Photocatalytic upgrading of 5-hydroxymethylfurfural – aerobic or anaerobic? *Green Chemistry* **2024**, *26*, 2949-2966, doi:https://dx.doi.org/10.1039/D3GC04814D.
132. Yang, B.; Hu, W.; Wan, F.; Zhang, C.; Fu, Z.; Su, A.; Chen, M.; Liu, Y. Adjusting effect of additives on decatungstate-photocatalyzed HMF oxidation with molecular oxygen under visible light illumination. *Chemical Engineering Journal* **2020**, *396*, 125345, doi:https://dx.doi.org/10.1016/j.cej.2020.125345.
133. Gonzalez-Casamachin, D.A.; Rivera De La Rosa, J.; Lucio–Ortiz, C.J.; Sandoval-Rangel, L.; García, C.D. Partial oxidation of 5-hydroxymethylfurfural to 2,5-furandicarboxylic acid using O2 and a photocatalyst of a composite of ZnO/PPy under visible-light: Electrochemical characterization and kinetic analysis. *Chemical Engineering Journal* **2020**, *393*, 124699, doi:https://doi.org/10.1016/j.cej.2020.124699.
134. Wang, Y.; Cai, C. Photocatalytic Oxidation of 5-Hydroxymethylfurfural to Selective Products by Noble Metal-Free Z-Scheme Heterostructures α-Fe₂O₃/Zn_{0.5}Cd_{0.5}S. *ACS Catalysis* **2025**, *15*, 3451-3463, doi:https://dx.doi.org/10.1021/acscatal.4c07189.
135. Wu, R.; Yang, J.; Jiang, Y.; Xin, F. Advances and prospects for lactic acid production from lignocellulose. *Enzyme and Microbial Technology* **2025**, *182*, 110542, doi:https://dx.doi.org/10.1016/j.enzmictec.2024.110542.
136. Augustiniene, E.; Valanciene, E.; Matulis, P.; Syrpas, M.; Jonuskiene, I.; Malys, N. Bioproduction of <scp>l</scp>- and <scp>d</scp>-lactic acids: advances and trends in microbial strain application and engineering. *Critical Reviews in Biotechnology* **2022**, *42*, 342-360, doi:https://doi.org/10.1080/07388551.2021.1940088.
137. Pleissner, D.; Venus, J. Agricultural Residues as Feedstocks for Lactic Acid Fermentation. In *Green Technologies for the Environment*; ACS Symposium Series; American Chemical Society: 2014; Volume 1186, pp. 247-263.
138. Ren, Y.; Wang, X.; Li, Y.; Li, Y.-Y.; Wang, Q. Lactic Acid Production by Fermentation of Biomass: Recent Achievements and Perspectives. *Sustainability* **2022**, *14*, 14434, doi:https://dx.doi.org/10.3390/su142114434.
139. Guan, R.; Li, X.; Wachemo, A.C.; Yuan, H.; Liu, Y.; Zou, D.; Zuo, X.; Gu, J. Enhancing anaerobic digestion performance and degradation of lignocellulosic components of rice straw by combined biological and chemical pretreatment. *Science of The Total Environment* **2018**, *637-638*, 9-17, doi:https://doi.org/10.1016/j.scitotenv.2018.04.366.
140. Haokok, C.; Lunprom, S.; Reungsang, A.; Salakkam, A. Efficient production of lactic acid from cellulose and xylan in sugarcane bagasse by newly isolated Lactiplantibacillus plantarum and Levilactobacillus

 doi:10.20944/preprints202601.1587.v1

brevis through simultaneous saccharification and co-fermentation process. *Heliyon* **2023**, *9*, e17935, doi:https://doi.org/10.1016/j.heliyon.2023.e17935.

141. Abdel-Rahman, M.A.; Tashiro, Y.; Sonomoto, K. Lactic acid production from lignocellulose-derived sugars using lactic acid bacteria: Overview and limits. *Journal of Biotechnology* **2011**, *156*, 286-301, doi:https://doi.org/10.1016/j.jbiotec.2011.06.017.
142. Garde, A.; Jonsson, G.; Schmidt, A.S.; Ahring, B.K. Lactic acid production from wheat straw hemicellulose hydrolysate by Lactobacillus pentosus and Lactobacillus brevis. *Bioresource Technology* **2002**, *81*, 217-223, doi:https://doi.org/10.1016/s0960-8524(01)00135-3.
143. Oonkhanond, B.; Jonglertjunya, W.; Srimarut, N.; Bunpachart, P.; Tantinukul, S.; Nasongkla, N.; Sakdaronnarong, C. Lactic acid production from sugarcane bagasse by an integrated system of lignocellulose fractionation, saccharification, fermentation, and ex-situ nanofiltration. *Journal of Environmental Chemical Engineering* **2017**, *5*, 2533-2541, doi:https://doi.org/10.1016/j.jece.2017.05.004.
144. He, T.; Jiang, Z.; Wu, P.; Yi, J.; Li, J.; Hu, C. Fractionation for further conversion: from raw corn stover to lactic acid. *Scientific Reports* **2016**, *6*, 38623, doi:https://doi.org/10.1038/srep38623.
145. Maas, R.H.W.; Bakker, R.R.; Jansen, M.L.A.; Visser, D.; De Jong, E.; Eggink, G.; Weusthuis, R.A. Lactic acid production from lime-treated wheat straw by Bacillus coagulans: neutralization of acid by fed-batch addition of alkaline substrate. *Applied Microbiology and Biotechnology* **2008**, *78*, 751-758, doi:https://doi.org/10.1007/s00253-008-1361-1.
146. Wang, S.; Hussain, A.; Fei, X.; Venkiteshwaran, K.; Raghavan, V. Harnessing Bioelectrochemical and Anaerobic Systems for the Degradation of Bioplastics: Application Potential and Future Directions. *Fermentation* **2025**, *11*, 610, doi:https://dx.doi.org/10.3390/fermentation11110610.
147. Wang, Q.; Zhao, X.; Chamu, J.; Shanmugam, K.T. Isolation, characterization and evolution of a new thermophilic Bacillus licheniformis for lactic acid production in mineral salts medium. *Bioresource Technology* **2011**, *102*, 8152-8158, doi:https://dx.doi.org/10.1016/j.biortech.2011.06.003.
148. Ou, M.S.; Ingram, L.O.; Shanmugam, K.T. l(+)-Lactic acid production from non-food carbohydrates by thermotolerant Bacillus coagulans. *Journal of Industrial Microbiology & Biotechnology* **2011**, *38*, 599-605, doi:https://doi.org/10.1007/s10295-010-0796-4.
149. Ojo, A.O.; De Smidt, O. Lactic Acid: A Comprehensive Review of Production to Purification. *Processes* **2023**, *11*, 688, doi:https://doi.org/10.3390/pr11030688.
150. Miura, S.; Arimura, T.; Itoda, N.; Dwiarti, L.; Feng, J.B.; Bin, C.H.; Okabe, M. Production of l-lactic acid from corncob. *Journal of Bioscience and Bioengineering* **2004**, *97*, 153-157, doi:https://doi.org/10.1016/s1389-1723(04)70184-x.
151. Bai, D.-M.; Li, S.-Z.; Liu, Z.L.; Cui, Z.-F. Enhanced l -(+)-Lactic Acid Production by an Adapted Strain of Rhizopus oryzae using Corncob Hydrolysate. *Applied Biochemistry and Biotechnology* **2008**, *144*, 79-85, doi:https://doi.org/10.1007/s12010-007-8078-y.
152. Huang, L.P.; Jin, B.; Lant, P.; Zhou, J. Simultaneous saccharification and fermentation of potato starch wastewater to lactic acid by Rhizopus oryzae and Rhizopus arrhizus. *Biochemical Engineering Journal* **2005**, *23*, 265-276, doi:https://doi.org/10.1016/j.bej.2005.01.009.
153. Zhang, Z.Y.; Jin, B.; Kelly, J.M. Enhancement of l(+)-lactic acid production using acid-adapted precultures of Rhizopus arrhizus in a bubble column reactor. *Journal of Bioscience and Bioengineering* **2009**, *108*, 344-347, doi:https://dx.doi.org/10.1016/j.jbiosc.2009.04.009.
154. Salas-Navarrete, P.C.; Rosas-Santiago, P.; Suárez-Rodríguez, R.; Martínez, A.; Caspeta, L. Adaptive responses of yeast strains tolerant to acidic pH, acetate, and supraoptimal temperature. *Applied Microbiology and Biotechnology* **2023**, *107*, 4051-4068, doi:https://dx.doi.org/10.1007/s00253-023-12556-7.
155. Tsaruk, A.; Filip, K.; Sibirny, A.; Ruchala, J. Native and Recombinant Yeast Producers of Lactic Acid: Characteristics and Perspectives. *International Journal of Molecular Sciences* **2025**, *26*, 2007, doi:https://dx.doi.org/10.3390/ijms26052007.
156. Osawa, F.; Fujii, T.; Nishida, T.; Tada, N.; Ohnishi, T.; Kobayashi, O.; Komeda, T.; Yoshida, S. Efficient production of <scp>L</scp>-lactic acid by Crabtree-negative yeast Candida boidinii. *Yeast* **2009**, *26*, 485-496, doi:https://doi.org/10.1002/yea.1702.

157. Wakai, S.; Yoshie, T.; Asai-Nakashima, N.; Yamada, R.; Ogino, C.; Tsutsumi, H.; Hata, Y.; Kondo, A. l-lactic acid production from starch by simultaneous saccharification and fermentation in a genetically engineered Aspergillus oryzae pure culture. *Bioresource Technology* **2014**, *173*, 376-383, doi:https://dx.doi.org/10.1016/j.biortech.2014.09.094.
158. Zhao, J.; Xu, L.; Wang, Y.; Zhao, X.; Wang, J.; Garza, E.; Manow, R.; Zhou, S. Homofermentative production of optically pure L-lactic acid from xylose by genetically engineered Escherichia coli B. *Microbial Cell Factories* **2013**, *12*, 57, doi:https://dx.doi.org/10.1186/1475-2859-12-57.
159. Miah, M.R.; Dong, Y.; Wang, J.; Zhu, J. Recent Progress on Sustainable 2,5-Furandicarboxylate-Based Polyesters: Properties and Applications. *ACS Sustainable Chemistry & Engineering* **2024**, *12*, 2927-2961, doi:https://doi.org/10.1021/acssuschemeng.3c06878.
160. Mendieta, C.M.; González, G.; Vallejos, M.E.; Area, M.C. Bio-polyethylene furanoate (Bio-PEF) from lignocellulosic biomass adapted to the circular bioeconomy. *BioResources* **2022**, *17*, 7313-7337, doi:https://doi.org/10.15376/biores.17.4.mendieta.
161. Walkowiak, K.; Paszkiewicz, S. Modifications of Furan-Based Polyesters with the Use of Rigid Diols. *Polymers* **2024**, *16*, 2064, doi:https://dx.doi.org/10.3390/polym16142064.
162. Xu, C.; Shi, X.; Cui, L.; Gao, S.; Wu, S. From biomass to biopolymer: strategic development of <scp>PEF</scp> for sustainable material solutions. *Biofuels, Bioproducts and Biorefining* **2025**, doi:https://dx.doi.org/10.1002/bbb.70000.
163. Fei, X.; Wang, J.; Zhang, X.; Jia, Z.; Jiang, Y.; Liu, X. Recent Progress on Bio-Based Polyesters Derived from 2,5-Furandicarbonxylic Acid (FDCA). *Polymers* **2022**, *14*, 625, doi:https://www.mdpi.com/2073-4360/14/3/625.
164. Loos, K.; Zhang, R.; Pereira, I.; Agostinho, B.; Hu, H.; Maniar, D.; Sbirrazzuoli, N.; Silvestre, A.J.D.; Guigo, N.; Sousa, A.F. A Perspective on PEF Synthesis, Properties, and End-Life. *Frontiers in Chemistry* **2020**, *8*, doi:https://doi.org/10.3389/fchem.2020.00585.
165. Righetti, M.C.; Marchese, P.; Vannini, M.; Celli, A.; Lorenzetti, C.; Cavallo, D.; Ocando, C.; Müller, A.J.; Androsch, R. Polymorphism and Multiple Melting Behavior of Bio-Based Poly(propylene 2,5-furandicarboxylate). *Biomacromolecules* **2020**, *21*, 2622-2634, doi:https://dx.doi.org/10.1021/acs.biomac.0c00039.
166. Toledano, O.; Gálvez, O.; Sanz, M.; Garcia Arcos, C.; Rebollar, E.; Nogales, A.; García-Gutiérrez, M.C.; Santoro, G.; Irska, I.; Paszkiewicz, S.; et al. Study of the Crystal Structure and Hydrogen Bonding during Cold Crystallization of Poly(trimethylene 2,5-furandicarboxylate). *Macromolecules* **2024**, *57*, 2218-2229, doi:https://dx.doi.org/10.1021/acs.macromol.3c02471.
167. Li, Y.; Li, C.; Ren, Y.; Zhou, W.; Yang, S.; Lin, Y.; Yuan, M.; Li, H.; Xu, C. Highly stretchable and degradable bio-based poly (butanediol 2,5-furandicarboxylate-co-ε-caprolactone): Regulating structure and performance via ε-caprolactone content. *Materials Today Communications* **2025**, *49*, 113879, doi:https://doi.org/10.1016/j.mtcomm.2025.113879.
168. Terzopoulou, Z.; Kasmi, N.; Tsanaktsis, V.; Doulakas, N.; Bikiaris, D.N.; Achilias, D.S.; Papageorgiou, G.Z. Synthesis and Characterization of Bio-Based Polyesters: Poly(2-methyl-1,3-propylene-2,5-furanoate), Poly(isosorbide-2,5-furanoate), Poly(1,4-cyclohexanedimethylene-2,5-furanoate). *Materials* **2017**, *10*, 801, doi:https://dx.doi.org/10.3390/ma10070801.
169. Weinland, D.H.; Van Putten, R.-J.; Gruter, G.-J.M. Evaluating the commercial application potential of polyesters with 1,4:3,6-dianhydrohexitols (isosorbide, isomannide and isoidide) by reviewing the synthetic challenges in step growth polymerization. *European Polymer Journal* **2022**, *164*, 110964, doi:https://dx.doi.org/10.1016/j.eurpolymj.2021.110964.
170. Wang, Y.; Guo, W.; Yue, J.; Heeres, H.J.; Zhao, L.; Xi, Z. Experimental Study on the Synthesis of Biobased Poly(ethylene-2,5-furandicarboxylate) and Kinetic Modeling on the Esterification of 2,5-Furandicarboxylic Acid and Ethylene Glycol. *ACS Sustainable Chemistry & Engineering* **2025**, *13*, 7299-7317, doi:https://dx.doi.org/10.1021/acssuschemeng.5c02516.
171. Zhao, D.; Delbecq, F.; Len, C. One-Pot FDCA Diester Synthesis from Mucic Acid and Their Solvent-Free Regioselective Polytransesterification for Production of Glycerol-Based Furanic Polyesters. *Molecules* **2019**, *24*, 1030, doi:https://dx.doi.org/10.3390/molecules24061030.

 doi:10.20944/preprints202601.1587.v1

172. Yi, J.; Dai, Y.; Li, Y.; Zhao, Y.; Wu, Y.; Jiang, M.; Zhou, G. −COOH & −OH Condensation Reaction Utilization for Biomass FDCA-based Polyesters. *ChemSusChem* **2024**, *17*, doi:https://doi.org/10.1002/cssc.202301681.
173. Sadraoui, C.; Trapasso, G.; Abid, F.; Lacerda, P.S.S.; Sousa, A.F.; Aricò, F. A Greener Approach to 2,5-Furandicarboxylate Macrocycles and their Entropically Driven Ring Opening Polymerization. *European Journal of Organic Chemistry* **2025**, doi:https://dx.doi.org/10.1002/ejoc.202500737.
174. Rosenboom, J.-G.; Hohl, D.K.; Fleckenstein, P.; Storti, G.; Morbidelli, M. Bottle-grade polyethylene furanoate from ring-opening polymerisation of cyclic oligomers. *Nature Communications* **2018**, *9*, doi:https://dx.doi.org/10.1038/s41467-018-05147-y.
175. Fei, X.; Wang, J.; Zhu, J.; Wang, X.; Liu, X. Biobased Poly(ethylene 2,5-furancoate): No Longer an Alternative, but an Irreplaceable Polyester in the Polymer Industry. *ACS Sustainable Chemistry & Engineering* **2020**, *8*, 8471-8485, doi:https://doi.org/10.1021/acssuschemeng.0c01862.
176. Wang, B.; Jia, Z.; Meng, L.; Zhang, W.; Sang, L.; Chan, W.; Zhang, Y.; Wang, L.; Qi, M.; Wei, Z. Scale-Up Preparation of Biobased Poly(ethylene furanoate) Biaxial Orientation Films with Enhanced Mechanical and Barrier Properties for Packaging. *ACS Sustainable Chemistry & Engineering* **2024**, *12*, 16409-16422, doi:https://doi.org/10.1021/acssuschemeng.4c06817.
177. Xie, W.; Zhang, X.; Tang, Y.; Ke, X.; Li, T.; Fang, H.; Lin, L.; Tang, X. Impact of impurities in 2,5-furandicarboxylic acid on the synthesis of Poly(ethylene 2,5-furandicarboxylate) and its purification by crystallization in a binary solvent system. *Chinese Journal of Chemical Engineering* **2025**, *85*, 38-48, doi:https://dx.doi.org/10.1016/j.cjche.2025.03.020.
178. Duh, B. Effect of antimony catalyst on solid-state polycondensation of poly(ethylene terephthalate). *Polymer* **2002**, *43*, 3147-3154, doi:https://doi.org/10.1016/s0032-3861(02)00138-6.
179. Jiang, M.; Liu, Q.; Zhang, Q.; Ye, C.; Zhou, G. A series of furan-aromatic polyesters synthesized via direct esterification method based on renewable resources. *Journal of Polymer Science Part A: Polymer Chemistry* **2012**, *50*, 1026-1036, doi:https://doi.org/10.1002/pola.25859.
180. Zhou, Q.; Zhao, Y.; Shi, Y.; Zheng, R.; Guo, L. Acidic Metal-Based Functional Ionic Liquids Catalyze the Synthesis of Bio-Based PEF Polyester. *Polymers* **2023**, *16*, 103, doi:https://dx.doi.org/10.3390/polym16010103.
181. Thiyagarajan, S.; Meijlink, M.A.; Bourdet, A.; Vogelzang, W.; Knoop, R.J.I.; Esposito, A.; Dargent, E.; Van Es, D.S.; Van Haveren, J. Synthesis and Thermal Properties of Bio-Based Copolyesters from the Mixtures of 2,5- and 2,4-Furandicarboxylic Acid with Different Diols. *ACS Sustainable Chemistry & Engineering* **2019**, *7*, 18505-18516, doi:https://dx.doi.org/10.1021/acssuschemeng.9b04463.
182. Wang, B.; Jia, Z.; Meng, L.; Zhang, W.; Sang, L.; Chan, W.; Zhang, Y.; Wang, L.; Qi, M.; Wei, Z. Scale-Up Preparation of Biobased Poly(ethylene furanoate) Biaxial Orientation Films with Enhanced Mechanical and Barrier Properties for Packaging. *ACS Sustainable Chemistry & Engineering* **2024**, *12*, 16409-16422, doi:10.1021/acssuschemeng.4c06817.
183. Papageorgiou, G.Z.; Nikolaidis, G.N.; Ioannidis, R.O.; Rinis, K.; Papageorgiou, D.G.; Klonos, P.A.; Achilias, D.S.; Kapnisti, M.; Terzopoulou, Z.; Bikiaris, D.N. A Step Forward in Thermoplastic Polyesters: Understanding the Crystallization and Melting of Biobased Poly(ethylene 2,5-furandicarboxylate) (PEF). *ACS Sustainable Chemistry & Engineering* **2022**, *10*, 7050-7064, doi:https://doi.org/10.1021/acssuschemeng.2c00995.
184. Codou, A.; Guigo, N.; Van Berkel, J.; De Jong, E.; Sbirrazzuoli, N. Non-isothermal Crystallization Kinetics of Biobased Poly(ethylene 2,5-furandicarboxylate) Synthesized via the Direct Esterification Process. *Macromolecular Chemistry and Physics* **2014**, *215*, 2065-2074, doi:https://doi.org/10.1002/macp.201400316.
185. Banella, M.B.; Bonucci, J.; Vannini, M.; Marchese, P.; Lorenzetti, C.; Celli, A. Insights into the Synthesis of Poly(ethylene 2,5-Furandicarboxylate) from 2,5-Furandicarboxylic Acid: Steps toward Environmental and Food Safety Excellence in Packaging Applications. *Industrial & Engineering Chemistry Research* **2019**, *58*, 8955-8962, doi:https://doi.org/10.1021/acs.iecr.9b00661.
186. Wang, B.; Tu, Z.; Zhang, X.; Sang, L.; Chan, W.; Wang, L.; Pu, X.; Ling, F.; Qi, M.; Wei, Z. New advance in biorenewable FDCA-based polyesters: Multiple scale-up from lab bench to pilot plant. *Chemical Engineering Journal* **2023**, *474*, 145911, doi:https://dx.doi.org/10.1016/j.cej.2023.145911.

187. Gomes, M.; Gandini, A.; Silvestre, A.J.D.; Reis, B. Synthesis and characterization of poly(2,5-furan dicarboxylate)s based on a variety of diols. *Journal of Polymer Science Part A: Polymer Chemistry* **2011**, *49*, 3759-3768, doi:https://doi.org/10.1002/pola.24812.
188. Gandini, A.; Coelho, D.; Gomes, M.; Reis, B.; Silvestre, A. Materials from renewable resources based on furan monomers and furan chemistry: work in progress. *Journal of Materials Chemistry* **2009**, *19*, 8656, doi:https://doi.org/10.1039/b909377j.
189. Atta, S.; Cohen, J.; Kohn, J.; Gormley, A.J. Ring opening polymerization of ε-caprolactone through water. *Polymer Chemistry* **2021**, *12*, 159-164, doi:https://doi.org/10.1039/d0py01481h.
190. Guy, N.; Giani, O.; Blanquer, S.; Pinaud, J.; Robin, J.-J. Photoinduced ring-opening polymerizations. *Progress in Organic Coatings* **2021**, *153*, 106159, doi:https://doi.org/10.1016/j.porgcoat.2021.106159.
191. Liu, Y.; Ou, S.; Wu, J.; Zhao, R.; Hou, R.; Li, X.; Sun, Y.; Li, Y.; Hu, X.; Zhu, N.; et al. Continuous flow ring-opening polymerization and ring-opening metathesis polymerization. *European Polymer Journal* **2024**, *216*, 113288, doi:https://doi.org/10.1016/j.eurpolymj.2024.113288.
192. Li, J.; Tu, Y.; Lu, H.; Li, X.; Yang, X.; Tu, Y. Rapid synthesis of sustainable poly(ethylene 2,5-furandicarboxylate)-block-poly(tetramethylene oxide) multiblock copolymers with tailor-made properties via a cascade polymerization route. *Polymer* **2021**, *237*, 124313, doi:https://doi.org/10.1016/j.polymer.2021.124313.
193. Carlos Morales-Huerta, J.; Martínez De Ilarduya, A.; Muñoz-Guerra, S. Poly(alkylene 2,5-furandicarboxylate)s (PEF and PBF) by ring opening polymerization. *Polymer* **2016**, *87*, 148-158, doi:https://doi.org/10.1016/j.polymer.2016.02.003.
194. Samant, K.D.; Ng, K.M. Synthesis of prepolymerization stage in polycondensation processes. *AIChE Journal* **1999**, *45*, 1808-1829, doi:https://dx.doi.org/10.1002/aic.690450816.
195. Terzopoulou, Z.; Karakatsianopoulou, E.; Kasmi, N.; Tsanaktsis, V.; Nikolaidis, N.; Kostoglou, M.; Papageorgiou, G.Z.; Lambropoulou, D.A.; Bikiaris, D.N. Effect of catalyst type on molecular weight increase and coloration of poly(ethylene furanoate) biobased polyester during melt polycondensation. *Polymer Chemistry* **2017**, *8*, 6895-6908, doi:https://dx.doi.org/10.1039/C7PY01171G.
196. Cai, Q.; Li, X.; Zhu, W. High Molecular Weight Biodegradable Poly(ethylene glycol) via Carboxyl-Ester Transesterification. *Macromolecules* **2020**, *53*, 2177-2186, doi:https://doi.org/10.1021/acs.macromol.9b02177.
197. Vogelzang, W.; J. I. Knoop, R.; Van Es, D.S.; Blaauw, R.; Maaskant, E. Biobased high-performance polyesters: Synthesis and thermal properties of poly(isoidide furanoate) and co-polyesters. *European Polymer Journal* **2023**, *200*, 112516, doi:https://dx.doi.org/10.1016/j.eurpolymj.2023.112516.
198. Wang, J.; Liu, X.; Zhu, J.; Jiang, Y. Copolyesters Based on 2,5-Furandicarboxylic Acid (FDCA): Effect of 2,2,4,4-Tetramethyl-1,3-Cyclobutanediol Units on Their Properties. *Polymers* **2017**, *9*, 305, doi:https://dx.doi.org/10.3390/polym9090305.
199. Knoop, R.J.I.; Vogelzang, W.; Van Haveren, J.; Van Es, D.S. High molecular weight poly(ethylene-2,5-furanoate); critical aspects in synthesis and mechanical property determination. *Journal of Polymer Science Part A: Polymer Chemistry* **2013**, *51*, 4191-4199, doi:https://doi.org/10.1002/pola.26833.
200. Papageorgiou, G.Z.; Tsanaktsis, V.; Bikiaris, D.N. Synthesis of poly(ethylene furandicarboxylate) polyester using monomers derived from renewable resources: thermal behavior comparison with PET and PEN. *Phys. Chem. Chem. Phys.* **2014**, *16*, 7946-7958, doi:https://doi.org/10.1039/c4cp00518j.
201. Benyathiar, P.; Kumar, P.; Carpenter, G.; Brace, J.; Mishra, D.K. Polyethylene Terephthalate (PET) Bottle-to-Bottle Recycling for the Beverage Industry: A Review. *Polymers* **2022**, *14*, 2366, doi:https://doi.org/10.3390/polym14122366.
202. Khouri, N.G.; Bahú, J.O.; Blanco-Llamero, C.; Severino, P.; Concha, V.O.C.; Souto, E.B. Polylactic acid (PLA): Properties, synthesis, and biomedical applications – A review of the literature. *Journal of Molecular Structure* **2024**, *1309*, 138243, doi:https://doi.org/10.1016/j.molstruc.2024.138243.
203. Momeni, S.; Craplewe, K.; Safder, M.; Luz, S.; Sauvageau, D.; Elias, A. Accelerating the Biodegradation of Poly(lactic acid) through the Inclusion of Plant Fibers: A Review of Recent Advances. *ACS Sustainable Chemistry & Engineering* **2023**, *11*, 15146-15170, doi:https://doi.org/10.1021/acssuschemeng.3c04240.

204. Lee, K.W.A.; Chan, L.K.W.; Lee, A.W.K.; Lee, C.H.; Wong, S.T.H.; Yi, K.-H. Poly-d,l-lactic Acid (PDLLA) Application in Dermatology: A Literature Review. *Polymers* **2024**, *16*, 2583, doi:https://doi.org/10.3390/polym16182583.
205. Srisuwan, Y.; Baimark, Y. Mechanical properties and heat resistance of stereocomplex polylactide/copolyester blend films prepared by in situ melt blending followed with compression molding. *Heliyon* **2018**, *4*, e01082, doi:https://dx.doi.org/10.1016/j.heliyon.2018.e01082.
206. Senila, L.; Kovacs, E.; Senila, M. A Review of Polylactic Acid (PLA) and Poly(3-hydroxybutyrate) (PHB) as Bio-Sourced Polymers for Membrane Production Applications. *Membranes* **2025**, *15*, 210, doi:https://dx.doi.org/10.3390/membranes15070210.
207. Yu, J.; Xu, S.; Liu, B.; Wang, H.; Qiao, F.; Ren, X.; Wei, Q. PLA bioplastic production: From monomer to the polymer. *European Polymer Journal* **2023**, *193*, 112076, doi:https://doi.org/10.1016/j.eurpolymj.2023.112076.
208. Pang, K.; Kotek, R.; Tonelli, A. Review of conventional and novel polymerization processes for polyesters. *Progress in Polymer Science* **2006**, *31*, 1009-1037, doi:https://doi.org/10.1016/j.progpolymsci.2006.08.008.
209. Mathew, A.P.; Oksman, K.; Sain, M. Mechanical properties of biodegradable composites from poly lactic acid (PLA) and microcrystalline cellulose (MCC). *Journal of Applied Polymer Science* **2005**, *97*, 2014-2025, doi:https://doi.org/10.1002/app.21779.
210. Senila, L.; Gál, E.; Kovacs, E.; Cadar, O.; Dan, M.; Senila, M.; Roman, C. Poly(3-hydroxybutyrate) Production from Lignocellulosic Wastes Using Bacillus megaterium ATCC 14581. *Polymers* **2023**, *15*, 4488, doi:https://dx.doi.org/10.3390/polym15234488.
211. De França, J.O.C.; Da Silva Valadares, D.; Paiva, M.F.; Dias, S.C.L.; Dias, J.A. Polymers Based on PLA from Synthesis Using D,L-Lactic Acid (or Racemic Lactide) and Some Biomedical Applications: A Short Review. *Polymers* **2022**, *14*, 2317, doi:https://doi.org/10.3390/polym14122317.
212. Chen, C.-C.; Chueh, J.-Y.; Tseng, H.; Huang, H.-M.; Lee, S.-Y. Preparation and characterization of biodegradable PLA polymeric blends. *Biomaterials* **2003**, *24*, 1167-1173, doi:https://doi.org/10.1016/s0142-9612(02)00466-0.
213. Inkinen, S.; Hakkarainen, M.; Albertsson, A.-C.; Södergård, A. From Lactic Acid to Poly(lactic acid) (PLA): Characterization and Analysis of PLA and Its Precursors. *Biomacromolecules* **2011**, *12*, 523-532, doi:https://doi.org/10.1021/bm101302t.
214. Vink, E.T.H.; Rábago, K.R.; Glassner, D.A.; Gruber, P.R. Applications of life cycle assessment to NatureWorks™ polylactide (PLA) production. *Polymer Degradation and Stability* **2003**, *80*, 403-419, doi:https://dx.doi.org/10.1016/S0141-3910(02)00372-5.
215. Kim, K.W.; Woo, S.I. Synthesis of High-Molecular-Weight Poly(L-lactic acid) by Direct Polycondensation. *Macromolecular Chemistry and Physics* **2002**, *203*, 2245-2250, doi:https://doi.org/10.1002/1521-3935(200211)203:15<2245::aid-macp2245>3.0.co;2-3.
216. Shaikh, T.; Kaur, H. Synthesis and characterization of nanosized polylactic acid/TiO2 particle brushes by azeotropic dehydration polycondensation of lactic acid. *Journal of Polymer Research* **2018**, *25*, doi:https://dx.doi.org/10.1007/s10965-017-1412-3.
217. Hu, Y.; Daoud, W.; Cheuk, K.; Lin, C. Newly Developed Techniques on Polycondensation, Ring-Opening Polymerization and Polymer Modification: Focus on Poly(Lactic Acid). *Materials* **2016**, *9*, 133, doi:https://doi.org/10.3390/ma9030133.
218. Gkountela, C.I.; Vouyiouka, S.N. Enzymatic Polymerization as a Green Approach to Synthesizing Bio-Based Polyesters. *Macromol* **2022**, *2*, 30-57, doi:https://doi.org/10.3390/macromol2010003.
219. Gurunathan, T.; Mohanty, S.; Nayak, S.K. A review of the recent developments in biocomposites based on natural fibres and their application perspectives. *Composites Part A: Applied Science and Manufacturing* **2015**, *77*, 1-25, doi:https://doi.org/10.1016/j.compositesa.2015.06.007.
220. Zahra, N.; Wardhono, E.Y.; Ni'Mah, H.; Widjaja, T. Impact of Ultrasound-Assisted Dehydration on the Properties of Poly Lactic Acid Produced by Ring-Opening Polymerization. *International Journal of Technology* **2025**, *16*, 458, doi:https://dx.doi.org/10.14716/ijtech.v16i2.6521.
221. Matsumoto, K.I.; Taguchi, S. Enzymatic and whole-cell synthesis of lactate-containing polyesters: toward the complete biological production of polylactate. *Applied Microbiology and Biotechnology* **2010**, *85*, 921-932, doi:https://doi.org/10.1007/s00253-009-2374-0.

 doi:10.20944/preprints202601.1587.v1

222. Singhvi, M.S.; Zinjarde, S.S.; Gokhale, D.V. Polylactic acid: synthesis and biomedical applications. *Journal of Applied Microbiology* **2019**, *127*, 1612-1626, doi:https://dx.doi.org/10.1111/jam.14290.
223. Chanfreau, S.; Mena, M.; Porras-Domínguez, J.R.; Ramírez-Gilly, M.; Gimeno, M.; Roquero, P.; Tecante, A.; Bárzana, E. Enzymatic synthesis of poly-l-lactide and poly-l-lactide-co-glycolide in an ionic liquid. *Bioprocess and Biosystems Engineering* **2010**, *33*, 629-638, doi:https://doi.org/10.1007/s00449-009-0388-8.
224. Kumar, R.; Lalnundiki, V.; Shelare, S.D.; Abhishek, G.J.; Sharma, S.; Sharma, D.; Kumar, A.; Abbas, M. An investigation of the environmental implications of bioplastics: Recent advancements on the development of environmentally friendly bioplastics solutions. *Environmental research* **2024**, *244*, 117707, doi:https://doi.org/10.1016/j.envres.2023.117707.
225. Blanc, S.; Massaglia, S.; Brun, F.; Peano, C.; Mosso, A.; Giuggioli, N.R. Use of bio-based plastics in the fruit supply chain: An integrated approach to assess environmental, economic, and social sustainability. *Sustainability* **2019**, *11*, 2475, doi:https://doi.org/10.3390/su11092475.
226. Atiwesh, G.; Mikhael, A.; Parrish, C.C.; Banoub, J.; Le, T.-A.T. Environmental impact of bioplastic use: A review. *Heliyon* **2021**, *7*, doi:https://doi.org/10.1016/j.heliyon.2021.e07918.
227. Khatami, K.; Perez-Zabaleta, M.; Owusu-Agyeman, I.; Cetecioglu, Z. Waste to bioplastics: How close are we to sustainable polyhydroxyalkanoates production? *Waste Management* **2021**, *119*, 374-388, doi:https://doi.org/10.1016/j.wasman.2020.10.008.
228. Kakadellis, S.; Lee, P.-H.; Harris, Z.M. Two birds with one stone: bioplastics and food waste anaerobic co-digestion. *Environments* **2022**, *9*, 9, doi:https://doi.org/10.3390/environments9010009.
229. Liu, H.; Han, P. Renewable energy development and carbon emissions: The role of electricity exchange. *Journal of Cleaner Production* **2024**, *439*, 140807, doi:https://doi.org/10.1016/j.jclepro.2024.140807.
230. Yadav, K.; Nikalje, G.C. Comprehensive analysis of bioplastics: life cycle assessment, waste management, biodiversity impact, and sustainable mitigation strategies. *PeerJ* **2024**, *12*, e18013, doi:https://doi.org/10.7717/peerj.18013.
231. Benavides, P.T.; Lee, U.; Zarè-Mehrjerdi, O. Life cycle greenhouse gas emissions and energy use of polylactic acid, bio-derived polyethylene, and fossil-derived polyethylene. *Journal of Cleaner Production* **2020**, *277*, 124010, doi:https://doi.org/10.1016/j.jclepro.2020.124010.
232. Van Roijen, E.C.; Miller, S.A. A review of bioplastics at end-of-life: Linking experimental biodegradation studies and life cycle impact assessments. *Resources, Conservation and Recycling* **2022**, *181*, 106236, doi:https://doi.org/10.1016/j.resconrec.2022.106236.
233. Moshood, T.D.; Nawanir, G.; Mahmud, F. Sustainability of biodegradable plastics: a review on social, economic, and environmental factors. *Critical Reviews in Biotechnology* **2022**, *42*, 892-912, doi:https://doi.org/10.1080/07388551.2021.1973954.
234. Spierling, S.; Knüpffer, E.; Behnsen, H.; Mudersbach, M.; Krieg, H.; Springer, S.; Albrecht, S.; Herrmann, C.; Endres, H.-J. Bio-based plastics-A review of environmental, social and economic impact assessments. *Journal of Cleaner Production* **2018**, *185*, 476-491, doi:https://doi.org/10.1016/j.jclepro.2018.03.014.
235. Symons, J. *ENVIRONMENTAL & ECONOMIC IMPLICATIONS OF BIOBASED PACKAGING*; 2022.
236. Moodley, P.; Trois, C. Circular closed-loop waste biorefineries: Organic waste as an innovative feedstock for the production of bioplastic in South Africa. *South African Journal of Science* **2022**, *118*, doi:https://doi.org/10.17159/sajs.2022/12683.
237. Keith, M.; Koller, M.; Lackner, M. Carbon recycling of high value bioplastics: a route to a zero-waste future. *Polymers* **2024**, *16*, 1621, doi:https://doi.org/10.3390/polym16121621.